UNIVERSITAT DE BARCELONA

Optimization of therapeutic options against multidrug resistant microorganisms

Berta Puig Collderram

UNIVERSITAT DE BARCELONA
FACULTAT DE FARMÀCIA I CIÈNCIES
DE L'ALIMENTACIÓ

OPTIMIZATION OF THERAPEUTIC OPTIONS AGAINST MULTIDRUG RESISTANT MICROORGANISMS

BERTA PUIG COLLDERRAM
2025

UNIVERSITAT DE BARCELONA

FACULTAT DE FARMÀCIA I CIÈNCIES DE L'ALIMENTACIÓ

DRUG RESEARCH, DEVELOPMENT AND CONTROL

LABORATORI DE REFERÈNCIA DE CATALUNYA

OPTIMIZATION OF THERAPEUTIC OPTIONS AGAINST MULTIDRUG RESISTANT MICROORGANISMS

Optimització d'opcions terapèutiques contra microorganismes multirresistents

Memòria presentada per Berta Puig Collderram per optar al títol de doctor per la Universitat de Barcelona

Dra. Núria Prim Bosch

Dr. Juan Ramón González

Berta Puig Collderram

Dra. Ana Maria Marques Villavecchia

Dedicatories, Agraïments

Quina sort la meva, tenir tantes coses per agraïr, i en tants idiomes diferents.

Que suerte la mía, tener tantas cosas por agradecer, y en tantos idiomas diferentes.

How lucky I am, to have so many things to be thankful for, in so many different languages.

Was für ein Glück, dass ich so viele Dinge habe, für die ich dankbar sein kann,

in so vielen verschiedenen Sprachen.

A la Concha i a la Núria, per ensenyar-me a fer i a escriure ciència. Per les incomptables hores compartides i les dificultats superades. Per ser-hi no només de manera professional si no també de manera personal. Font d'inspiració i suport constant.

A Rafa, que desde el más allá seguro que sigue refunfuñando por las reuniones interminables de esta tesis.

A Juan, por su atención, asesoramiento y soporte.

A Eduardo, por creer siempre en mí y apostar por mí. Por la confianza y las confidencias compartidas.

A Mila, por tantos consejos y por ser alegría y energía siempre.

A la Sandra, per ser-hi de manera incondicional cuando la vida aprieta y ahoga y, cuando no, también. Encordades 4ever.

Al Santi, al Dani, a la Luisa i a la Sonia, per les seves aportacions en moments claus d'aquest doctorat.

A Juan Pablo, por sus aportacions en esta tesis.

A les meves alumnes de màster, la Clàudia, la Jana, les Natàlies i l'Alba. Per haver compartit l'amor (i desamor) per la recerca.

A la meva família, per les arrels i per les ales. Gràcies per donar-me sempre les eines per poder escollir i deixar-me lliure per prendre les meves decisions. Al meu pare i a la meva mare per ser refugi i experiència sempre. Al meu germà, guia i complice. A la meva tieta, que sempre ha sigut vitamina. A la meva àvia Carmen i al tiet Pau, als que penso, estimo i anyoro cada dia.

An Omar, defür, dass ich mich bi dir dihei fühl. Defür, dass du mich nöd nur so fest liebsch, sondern dass du mich au so guet liebsch.

Als Soutos, per escollir ser familia i ser-hi sempre. Celebrant els bons moments i no fallant mai en els dolents.

A la Lena i la Judit, per tot el que hem après i descobert fent-nos grans juntes. Tan de bo i això no canviï. Sempre sereu casa.

A la Paola, mi partner in crime. Por el peligro que tenemos cuando nos juntamos, por todo lo que podemos contar, pero sobre todo por todo lo que no. Por no juzgarnos nunca y por acompañarnos siempre tan bien.

A la meva cosina Noa i a la connexió tan especial que tenim. Espero ser exemple no només dels encerts, si no també dels errors.

A les Biogirls, les meves amigues de la universitat, per continuar essent una petita familia tot i la distància i el temps.

A la Judith, quina sort trobar-nos, tantíssim après (i desaprès) en tant poc temps.

Al Bernat i a l'Alba, per sostenir-me quan més ho necessitava, desbloquejar pors i compartir felicitat. Em grabo el "lo que puedes dar se agradece y se aprecia, y lo que no puedes no existe".

A les Zürines, la meva bombolla a Zürich. Per ser zona de confort on tot és extrany.

A tots els que han compartit energia amb mi practicant Navakarana. En català, en castellà, en anglès i/o en sanskrit. Mestres, alumnes i companyes, gràcies.

To my little phage family, colleagues and supervisors from Universitätklinic Balgrist in Zürich. One worry at a time; could be worse!

Als meus excompanys de la FNAC, por hacer fácil lo difícil, por conseguir que estudiar y trabajar no solo fuera posible, sino también divertido.

Al Laboratori de Referència de Catalunya i als seus treballadors, pel suport rebut durant la realització d'aquesta tesi, ajudant-me a crèixer com a profesional i com a persona.

A Promega Iberia, por la ayuda y el soporte técnico.

There and back again

A hobbit tale about academic research,
by Berta Baggins

Resum

L'increment de la resistència als antibiòtics representa un greu problema de salut pública a escala global. *Pseudomonas aeruginosa* i *Klebsiella pneumoniae* són dues de les espècies involucrades amb més freqüència en infeccions nosocomials, sovint causades per soques multiresistents. Les combinacions d'antibiòtics són una de les opcions terapèutiques disponibles per a combatre infeccions causades per bacteris multiresistents. La corba de letalitat (*time-kill*, TK) és un mètode *in vitro* que permet estudiar l'activitat de les combinacions d'antibiòtics al llarg d'un temps determinat. El recompte d'unitats formadores de colònies (UFC) és el mètode tradicional d'obtenció de resultats en les TK. La possibilitat d'emprar una tècnica de bioluminescència basada en l'ATP suposaria una alternativa més ràpida i menys laboriosa que el recompte convencional. Una de les combinacions d'antibiòtics utilitzades habitualment per tractar de manera empírica infeccions causades per bacils gramnegatius és meropenem i amikacina. No obstant, l'instant d'administració de l'amikacina no està ben definit a la pràctica clínica. Els règims simultanis i esglaonats d'aquesta combinació podrien tenir diferents impactes clínics.

L'objectiu principal d'aquest estudi va ser 1) estandarditzar i avaluar una tècnica d'ATP com alternativa al mètode convencional de recompte de colònies en estudis de combinacions d'antibiòtics mitjançant TK i, 2) determinar el règim d'administració òptim de meropenem i amikacina contra *P. aeruginosa* extremadament resistents (XDR) i *K. pneumoniae* productores de carbapenemases (CP-KP) mitjançant experiments TK.

La tècnica d'ATP es va realitzar amb el GloMax®96 Microplate Luminometer (Promega), que mesura la bioluminescència en unitats relatives de llum (RLU). Per estandarditzar la tècnica, es va determinar el *background*, la linealitat i el límit de detecció. Es van dur a terme TKs de 24 h, i els resultats es van analitzar en paral·lel mitjançant el mètode convencional de recompte de cèl·lules i la tècnica d'ATP. El mètode convencional es va utilitzar com a *gold standard* per establir els punts de tall en el mètode d'ATP. L'estandardització es va fer amb *P. aeruginosa*, *K. pneumoniae* i *Enterococcus faecium*. La solució salina neutra (NSS) es va establir com a medi de rentat i/o dilució ja que va mostrar una major linealitat i un límit de detecció més baix que el medi de cultiu amb cations ajustats Mueller Hinton (CA-MH). Les RLU van correlacionar amb les UFC dins del rang lineal. La categorització dels paràmetres farmacodinàmics utilitzant la tècnica d'ATP va ser equivalent al mètode de recompte de colònies. Els punts de tall per a l'efecte bactericida i la sinergia van ser de 1,348 log RLU/mL (93% sensibilitat, 78.5% especificitat) i 0,9 log RLU/mL (95% de sensibilitat, 88% d'especificitat) per a *P. aeruginosa*, i de 0,764 log RLU/mL (sensibilitat del 100%, especificitat del 76%) i 2,95 log RLU/mL (78.6% de sensibilitat, 100% d'especificitat) per a *K. pneumoniae*, respectivament.

Diferents règims d'administració de meropenem (MEM) i amikacina (AK) es van evaluar en set soques clíniques de XDR *P. aeruginosa* i en cinc aïllats clínics de CP-KP mitjançant TKs de 24 h. Les concentracions d'antibiòtics utilitzades van correspondre a AK8 (8,17 mg/L) i MEM17 (17,71 mg/L). També es va avaluar una concentració més elevada de MEM32 (32 mg/L) en tots els aïllats de CP-KP i en quatre soques seleccionades de *P. aeruginosa* amb diferents mecanismes de resistència. Es va testar una concentració més

alta d'AK40 (40 mg/L) en quatre soques de *P. aeruginosa* amb diferents concentracions mínimes inhibitòries (CMI) d'aquest antibiòtic i en dues CP-KP amb resistència d'alt nivell a AK. Ambdós antibiòtics es van administrar alhora a l'inici de la corba en els règims simultanis. En els règims esglaonats, el segon antibiòtic es va afegir 2 hores després del primer, AK després de MEM o viceversa. El recompte de cèl·lules viables (log UFC/mL) es va analitzar a diferents temps al llarg de la corba.

Els règims simultanis d'amikacina i meropenem van causar una reducció inicial de la càrrega bacteriana a la majoria dels aïllats de XDR *P. aeruginosa* i CP-KP. Els règims esglaonats van causar una reducció inicial de la càrrega bacteriana quan la concentració del primer antibiòtic va ser superior a la CMI d'aquell antibiòtic, independentment del mecanisme de resistència.

En conclusió, l'assaig d'ATP va ser útil per avaluar les combinacions d'antibiòtics mitjançant experiments TK. Aquest mètode, menys laboriós i més ràpid que el mètode de recompte de colònies, podria ser fàcilment implementat en laboratoris de microbiologia clínica. Els nostres resultats suggereixen que l'administració simultània d'amikacina i meropenem hauria de ser la primera opció en els tractaments empírics per tal de buscar una major reducció inicial de la càrrega bacteriana quan es desconeix la sensibilitat de l'agent infecciós a aquells antibiòtics.

Paraules clau de la tesi: TESAURO (Codis UNESCO)
Ciències clíniques, microbiologia, farmacodinàmica, acció dels medicaments

Abstract

Antibiotic resistance has become a public health concern. Combining antibiotics is a strategy to overcome the limited therapeutic options against multidrug-resistant bacteria, including extensively-drug resistant (XDR) *Pseudomonas aeruginosa* and carbapenemase-producing *Klebsiella pneumoniae* (CP-KP). Time-kill curves (TK) are used to study antibiotic combinations, but the colony count method to obtain the results is time-consuming. A bioluminescent ATP assay to analyze the results of TKs would allow the implementation of studies of antibiotic combination in clinical microbiology laboratories. The combination of meropenem and amikacin is commonly used to empirically treat infections caused by Gram-negative bacilli, but the time of amikacin administration is not well stablished. Simultaneous and staggered schedules of this combination may have different clinical impacts.

The main aims of this study were 1) to standardize and evaluate an ATP assay as an alternative to the conventional colony count method in TK studies of antibiotic combinations, and 2) to determine the optimal dosing schedule of meropenem plus amikacin against XDR *P. aeruginosa* and CP-KP by means of TK experiments.

The ATP assay was performed using the GloMax®96 Microplate Luminometer (Promega) that measures bioluminescence in relative light units (RLU). Background, linearity and detection limit were determined to standardize this assay. Twenty-four-hour TKs were performed, and results were analyzed in parallel using the conventional cell count method and the ATP assay. The conventional method was used as gold standard to establish the breakpoints in the ATP method. Standardization was performed with *P. aeruginosa*, *K. pneumoniae* and *Enterococcus faecium*.

Different dosing schedules of meropenem (MEM) and amikacin (AK) were tested against seven XDR *P. aeruginosa* and five CP-KP clinical isolates by 24-hour TKs. The antibiotic concentrations AK8 (8.17 mg/L) and MEM17 (17.71 mg/L) were assessed against all isolates. A higher dose of MEM32 (32 mg/L) was also assessed on all CP-KP isolates and four selected *P. aeruginosa* isolates with different mechanisms of resistance. A higher concentration of AK40 (40 mg/L) was evaluated against four *P. aeruginosa* with different amikacin minimum inhibitory concentrations (MIC), and against the two high-level amikacin-resistant CP-KP. Simultaneous schedules included both antibiotics at the start of the curve. In staggered schedules the second antibiotic was added two hours after the first antibiotic: AK after meropenem or conversely. Viable cell count (log CFU/mL) was analysed at different times. The initial bacterial load reduction was evaluated for each dosing schedule.

Neutral saline solution (NSS) showed wider linearity and a lower detection limit than Cation-adjusted Mueller Hinton (CA-MH) in the ATP assay. Therefore, NSS was established as washing/dilution medium. Relative light forming units (RLU) signal correlated with colony forming units (CFU) when the assay was performed within the linear range. Categorization of the pharmacodynamic parameters using the ATP assay was equivalent to the colony-count method in the TKs. The bactericidal effect and synergy breakpoints were 1.348 (sensitivity 93%, specificity 78.5%) and 0.9 (98% sensitivity, 88% specificity) log RLU/ml for *P. aeruginosa,* and 0.764 (sensitivity 100%,

specificity 76%) and 2.95 (78.6% sensitivity, 100% specificity) log RLU/ml for *K. pneumoniae*, respectively.

Simultaneous schedules of amikacin and meropenem caused an initial bacterial load reduction in most of the XDR *P. aeruginosa* and CP-KP isolates. Staggered schedules caused an initial bacterial load reduction when the concentration of the first antibiotic was above the MIC, regardless of the mechanism of resistance.

Summing up, the ATP assay was useful to determine the effectiveness of antibiotic combinations in TKs. This method, less laborious and faster than the colony count method, could be more easily performed in clinical microbiology laboratories. According to our results, simultaneous dosing schedules of amikacin and meropenem should be of choice in empirical treatments when the antibiotic susceptibility results of the infectious agent are unknown.

Thesis keywords: THESAURUS (UNESCO Codes)
Clinical sciences, microbiology, pharmacodynamics, drug action

Índex

Tables and figures

Tables

Tables and figures
Figures

List of Abbreviations

AK – Amikacin
AMR – Antimicrobial Resistance
ARG – Antibiotic Resistance Gen
AST – Antibiotic Susceptibility Testing
ATP - Adenosine Triphosphate
AUC – Area Under the Curve
AUC24 – Area Under the Concentration-time Curve from 0 to 24h
BLBLI – β-lactam/β-lactamase Inhibitors
CA-MH – Cation-adjusted Mueller Hinton
CFU – Colony Forming Units
CG – Clonal Group
CLSI – Clinical and Laboratory Standards Institute
CP-KP – Carbapenemase-producing *Klebsiella pneumoniae*
DHFR – Dihydrofolate Reductase
EMA – European Medicines Agency
EPS – Exopolysaccharides
ERIC – Enterobacterial Repetitive Intergenic Consensus
ESBL – Extended-spectrum β-lactamases
EUCAST – European Committee on Antimicrobial Susceptibility Testing
FDA – Food and Drug Administration
HPLC – High Performance Liquid Chromatography (HPLC)
HVKP – Hypervirulent *Klebsiella pneumoniae*
I – Susceptible, Increased Exposure
ICC – Intraclass Correlation Coefficient
LPS – Lipopolysaccharide
MBL – Metallo-β-lactamase
MDR – Multi-drug Resistant Microorganism
MEM – Meropenem
MIC – Minimum Inhibitory Concentration
MLST – Multilocus Sequence Typing
MLVA – Multilocus Variable-number Tandem-repeat Analysis
MPC – Mutant Prevention Concentration
NSS – Neutral Saline Solution
OMP – Outer Membrane Protein
ORWG – Outreach Working Group
PABA – Para-aminobenzoic Acid

PAE – Post-antibiotic Effect
PAP – Population Analysis Profile
PBP – Penicillin Binding Protein
PCH – Pyochelin
PDR – Pandrug Resistant Microorganism
PFGE – Pulsed-field Gel Electrophoresis
PK/PD – Pharmacokinetic/pharmacodynamic
PVD – Pyoverdine
R – Resistant
RAPD – Randomly Amplified Polymorphic DNA
RLU – Relative Light Forming Units
RNAP – DNA-dependent RNA Polymerase
ROC – Receiver Operating Characteristic Curves
S – Susceptible
ST – Sequence Type
TLR4 – Toll-like Receptor 4
UA – Unweighted Accuracy
WHO – World Health Organization
WWTPS – Wastewater Treatment Plants
XDR – Extensively Drug-resistant Microorganism

01
Introduction

1. Introduction

Antibiotics have been used to fight bacteria since the 20th century.[1] Infectious diseases were thought to be controlled during the antibiotic golden age, but the current situation is far from what was expected.[2] Misuse and abuse of antibiotics have occurred since their deployment, not only in human medicine but also in veterinary medicine. This fact has led to the current increasing rates of antibiotic-resistant microorganisms in most clinical settings. Infections caused by multi-drug resistant (MDR) bacteria are more difficult to treat, which causes higher mortality and morbidity rates and substantial economic burden.[3] According to a group of experts chaired by Jim O'Neal, 10 million deaths worldwide could be attributed to antimicrobial resistance (AMR) every year by 2050 if no actions are taken to tackle this threat.[4] The success of modern medicine is linked to the capacity to treat infections. Medical achievements such as cancer chemotherapy and major surgeries may be at risk without effective antimicrobial treatments. Given this concerning scenario, the World Health Organization (WHO) declared AMR as one of the top ten threats that global health is facing.[5]

AMR is a natural phenomenon that existed well before the antibiotic era. Microorganisms live in complex communities, in constant competition for space and resources.[6] The production of antimicrobial compounds helps microorganisms mediate competition against other species and dominate an ecological niche. Bacteria also have strategies to protect themselves from these natural antibiotics in their environment.[6] However, this

natural equilibrium has been completely disrupted due to the anthropogenic impact of massive use of antibiotics.

The deployment of every antimicrobial compound has been followed by emergence of resistance (Figure 1). Given this extraordinary capacity of bacteria to quickly evolve and adapt to changing environments, the discovery/development of new antibiotics has become a bottleneck and a nonstop race against increasing bacterial resistance[7].

Antibiotic pressure is a key driver for AMR because susceptible bacteria are killed while antibiotic-resistant bacterial subpopulations are selected and enlarged (Figure 2).[8] Misuse of antimicrobials in both human medicine and veterinary medicine causes selective pressure that leads to increasing AMR rates in different ecological niches. Appropriate use of antibiotics is paramount to delay this race, and this is the goal of antibiotic stewardship programs in human medicine.

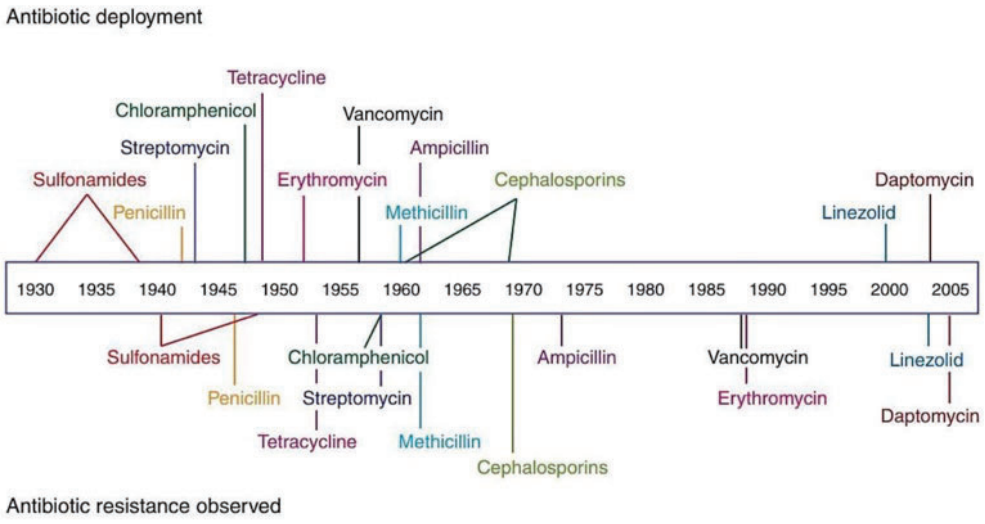

Figure 1. Timeline of antibiotic deployment and emergence of antibiotic resistance. Year of antibiotic deployment (above), and year of emergence of resistance (below)[9].

Antimicrobial resistance genes (ARGs) are either intrinsically present in bacteria, further developed through mutations, or acquired from nearby bacteria by horizontal gene transfer (HGT).[10] The term antibiotic resistome includes not only all ARGs present in an ecological niche but also their precursors and other potential resistance mechanisms that may require further modifications to confer resistance.[10] Interactions between microbial populations are complex drivers of AMR. The human gut microbiome harbours an assorted dynamic resistome that is potentially shaped by many facets, including geographical factors, biological factors (antibiotic selection pressure, HGT), health condition (co-morbidities, hospitalizations), and individual behaviour (nutrition, travels).[11]

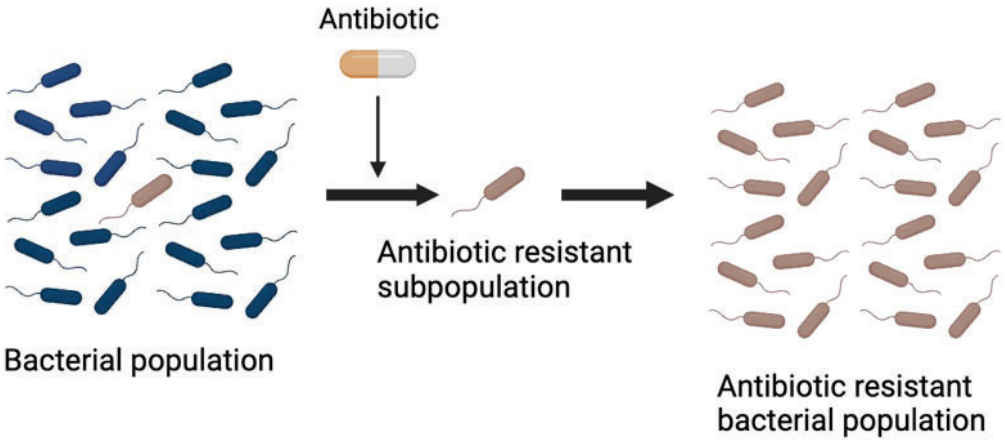

Figure 2. Antibiotic selection pressure. This figure shows the effect of antibiotic selection on bacterial populations. Susceptible cells (in blue) and resistance cells (brown). Created by Biorender.

Antibiotic resistance is not confined to clinical settings as human, animal and environmental microbiomes are connected.[8,12] There is large exchange and dissemination of both ARGs and antibiotic-resistant bacteria across different ecosystems. Medical facilities and farms but also environmental niches such as water and soil are hotspots for emerging AMR.[13] River sediments near water waste sources and soils contaminated with manure have increased potential for selection and HGT.[14] The massive release of antimicrobials into the environment contributes to this process. A recent United Nations report highlighted the impact of different anthropogenic activities on the emergence and spread of AMR in the environment.[14]

The concept of One Health (Figure 3) refers to the interconnection between human, animal and environmental health.[15] Some worldwide-spread AMR determinants such as CTX-M extended-spectrum *β-lactamases* emerged from environmental bacteria.[16] Understanding the human resistome dynamics related to the other One-Health sectors is imperative to control ARG flow to the human sector, particularly ARG transmission to nosocomial pathogens.[10] Preserving the effectiveness of antibiotics is paramount. As emerging AMR is linked to the constant exchange among different ecosystems, this global health problem must be tackled following a One-health approach, which requires the collaborative effort of multiple disciplines working locally, nationally, and globally.[14]

1.1 Antibiotics and their mechanisms of action

Antimicrobial agents interfere in biological processes that are essential for bacterial growth (Figure 4).[17] Naturally produced by microorganisms in nature or of synthetic or semi-synthetic origin, antibiotics used to treat or prevent infectious diseases should be as harmless as possible to the patient. Bactericidal agents kill the target bacteria

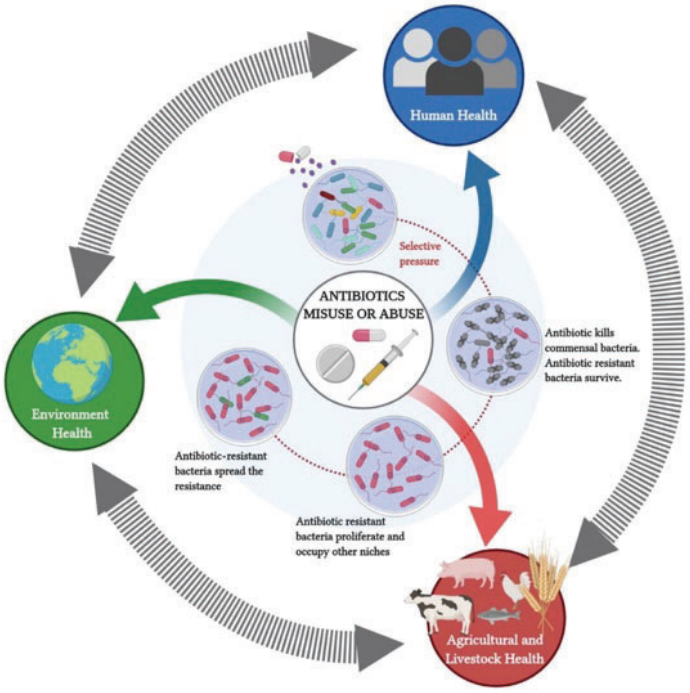

Figure 3. One Health Approach. Human health is connected to the health of animals, plants and our shared environment. The inner circle illustrates how antibiotic resistance is spread in a healthy and diverse bacterial population[15].

whereas bacteriostatic agents inhibit their growth. Bacteriostatic antimicrobials usually function via the inhibition of bacterial protein synthesis, and therefore they require a functioning host immune system to completely clear overgrowth.

Antibiotics have different mechanisms of action. These mechanisms include 1) inhibition of bacterial cell wall biosynthesis, 2) disruption of cell membrane, 3) inhibition of nucleic acid synthesis, 4) inhibition of protein synthesis, or 5) acting as antimetabolites.[18]

1.1.1 Inhibition of cell wall synthesis

The main antibiotic families that target the bacterial cell wall are β-lactams and glycopeptides. These antibiotics inhibit the cell wall biosynthesis by interfering in the polymerization of peptidoglycan, which is the major structural component of the bacterial cell wall.

The β-lactam family of antibiotics includes penicillins, cephalosporins, monobactams, and carbapenems. These bactericidal antibiotics have a four-member β-lactam ring (3-carbon and 1-nitrogen ring) and differ on the chemical nature of the radicals fused to β-lactam unit. They act by covalently and irreversibly binding to penicillin-binding

proteins (PBPs), which are essential in the formation of cross-bridges between peptide chains of peptidoglycan to ensure cell wall stability.[18] Inhibition of PBPs leads to malfunction of the cell wall biosynthesis machinery, resulting in a futile cycle where the cell wall is continuously synthesized and degraded without assembly.[19] This causes depletion of cellular energy that enhances the bactericidal effect of these antibiotics. Osmotic pressure occurs as the structural integrity of cell wall is weakened, finally leading to lysis of the bacterial cell. Some β-lactamase inhibitors (e.g. clavulanic acid, tazobactam) also contain a β-lactam ring structure but they act by inhibiting these enzymes instead of binding to PBPs. These inhibitors are commonly used in combination to protect the other β-lactam antibiotic.

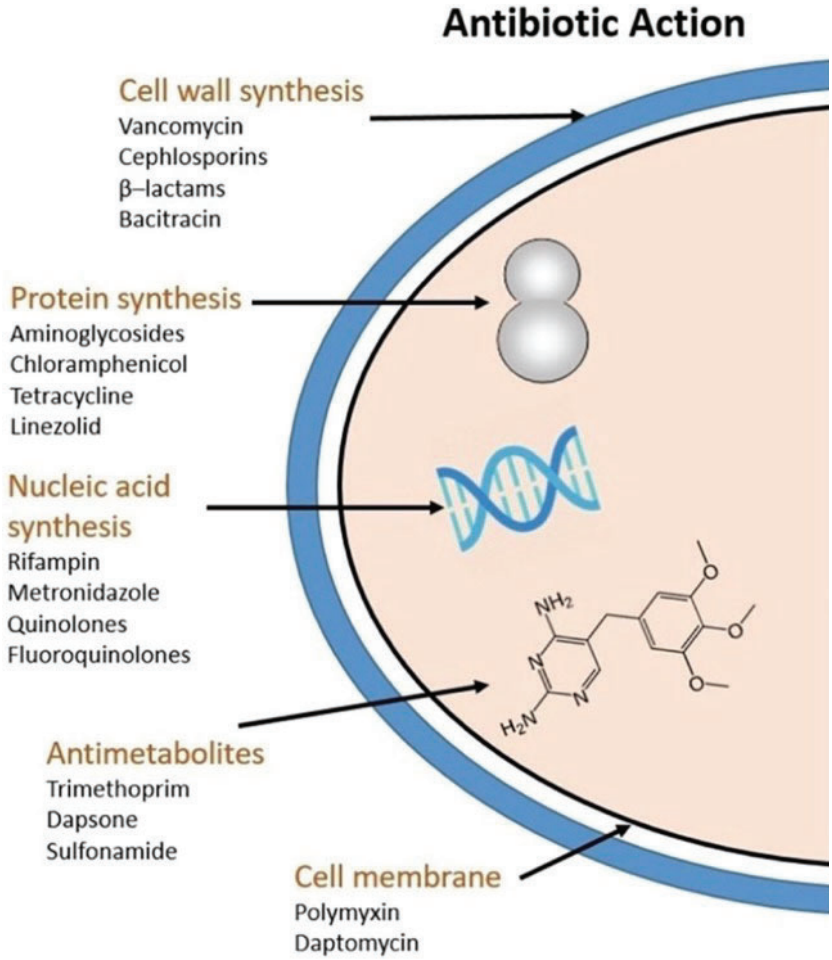

Figure 4. Action mechanisms of antibiotics. Modified from Uluseker C et al. 2021[7].

The different classes of β-lactam antibiotics have different spectrum of activity. Carbapenems (e.g. imipenem, meropenem) are broad-spectrum antibiotics, having activity against many MDR bacilli. Members in this β-lactam class are relatively resistant to most β-lactamases except for carbapenemases.[20]

Glycopeptides are large and complex molecules that inhibit peptidoglycan biosynthesis in Gram-positive bacteria. They are composed of a cyclic glycosylated peptide structure with seven amino acids. This heptapeptide backbone binds to the C-terminal L-Lys-D-Ala-D-Ala subunit of the peptidoglycan precursor lipid II, preventing the addition of new units.[18] The glycopeptide family of antibiotics includes vancomycin, teicoplanin, telavancin and the more recently deployed dalbavancin and oritavancin. Glycopeptides have different toxicity profiles, with vancomycin associated with nephrotoxicity, ototoxicity and the requirement of drug monitoring. The new lipoglycopeptides (dalbavancin and oritavancin) have minimal toxicity profiles and a long half-life that helps reduce the need for hospitalization.[21,22]

1.1.2 Disruption of the cell membrane

The main bactericidal antibiotic classes that disrupt the integrity of the cell membrane are cyclic lipopeptides (daptomycin) and polymyxins (colistin and polymyxin B).

Daptomycin is active against Gram-positive bacteria, and it has a unique structure with a 13-amino-acid peptide linked to a decanoyl side chain. Daptomycin requires calcium for activity. The insertion of the Ca2+-daptomycin complex into the cell membrane forms a channel that causes depolarization due to leakage of ions and loss of cell membrane integrity, leading to bacterial cell death.

Polymyxins are active against many Gram-negative bacteria. Polymyxin B was isolated from Bacillus polymyxa in the late 1940s, which was followed by the discovery of other polymyxins.[23] Polymyxin E (colistin) and polymyxin B were extensively used in human medicine until new safer antibiotics were introduced in the 1970s. Polymyxins are cationic polypeptides composed of a heptapeptide ring attached to an acylated fatty acid chain at the N-terminal end.[23,24] The hydrophilic cationic peptide ring and the hydrophobic fatty acids form a unique amphipathic structure. The cationic peptide binds electrostatically to the negatively charged lipopolysaccharide (LPS) molecules of the bacterial outer membrane (OM) and causes the displacement of membrane-stabilizing cations (Ca2+ and Mg2+). This local disturbance allows the interaction of the fatty acid chain of polymyxin with the lipid A portion in LPS. This leads to an increase in the OM permeability and allows the entry of antibiotic molecules.[25] Osmotic imbalance and loss of cell membrane integrity contribute to the cell disruption and bacterial death caused by polymyxins.[25]

1.1.3 Inhibition of the nucleic acid synthesis

Some antibiotic families directly inhibit nucleic acid synthesis. These antibiotics may interfere with DNA replication by targeting essential enzymes for bacterial DNA synthesis (i.e. quinolones, novobiocin), or with RNA synthesis by targeting bacterial RNA polymerase (i.e. rifamycins).

Quinolones are bactericidal antibiotics that act on DNA synthesis. They target two type II topoisomerase enzymes that are essential in the replication fork: DNA-gyrase and

topoisomerase IV. [26] Nalidixic acid was the first quinolone antibiotic discovered in 1962. This first generation of quinolones was replaced by fluoroquinolones with a broader spectrum of bactericidal activity and expanded pharmacological properties. Improved activity in fluoroquinolones is due to a fluorine atom at position 6 and different sides chain substitutions added to the nalidixic acid quinolone core. Several generations of fluoroquinolones have been deployed to increase these properties, ranging from norfloxacin, ofloxacin and ciprofloxacin, to levofloxacin, moxifloxacin and novel members such as delafloxacin.[27]

Rifamycins are bactericidal antibiotics that prevent RNA synthesis by binding to the β-subunit of prokaryotic DNA-dependent RNA-polymerase near its catalytic center. [28] The inhibition occurs by sterically blocking the path of the elongating RNA at its 5´ end, and by reducing the affinity of this RNA-polimerase for short RNA transcripts. Consequently, transcriptional activity is inhibited, leading to bacterial death.[29] Rifamycins are used usually in combination against *Mycobacterium tuberculosis* or some Gram-positive bacteria.

1.1.4 Inhibition of protein synthesis

Antibiotics that inhibit protein synthesis target the ribosomal machinery in prokaryotic cells. The main families of antibiotics with this mechanism of action are tetracyclines, aminoglycosides, macrolides and oxazolidinones.[30]

Tetracyclines are considered bacteriostatic antibiotics. Members of this antibiotic family differ in the moieties attached to a core structure that consists of four flat aromatic hydrocarbon rings.[31] These antibiotics form complexes with magnesium in aqueous solutions. These tetracycline-metal complexes attach to the 30S subunit in the bacterial ribosome, blocking aminoacyl-tRNA binding to the A-site and inhibiting translation. Tetracyclines are active against a wide range of Gram-positive and Gram-negative bacteria, including some intracellular pathogens and spirochetes.

Aminoglycosides are potent antibiotics that act through inhibition of protein synthesis. The use of aminoglycoside antibiotics started in the mid 1940s. The first aminoglycoside to be discovered was streptomycin obtained from the soil bacterium *Streptomyces griseus* in 1943.[32] This was followed by the discovery of new aminoglycosides (e.g. neomycin, gentamicin, tobramycin, kanamycin) obtained from other *Actinomycetales* throughout the next decades.[33] Starting in the 1970s, semi-synthetic aminoglycosides such as amikacin were developed to improve their pharmacological properties and to overcome resistance issues.[33] Development of new aminoglycosides continued in the present century, leading to FDA approval of plazomicin in 2018.[34] Aminoglycosides are broad-spectrum antibiotics, being active against many Gram-positive and Gram-negative bacteria, but they have no inherent activity against anaerobes because active electron transport is required for their uptake.[35]

Aminoglycosides have a core of amino sugars linked via a glycosidic bond to an aminocyclitol ring (streptamine, 2-deoxystreptamine, or streptidine). The position of their amino and hydroxyl substituents influences their binding specificity to the 16S rRNA in the 30S ribosomal subunit and determines their mechanism of action.[35] Aminoglycoside uptake occurs in distinct stages. Firstly, these polycationic molecules bind electrostatically to negatively charged membrane components such

as phospholipids and LPS, displacing magnesium ions and disrupting membrane integrity. This enhances permeability and facilitates energy-dependent transport into the cytoplasm where aminoglycosides bind to the A-site of 16S rRNA. This interaction causes mRNA misreading and mistranslation, which leads to faulty proteins that integrate into the cytoplasmic membrane, further compromising permeability, disrupting transmembrane transport, and promoting increased aminoglycoside influx into the cell [36]. Some aminoglycosides also inhibit polypeptide synthesis by blocking the formation of the initiation complex or the translocation of peptidyl-tRNA.[36] Unlike bacteriostatic antibiotics that inhibit protein synthesis, aminoglycosides are bactericidal, showing concentration-dependent killing and a post-antibiotic effect (PAE), suppressing bacterial growth even after their concentration falls below the minimum inhibitory concentration (MIC) value.[35]

Macrolides and lincosamides bind to the large 50S ribosomal subunit, inhibiting translation. Macrolides are hydrophobic antibiotics that have a macrolactone ring with neutral or amino sugar groups. They inhibit peptide chain elongation by reversible binding to 23S rRNA at the peptidyl-tRNA binding region. This binding blocks the exiting channel for the nascent peptide, translocation is inhibited, and peptidyl-tRNA drop off ultimately aborts translation. Macrolides are classified according to the number carbon atoms in their lactone ring (14-, 15- and 16-member). Each subclass differs in stability, pharmacokinetics and spectrum activity. Erythromycin was the first macrolide discovered, clarithromycin and other 14-derivatives were later introduced, followed by 15-member azithromycin and 16-members (e.g. josamycin) with improved pharmacological properties. The basic structure of lincosamides consists of an amino acid derivative connected to a sugar moiety via an amide bond. Lincosamycin and clindamycin bind to the 23S rRNA in the central part of peptidyl transferase center blocking A-site tRNA positioning and thus inhibiting the peptide-bond formation in the initial phase of elongation. Both macrolides and lincosamides are bacteriostatic antibiotics, but they can exhibit bactericidal activity at high concentrations and against low bacterial inocula.[37] Macrolides are being broadly used to treat respiratory, skin and soft tissue, and sexually-transmitted infections, as well as some gastrointestinal infections.[38]

1.1.5 Interference in metabolic pathways

Some antibiotics act by disrupting metabolic pathways that are essential for bacteria. One of the best-known examples is the inhibition of folic acid synthesis in bacterial cells by sulfonamides alone or by synergistic combination with trimethoprim (cotrimoxazole).[39] Sulfonamides compete with *para*-aminobenzoic acid for the active site of the dihydropteroate synthase in the folic acid synthesis pathway. Trimethoprim binds to the dihydrofolate reductase in the next step of this metabolic pathway. Folic acid is a cofactor in the synthesis of nucleotides and some amino acids, and therefore essential in DNA replication and protein synthesis. Bacterial growth is inhibited when folate stores in cells are depleted.[39]

1.2 Mechanisms of antibiotic resistance

The diversity of mechanisms of antibiotic resistance can be summarized in few groups. Antibiotic resistance may be due to 1) inactivation or modification of the antimicrobial

agent, 2) modification of the antimicrobial binding site, 3) changes in porins, and 4) changes in active efflux pumps. Both decreased expression of porins and changes in efflux pumps may lower antibiotic concentration within the bacterial cell (Figure 5).[40]

Bacterial species have their own natural antibiotic resistance. Traditionally termed intrinsic resistance, it is due to the specific inherent mechanisms present in each species and it is predictable. Recently EUCAST replaced the term intrinsic resistance with the concepts of expected resistant and expected susceptible phenotypes.[41] Expected resistant phenotype should be used when most of the wild-type isolates (≥90%) within a bacterial species have MIC values for a specific antibiotic above the PK/PD-based resistance breakpoint, and therefore this agent should not be considered for either therapy or even clinical susceptibility testing. The definition of expected susceptible phenotype should be used when most of the isolates within a bacterial species (>99%) has MICs below or equal to the susceptible PK/PD breakpoint.

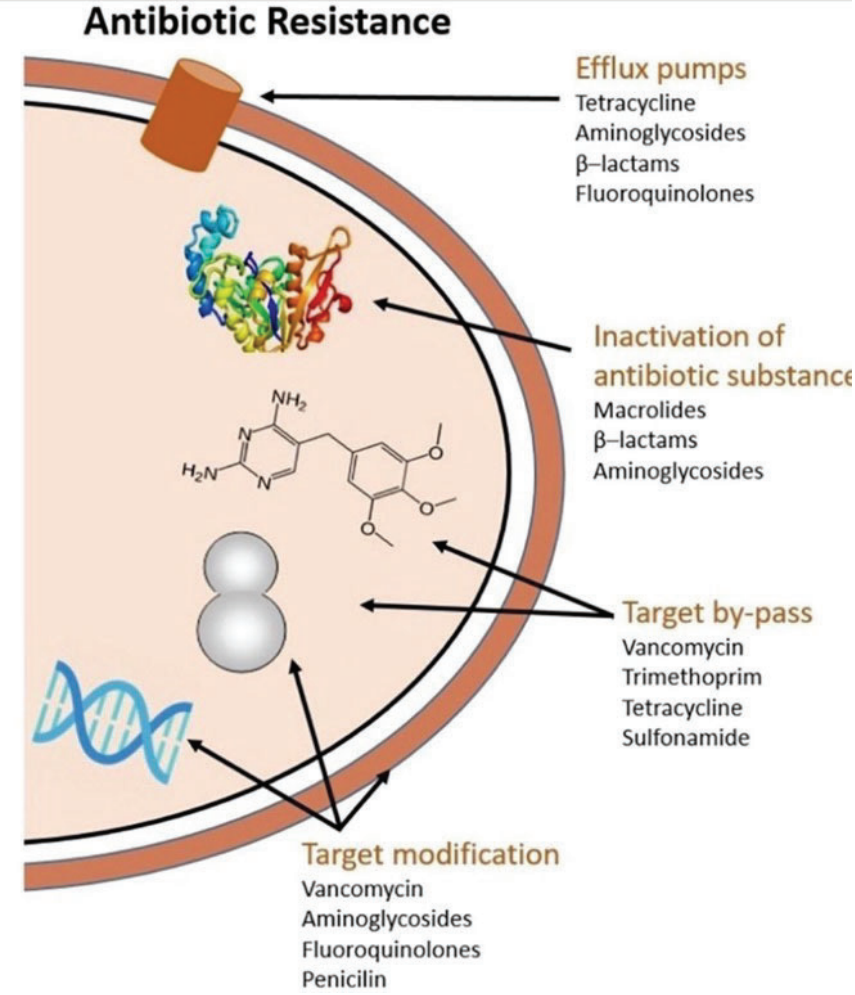

Figure 5. Mechanisms of antibiotic resistance. Modified from Uluseker C et al. 2021[17]

Acquired resistance to antimicrobials is an issue challenging the health system. AMR acquisition may occur through mutations in chromosomal genes or by HGT via plasmids or other mobile genetic elements.[42] Some bacteria may also present adaptive antibiotic resistance under certain environmental stimuli and reversion to the susceptible phenotype occurs when these stimuli disappear.[43] Additionally, biofilm formation may also contribute to resistance as it involves phenotypic changes that shield bacteria from many antibiotics.[3]

Chromosomal mutations may have an impact in genes involved in mechanisms of resistance, including membrane permeability, efflux pump regulation, antibiotic targets, or expression of antibiotic-modifying enzymes.[44,45] In the case of fluoroquinolones, mutations in the quinolone resistance-determining region (QRDR) of *gyrA* and *parC* genes encoding DNA gyrase and topoisomerase IV, respectively, reduce antibiotic binding affinity, leading to resistance.[46] In a comparable manner, resistance to β-lactams can emerge through mutations that modify PBP affinity for these antibiotics.[47]

Porins are β-barrel channel proteins that play an essential role in the passage of small molecules, facilitating the entrance of hydrophilic antibiotics like β-lactams.[48] Chromosomal mutations may cause altered expression of porins in Gram-negative bacteria. Decreased permeability can be relevant in β-lactam resistance. The decrease in porin-mediated antibiotic uptake can act synergistically with efflux pumps or other resistance mechanisms.

Efflux pumps are membrane-bound transporters that actively expel antibiotics out of the cell, lowering their intracellular concentration.[49] Many of these pumps can expel a broad range of antimicrobial compounds. Efflux pumps can be intrinsic or acquired via horizontal gene transfer. Mutations in regulatory genes can lead to their overexpression, increasing antibiotic resistance.

β-lactamases are β-lactam-hydrolyzing enzymes that can be either naturally present in bacteria or acquired through mobile genetic elements.[50] The Ambler classification is based on their molecular structure and divides β-lactamases into four classes (A, B, C, and D).[51] Classes A, C, and D have a serine residue in their active site, whereas class B enzymes are metallo-β-lactamases that require zinc for hydrolytic activity. Class A includes some narrow spectrum enzymes, many extended-spectrum β-lactamases (ESBLs) and some carbapenemases. Class C comprises AmpC cephalosporinases whereas class D includes OXA-type enzymes (oxacillinases). In contrast, class-B, metallo-β-lactamases (MBLs) are a unique group of enzymes because of their requirement for a zinc ion at the active site. The Bush-Jacoby classification (groups 1, 2 and 3) is based on their functional characteristics, namely substrate and inhibitor profiles.50 Group 1 includes serine cephalosporinases (AmpC enzymes), which are not inhibited by clavulanic acid. Group 2 is the largest and most heterogeneous category, comprising serine β-lactamases (class A and D in Ambler's classification) with different range of hydrolytic activity and inhibited by clavulanic acid. Group 3 are all MBLs, which can hydrolyze carbapenems (carbapenemases) and have poor affinity for monobactam.[52]

Other acquired enzymes, apart from β-lactamases, play a significant role in AMR by modifying antibiotics or their targets.[53] These include aminoglycoside-modifying enzymes (AMEs) such as acetyltransferases and phosphotransferases, rRNA methyltransferases

that methylate ribosomal targets and may conferring resistance to aminoglycosides or macrolides (Erm), and phosphoethanolamine transferases (*mcr* genes) that confer resistance to colistin by modifying bacterial membrane.

The definition of multidrug-resistant (MDR) microorganism was a controversial issue in the past. Experts from the European Center for Disease Control (ECDC) and Prevention (CDC) proposed an interim of definitions accepted by the international community in 2012 (Figure 6).[54] A MDR strain is defined as that strain with acquired resistance to at least one antibiotic from three or more categories of antimicrobials. An extensively resistant strain (XDR) has susceptibility to only one or two categories of antimicrobials and a pan-resistant strain (PDR) has resistance to all antimicrobial agents. This common terminology allowed to report comparable data and facilitated the exchange of information among the medical community. More recently, the term "difficult-to-treat resistance" (DTR) was introduced as a new definition for AMR in Gram-negative bacteria.[55] Antibiotics are not equally weighed in this definition in contrast to the 2012 interim proposal. DTR was defined as non-susceptibility to all first-line antibiotics, which considers high-efficacy and low-toxicity agents (namely fluoroquinolones and all β-lactams, including carbapenems).[55] However, the concept of DTR may evolve over time due to the introduction of new antibiotics, requiring further reassessment.[56]

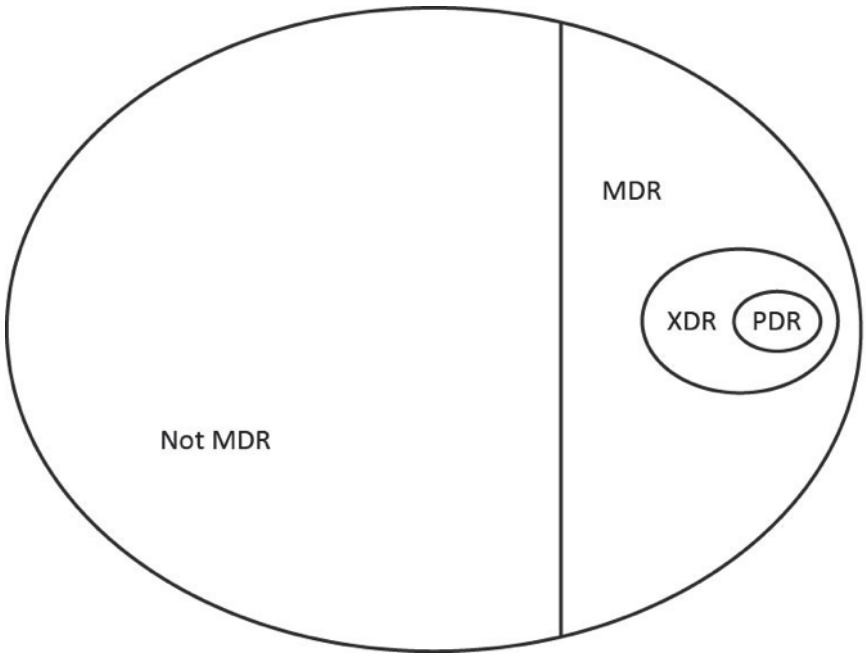

Figure 6 Population structure in terms of antibiotic resistance within a bacterial species. This diagram shows the relationship of MDR, XDR and PDR to each other[54]. MDR: multi-drug resistant, XDR: extensively drug resistant, PDR: pandrug resistant.

1.3 ESKAPE pathogens

The emergence of antibiotic resistance in bacteria involved in nosocomial infections is especially alarming because lives of critical and/or immunosuppressed patients may be compromised. In 2008, Rice was first to report as ESKAPE pathogens a group of six bacteria with the ability of evading bactericidal activity of antibiotics and usually involved in nosocomial infections.[57] The term ESKAPE was used thereafter to jointly refer to *Enterococcus faecium*, *Staphylococcus aureus*, *Klebsiella pneumoniae*, *Acinetobacter baumanni, Pseudomonas aeruginosa* and *Enterobacter* spp[58]. WHO published the first list of antibiotic-resistant priority pathogens in 2017. This list was defined according to the largest threat bacteria posed to human health, and ESKAPE pathogens were at the top.[59] The 2024 updated list includes carbapenem-resistant *A. baumanni* and MDR *Enterobacterales* in the group of critical pathogens whereas carbapenem-resistant *P. aeruginosa* and vancomycin-resistant *Enterococcus faecium* are considered as priority pathogens.[60]

The largest burden of AMR is due to the global spread of some successful AMR clones. Since the early 2010s, the term high-risk clone has been used to refer to those clones that are able to enhance AMR spread amongst different geographical locations.[61] Accordingly, high-risk clones are important reservoirs for the dissemination of AMR genetic components either by horizontal or vertical gene transmission.[62,63] High-risk clones not only possess a combination of AMR determinants and enhanced pathogenicity and/or fitness, but they are also able to colonize and persist in hosts. Some biological traits may increase their fitness, providing survival skills and edging out other isolates of the same species.[64] High-risk clones can compete against other bacteria and become the main part of a bacterial population. Initially as colonizers, they may eventually lead to infections. *P. aeruginosa* and *K. pneumoniae* are the most frequent Gram-negative bacilli associated with nosocomial infections worldwide, and MDR/XDR high-risk clones of these species are often involved.[62,65–67]

1.3.1 *Pseudomonas aeruginosa*

P. aeruginosa is a motile non-fermenting Gram-negative rod. This environmental bacterium was first described in 1882 from wound infections of soldiers whose bandages were blue and green.[68] This metabolically versatile bacterium can survive under a variety of environmental conditions, including soil, water and plants.[63] *P. aeruginosa* pangenome (~5.5-7 Mbp) encodes for many regulatory enzymes that provide this bacterium with metabolic versatility and high adaptability to environmental changes.[69] This bacterial species usually uses oxygen as the terminal electron acceptor, but it may adapt to hypoxic conditions in the environment. *P. aeruginosa* can use nitrate as the final acceptor of electrons through a process known as denitrification in anaerobic conditions.[70]

P. aeruginosa has an arsenal of virulence factors that contribute to pathogenicity by promoting bacterial adhesion, colonization, invasion of host tissues, dissemination and/or evasion of host immune response.[62] These factors are regulated by complex pathways and signaling systems that confer great plasticity to this bacterium. Some virulence factors are encoded by its core genome such as lipopolysaccharide (LPS), outer membrane proteins (OMPs) like porins, and exopolysaccharides, whereas many other factors related to pathogenicity are part of its accessory genome and may be found in pathogenicity islands.[71] Many of these factors are encoded in the core-genome,

including lipopolysaccharide (LPS), OMPs, secretion systems, exopolysaccharides (EPS) and siderophores.[71] The LPS is a component of the outer membrane of Gram-negative bacilli.[72] The LPS structure consists of three domains: lipid A (the anchor to the outer membrane), the core oligosaccharide region, and the O-polysaccharide (more distally located).[72] LPS has a key role in several biological functions, and it is a major virulence factor. It mediates interactions with host receptors and causes tissue damage due to its endotoxic activity.[73]

P. aeruginosa has different types of porins, including non-specific porins (OprF), specific and/or gated porins (OprD, OprB, OprH), and efflux porins (OprM, OprN, OprJ).[48,71] The well-characterized OprD facilitates uptake of basic amino acids and small peptides, and it is the primary channel for the entry of carbapenem antibiotics.[48,71] Other surface structures of *P. aeruginosa* are flagella and type IV pili.[74] This bacterium has a single polar flagellum with a filament made of helicoidally arranged flagellin (FliC), a cap protein (FliD), the hook at the filament base (FlgE), two filament-hook junction proteins (FlgKL), and basal body components across outer and inner membranes.[74] The flagellum is essential for swimming motility, which helps bacteria reach the surface to establish initial attachment. Flagella Type IV pili are hair-like filamentous appendages mainly composed by monomeric pilin subunits (PilA). These pili provide twitching motility and are crucial for host cell attachment. Both flagella and type IV pili also contribute to biofilm formation.[75]

Six types of secretion systems have been identified in *P. aeruginosa*.[71] These secretion systems secrete a wide variety of toxins and hydrolytic enzymes to attack the host.[74] Type 3 secretion system (T3SS) is a major virulence determinant in this bacterium. T3SS injects effector cytotoxins (ExoS, ExoU, ExoT and ExoY) into host cells, disrupting their membrane and inducing apoptosis.[71] The distribution of genes encoding these proteins is variable among strains, and their expression can significantly contribute to the pathogenic potential. ExoU is a potent phospholipase causing rapid membrane damage that may be directed against phagocytes and epithelium to promote bacterial dissemination. Therefore, ExoU has been associated with high bacterial virulence, acute infections and disease severity.[74] In contrast, ExoS is a bifunctional toxin with GTPase activating and adenosine-diphosphate-ribosyl-transferase activities. ExoS targets a wide range of cell factors and pathways, and it is more frequently associated with chronic infections.

P. aeruginosa secretes a variety of extracellular factors, including toxins, enzymes, exopolysaccharides, pigments and siderophores.[71] Secreted by type 2 secretion system (T2SS), exotoxin A is an ADP-ribosyl transferase that inhibits protein synthesis, inducing cell death and reducing the host response to infection.[75] Secreted enzymes (e.g. lipases, proteases, elastases) are involved in tissue destruction.

P. aeruginosa secretes several exopolysaccharides (alginate, Pel and Psl) that contribute to biofilm formation.[76] Alginate is the main exopolysaccharide produced by this bacterium, particularly involved in chronic infections like cystic fibrosis. Biofilm formation is a complex interplay of many genes and regulatory networks. This highly regulated process encompasses from the initial adhesion steps (type IV pili and flagella) to exopolysaccharide expression and Quorum Sensing molecules.[75] Biofilm impairs effective bacterial clearance by both inhibiting phagocytosis and hampering antibiotics treatments.[74,76,77]

P. aeruginosa produces several pigments with relevant biological properties such as iron acquisition and oxidative stress responses.[63] Pyocyanin (blue) and pyoverdine (yellow-green) are the most common pigments, whereas pyorubrin (reddish) and pyomelanin (brown) are minor pigments expressed by some strain under certain environmental conditions.[63] Pyocyanin is a T2SS-secreted redox-active phenazine with a significant role in the ecological fitness of *P. aeruginosa*.[74] Pyocyanin can generate reactive oxygen species (ROS) within host cells, which leads to oxidative stress and cell damage contributing to the severity of disease, particularly in chronic infections such as cystic fibrosis.[74]

Iron depletion during infection is an important feature in host defense.[78] Iron is essential for bacterial growth and virulence as it acts as redox catalyst in many proteins involved in oxygen and electron transport processes.[78] Secreted by bacteria to overcome this host defense mechanism, siderophores are iron-scavenging molecules that specifically chelate ferric iron (Fe^{3+}).[78] *P. aeruginosa* produces two siderophores as part of its arsenal of virulence factors, pyochelin and the fore mentioned yellow-green pigment pyoverdine.[78] Salicylate-based pyochelin has lower affinity for iron, whereas pyoverdine is the major siderophore expressed in low-iron conditions usually in acute infections. [74] Involved in iron uptake, pyoverdine is a complex fluorescent chromophore molecule that binds free Fe^{3+} with high affinity and it can also displace iron from transferrin.[78] Additionally, pyoverdine is a signal molecule for the expression of virulence factors such as exotoxin A.[78] Despite not being considered a siderophore, the redox activity of pyocyanin can also influence iron metabolism by reducing Fe^{3+} to the ferrous form (Fe^{2+}) that is more easily available for bacteria.[74]

P. aeruginosa is an opportunistic pathogen that is highly associated with nosocomial (hospital-acquired) infections[79]. This Gram-negative rod can easily be selected because of its natural resistance to many antibiotics commonly used in hospitals. This environmental bacterium can thrive in hospital settings, especially in wet areas (e.g. equipment such as nebulizers, dialysis, etc). This bacterium may also cause some community-acquired infections, usually associated with humid environments. Some examples of these community infections are folliculitis, keratitis and otitis, among others.[62] Although this environmental bacterium is not part of the normal human microbiota, once in-patients become colonized, they may also act as endogenous reservoir and further contribute to nosocomial spread.[80] *P. aeruginosa* is commonly involved in hospital-acquired pneumonia (including ventilator-associated pneumonia), urinary tract infections, bloodstream infections and surgical site infections. *P. aeruginosa* can easily invade and proliferate in nonviable tissues, becoming a major threat in patients with extensive burns.[70] It is also a major pathogen involved in chronic respiratory infections in cystic fibrosis and patients with chronic obstructive pulmonary disease.[81] Additionally, this bacterium may also be involved in some community infections, usually associated with wet environments (e.g. folliculitis, keratitis and otitis).[62]

1.3.1.1 Mechanisms of antibiotic resistance

P. aeruginosa is bestowed with a large intrinsic resistome. The expression of the chromosomally encoded resistance mechanisms is highly regulated.[82] This bacterium has natural (intrinsic) resistance to many antibiotics commonly used (e.g amoxicillin-clavulanic acid, ceftriaxone, ertapenem, tetracyclines, cotrimoxazole). This feature results in selection of this bacterium under certain antibiotic treatments.[83]

The mechanisms for natural antibiotic resistance in *P. aeruginosa* are mainly due to the low permeability of its outer membrane, expression of chromosomal enzymes and expression of efflux pumps.[48,84] This bacterium lacks large general diffusion porins and it has a limited number of porins that are highly selective, contributing to this low permeability.[48] *P. aeruginosa* has an inducible chromosomal AmpC β-lactamase with a significant role in its natural resistance to aminopenicillins (alone and combined with clavulanic acid), and to most of the older cephalosporins (including the third-generation cephalosporin cefotaxime).[82] These beta-lactam antibiotics are strong inducers of its expression and are efficiently hydrolysed by this cephalosporinase.

P. aeruginosa is armed with several efflux pumps that expulse antimicrobials and many other toxic compounds out of the bacterial cell, allowing this bacterium to adapt and succeed in different environments.[49] Known for their broad substrate specificity, the Resistance-Nodulation-Division (RND) family of efflux pumps is the most prominent in *P. aeruginosa*, being MexAB-OprM and MexXY-OprM the most relevant pumps in its natural antibiotic resistance.[82] Constitutive expression of MexAB-OprM contributes to the basal low-level resistance to most beta-lactams (except for imipenem), fluoroquinolones, tetracyclines, macrolides, chloramphenicol and sulphonamides.[82] Inducible expression of MexXY-OprM plays a role in low-level resistance to aminoglycosides and other antibiotics.[82]

Treatment of *P. aeruginosa* infections represents a therapeutic challenge due to its natural (intrinsic) resistance to many antibiotics commonly used. This characteristic contributes to the selection of this bacterium under antibiotic pressure backgrounds.[83] Additionally, *P. aeruginosa* can easily develop increased antibiotic resistance, mainly through chromosomal mutations.[85,86] Its high rate of spontaneous mutations contributes to this frequent antibiotic resistance development, especially in infections with high bacterial load such as pneumonia. The selection of a first mutation usually facilitates the subsequent selection of others, finally resulting in MDR/XDR phenotypes.[87]

Acquired resistance in *P. aeruginosa* is mainly caused by chromosomal gene mutations.[62] Chromosomal mutations can lead to the overproduction of chromosomal AmpC β-lactamase, changes in porin expression, or increased activity of efflux pumps.[71,84] Acquired carbapenem resistance often occurs through the loss or downregulation of OprD due to mutations in its structural gene, in its promoter region or in regulatory genes controlling expression.[69] The hyperexpression of efflux pumps allow bacteria to increase antimicrobial expelling.[49] Hyperexpression of efflux pumps is associated with resistance to carbapenems (excluding imipenem), to many other β-lactams, fluoroquinolones and other classes of antibiotics.MexAB-OprM is crucial for developing carbapenem resistance in *P. aeruginosa*.

Hyperproduction of the chromosomal AmpC enzyme is the most common mutation-driven mechanism of resistance to anti-pseudomonal penicillins (piperacillin), cephalosporins (ceftazidime or cefepime) and aztreonam.[88,89] Additionally, *ampC* upregulation may be driven by certain point mutations (i.e. D135N, G154R) that cause a conformational change in the transcriptional regulator AmpR.[89] Mutations leading to structural modifications of AmpC due to changes in the catalytic centre may also cause beta-lactams resistance, including the antibiotic combinations ceftolozane-tazobactam and ceftazidime-avibactam.[84,89]

P. aeruginosa can become more resistant by acquiring ARG through horizontal gene transfer and acquired β-lactamase genes (*bla* genes) are an important source of resistance.[89] Among carbapenemases, metallo-β-lactamases (mainly VIM, IMP, and NDM) have been frequently reported in *P. aeruginosa* clinical strains.[90] Amynoglucoside-modifying enzymes are also commonly acquired AMR determinants in *P. aeruginosa*.[91]

1.3.1.2 Pseudomonas aeruginosa high-risk clones

The population structure of this environmental bacterium is considered non-clonal.[92] However, some clonal lineages in *P. aeruginosa* are associated with multidrug resistance, increased virulence and the ability to cause nosocomial outbreaks. These MDR/XDR high-risk clones are predominantly associated with hospital infections and their worldwide spread has become a public health issue due to limited therapeutics options (Figure 7). Recently the following top ten high-risk lineages were listed in order of relevance according to their prevalence, their global spread, and their association with MDR/XDR/DTR profiles and acquired β-lactamases: ST235, ST111, ST233, ST244, ST357, ST308, ST175, ST277, ST654, and ST298.[89] Their virulence profile based on the presence of genes coding T3SS exotoxins ExoS and/or ExoU was also included.[89] Of these lineages, ST235, ST111 and ST175 are the most common high-risk clones in Europe.[62]

ST235 is the most relevant and widespread high-risk clone.[62] With an overwhelming presence of horizontally acquired determinants, this clone has been associated with over 60 acquired β-lactamases, including class A and class B carbapenemases.[62] ST235 has a hypervirulent phenotype associated with high mortality, in part due to the production of ExoU cytotoxin.[62,93] ST111 is the second most widespread high-risk clone after ST235, and it is found in Europe, Asia, and America.[62,93] Different β-lactamases have been associated with this clone, with VIM-2 being the most prevalent carbapenemase.[62]

ST175 is prevalent high-risk clone in Europe, especially in France and Spain.[62] A recent nation-wide five-year study showed that ST175 is still the predominant lineage in Spain but there has been a significant increase in ST235.[94] The MDR/XDR resistance profile of ST175 is mainly due to a combination of mutations leading to the inactivation of the OprD porin, hyperproduction of chromosomal beta-lactamase AmpC, and overexpression of efflux-pumps.[95] The characteristic beta-lactam mutational resistome of ST175 includes AmpR (G154R) mutation that causes AmpC hyperproduction, and the specific OprD (Q142X) mutation.[89] MexZ (G195E) mutation that leads to MexXY overexpression, and three QRDR mutations (GyrA T83I, D87N and ParC S87W) are also present. Occasionally acquired beta-lactamases like carbapenemases VIM and GES have also been found in this lineage.[89]

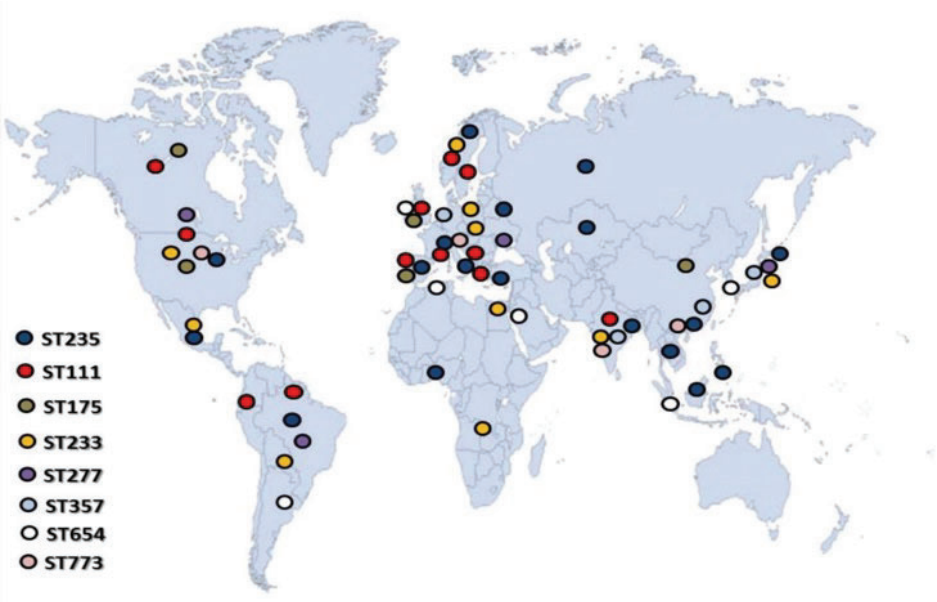

Figure 7 Geographic dissemination of the most frequently reported international high-risk clones of *P. aeruginosa*. Figure illustrates reported cases until 2020[96].

The capacity to cause severe infections and higher mortality in acute infections varies among the different *P. aeruginosa* high-risk clones.[96] The most virulent high-risk clone is the ST235 while ST175 seems to be less virulent. These high-risk clones were found to be defective in the three types of motilities and pigment (pyoverdine and pyocyanin) production. They also showed reduced fitness in vitro, elevated spontaneous mutant frequencies, and enhanced biofilm growth.[84] Associated with specific combinations of virulence factors, these differences have been particularly linked to the presence of either *exoU* or *exoS*.[75,97] As previously mentioned, ST235 is a virulent lineage that produces the potent cytotoxin ExoU. In contrast, ST111 and ST175 commonly produce ExoS.[75] However, ST175 has lower cytotoxicity, and it is less virulent than ST111, probably because the latter has other relevant factors contributing to its virulence.[89] Additionally, these three lineages were found to be defective in motility and pigment production compared to non-MDR clones, but they have enhanced biofilm growth and higher frequencies of spontaneous mutation.[84]

1.3.2 *Klebsiella pneumoniae*

K. pneumoniae is a non-motile Gram-negative rod first isolated and described by Carl Friedlander from a patient with pneumonia in 1882.[98] This non-fastidious aerobic and facultative anaerobic bacterium is included in the order *Enterobacterales* and the family *Enterobacteriaceae*.[99] *K. pneumoniae* ferments lactose and it has a distinctive mucoid phenotype when growing on agar plates due to the production of polysaccharide capsule.[72]

K. pneumoniae inhabits the gastrointestinal tract of healthy humans and animals.[58,100] *K. pneumoniae* is the second most frequent enterobacteria involved in opportunistic healthcare-associated infections after *E. coli*, including urinary tract infection, pneumonia, bacteremia, and wound site infections.[101,102] The ability of this organism to spread rapidly often leads to nosocomial outbreaks. Outside hospital settings, some strains are involved in community-acquired infections such as pyogenic liver abscess.

K. pneumoniae genomes (~5–6 Mbp in size) encode ~5,000–6,000 genes. Of these, approximately 1,700 are core genes preserved in all members of this species, whereas the remainder are accessory genes that are variably present.[103] *K. pneumoniae* clones can be distinguished from one another based on their accessory genome, which includes, among others, genes encoding acquired virulence factors and antimicrobial resistance determinants.

All *K. pneumoniae* strains have a subset of core genes that code for basic pathogenicity factors required to establish opportunistic infections in mammalian hosts.[103] Some of these virulence factors are adhesins, the variable capsular polysaccharide, lipopolysaccharide (LPS) and the siderophore enterobactin.[103,104] Adhesins are essential for mucosal colonization, which is an initial step that may lead later to infection. *K. pneumoniae* genome encodes for different types of fimbriae that promote bacterial adhesion to both epithelial cells and abiotic surfaces. The most well-characterized adhesins are type 1 and type 3 pili, encoded by *fim* and *mrkABCD* clusters, respectively.[105]

Capsule polysaccharide (K antigen) and LPS (O antigen) are the two major bacterial surface components that significantly contribute to *K. pneumoniae* pathogenesis. The diversity in these two antigens has been linked to the severity of disease in some cases. As previously mentioned, LPS is comprised of the O antigenic polysaccharide, the core oligosaccharide and lipid A. Modifications in the lipid A hamper recognition and binding to the Toll-like receptor 4 (TLR4) of host cells, contributing to immune system evasion.[106] The O-antigen provides resistance to complement-mediated killing and phagocytosis.[107] The main determinants of the O antigenic polysaccharide are located at the O locus (previously known as the *rfb* locus). Ten O-antigen have been serologically described in *K. pneumoniae* but some isolates are non-typeable, and 12 different O-loci have been identified.[108] O1 and O2 serogroups are the most common.

A distinctive feature in *K. pneumoniae* is its encapsulated morphology. Capsule polysaccharide is an important virulence factor that gives protection from serum factors and phagocytosis.[109] Genes involved in capsular polysaccharide synthesis (CPS) are found in a locus adjacent to O locus.[110] The CPS locus has a mosaic structure, with a group of six conserved genes at 5' (*galF, orf2, wzi, wza, wzb,* and *wzc*). Additionally, a set of highly diverse genes that encode the capsule-specific sugar synthesis are variably present.[108,111] Using the traditional K-typing, 79 capsular serotypes with diverse clinical implications and geographical distribution have been described.[112] Currently genotyping methods based on specific gene sequencing (e.g *wzi*) are used to determine capsular types in *K. pneumoniae*, which has led to the identification of 134 K-loci.[108,111] Recently an alternative typing approach based on Fourier transform infrared spectroscopy (FT-IR) has been proposed to cover the gaps between K serotyping and genotyping in this species.[113]

The ability to form biofilms is an important virulence trait in *K. pneumoniae*.[114] Several factors contribute to biofilm formation in this species, including fimbriae, the polysaccharide capsule, iron metabolism and quorum sensing, among others.[110,114,115]

The presence of siderophores is essential in *K. pneumoniae* virulence given the role of iron uptake in bacterial growth during infection.[110] Four types of iron-chelating systems have been found in this bacterial species, including the forementioned core siderophore enterobactin (Ent), and three accessory siderophores: yersiniabactin, salmochelin, and aerobactin (encoded *by ybt, iuc* and *iro*, respectively).[103,110] The expression and contribution of each siderophore to virulence vary, and additionally they are irregularly distributed in *K. pneumoniae* clones.[107] Present in all isolates, Ent is required for growth in most niches, but its iron-scavenging function is disrupted when bound by host lipocalin 2 secreted by neutrophils and epithelial cells. Salmochelin is an acquired glycosylated Ent that evades this binding while remaining active in iron scavenging. Aerobactin and yersiniabactin are not bound by lipocalin either but they have lower affinity for iron.[103]

K. pneumoniae strains are classified into three pathotypes according to their accessory genome: opportunistic, MDR and hypervirulent (hvKp).[116] First described in Taiwan in 1980s, hvKp was isolated mainly from pyogenic liver abscesses in the early reports.[117] While opportunistic strains cause infections in patients with predisposing factors, hvKp strains have been related to community-acquired, aggressive, and metastatic infections in immunocompetent patients.[118,119] A combination of several determinants of virulence is required to achieve this hypervirulent pathotype. Its main feature is a hypermucoviscosus phenotype that is commonly detected using the string test.[120] Although hvKp is mainly associated with capsular serotypes K1 and K2, other serotypes (e.g K28, K47, K63) have also been recently involved. Infections caused by hypervirulent K. pneumoniae are dominated by the same subset of lineages.[103] K1 serotype is strongly associated with ST23 whereas several other clones such as ST380 and ST375, may present K2 serotype and have been associated with hvKp strains.

The hypermucoviscosus phenotype in *K. pneumoniae* is developed by the expression of the mucoviscosity associated gene *magA* and gene *rmpA* enconding the regulator of the mucoid phenotype. An additional genetic marker is *iucABCD* operon that encodes aerobactin, a highly prevalent siderophore among hvKp. Enhanced siderophore activity has been demonstrated in hvKp strains compared to non-virulent strains.[103] Another distinctive feature of hvKp isolates used to be their antibiotic susceptibility but there are recent reports about hvKP combining virulence and resistance genes on mobile genetic elements.[121] Given the changing epidemiology in these strains, the European Centre for Disease Prevention and Control recently issued a warning about the increase in hypervirulent carbapenem-resistant *K. pneumoniae*.[122]

1.3.2.1 Mechanisms of antibiotic resistance

K. pneumoniae is naturally resistant to amino-penicillins and carboxy-penicillins. This resistance is due to its chromosomal penicillinase SHV-1, which is a short-spectrum class A β-lactamase and therefore inhibited by clavulanic acid.[123,124] Hyperproduction of this chromosomal enzyme may cause some degree of ceftazidime resistance, which might be misidentified with an ESBL due to presence of synergy with clavulanic acid.[123–125]

K. pneumoniae contributes to the dissemination of antimicrobial resistance genes from the environment to clinical settings.[123] Many clinical strains have become highly resistant to antibiotics mainly due to horizontal acquisition of antibiotic resistance determinants especially through large self-conjugating plasmids.[126]

Resistance to β-lactams in *K. pneumoniae* is mainly mediated by the acquired β-lactamases. Among these enzymes, class-A extended-spectrum β-lactamases (ESBL) are the most common cause of third-generation cephalosporin resistance in this species.[52,127] These enzymes confer resistance to penicillins, cephalosporins and monobactams but strains remain susceptible to carbapenems. The first ESBLs in *K. pneumoniae* were reported in the early 1980s and they were derivatives of the TEM-1, TEM-2 and SHV-1 enzymes.[128] In the late years of that decade a new ESBL family was detected and named CTX-M because these enzymes conferred resistance predominantly to cefotaxime rather than ceftazidime.[128]

The global spread of CTX-M ESBLs throughout the present century led to an increase in the use of carbapenems.[129] More recently, the emergence and spread of carbapenemases in this nosocomial pathogen has become a major challenge worldwide.[103] Serin-β-lactamases with carbapenem-hydrolyzing activity include class-A enzymes such as *K. pneumoniae* carbapenemase (KPC) and some class-D β-lactamases like OXA-48. The most prevalent MBLs in this bacterium are Verona integron-borne metallo-β-lactamase (VIM) and New Delhi metallo-β-lactamase (NDM).[100,123] However, carbapenemases show different geographical distribution trends.[130] The highest burden of carbapenem-resistant *K. pneumoniae* in Europe is found in some southern countries, especially in Greece where KPC is the main problem.[131] Originated in Turkey, OXA-48 is widespread in the Mediterranean area, and it is the most prevalent carbapenemase in Spain.[129] Currently strains harboring several acquired β-lactamases are commonly isolated worldwide, and the most frequent combination in our geographical area is CTX-M ESBL plus OXA-48 carbapenemase.[129,132]

Both modification of permeability and efflux pumps may also contribute to the acquisition of β-lactam resistance in *K. pneumoniae*. OmpK35 and OmpK36 porins are critical for the entry of β-lactam antibiotics. Another common mechanism in *K. pneumoniae* is the overexpression of active efflux pumps like AcrAB-TolC and oxqAB.[133]

Co-resistance to β-lactams and other antibiotic families is frequent in *K. pneumoniae*, drastically reducing the range of effective antibiotics.[126] Resembling other Gram-negative bacilli, the main resistance mechanism against aminoglycosides in this species is the acquisition of modifying enzymes (AMEs) with activities such as acetylation, adenylation or phosphorylation (*aac, aad* and *aph* genes).[100] In contrast to AMEs, plasmid-mediated 16S rRNA methyltransferases (ArmA, NpmA and Rmt) confer resistance to almost all aminoglycosides. Chromosomal mechanisms for aminoglycoside resistance in *K. pneumoniae* include alterations in AcrAB-TolC and KpnEF efflux pumps.[100]

Fluoroquinolone resistance is mainly due to point mutations in the quinolone resistance determining region (QRDR) of the genes that code for DNA gyrase (*gyrA* and *gyrB*) and topoisomerase IV (*parC* and *parE*).[133] The first target for quinolone resistance is *gyrA* followed by *parC*. Several simultaneous mutations in these genes contribute to high level resistance. Altered permeability and increased expression of efflux pumps

are also involved in quinolone resistance.[133] Additionally, quinolone resistance may be horizontally acquired, including Qnr proteins involved in target protection, some efflux pumps like OqxAB and QepA, and the aminoglycoside acetyltransferase AAC(6′)-Ib-cr that causes quinolone modification.[134] These plasmid-mediated mechanisms of quinolone resistance have frequently been associated with ESBLs, mainly in IncF-like plasmids.

Colistin-resistance in *K. pneumoniae* emerged soon after the recovery of polymyxins to treat infections caused by XDR carbapenemase-producing isolates.[100] Colistin-resistance may emerge during treatments with this last-line drug due to chromosomal mutations in the LPS modification system. These mutations usually involve one of the two-component regulator systems (PhoP-PhoQ, PmrA-PmrB or CrrAB), or inactivation of the regulator MgrB.[135] Since the first report on plasmid-mediated colistin resistance, several mcr genes encoding phosphoethanolamine transferases that modify lipid A have been detected worldwide in different bacterial species including *K. pneumoniae* but they remain predominant in *Escherichia coi*.[100,135]

1.3.2.2 High-risk clones

K. pneumoniae has a clonal population structure where some global MDR high-risk clones are predominant in hospital settings.[134] Among them, the clonal group (CG) CG258, which includes sequence types (ST) ST258, ST11 and ST512, stands out for being predominantly associated with nosocomial outbreaks.[100] Most CG258 members are XDR due to their multiple ARGs and are noteworthy for their contribution to the global dissemination of CTX-M ESBL and several types of carbapenemases.[100] Whole-genome sequencing revealed the linkage between KPC and the spread of ST258.[100] Other global MDR high-risk clones that contribute to the global expansion of resistance are CG15, CG17, CG37, CG101, and the emerging CG147 and CG307.[64,100] ST307 has begun to displace ST258 and ST512 among CR-KP in America and southern Europe and has become the dominant CR-KP lineage in South Africa.[64]

Carbapenemase OXA-48 is highly preponderant in *Enterobacterales* in Spain.[136] A catalan study showed that *K. pneumoniae* ST405 clone, usually carrying also CTX-M enzyme, played a major role in these high rates of OXA-48.[132] Changing epidemiological trends of CR-KP lineages in Spain have been recently reported, going from the predominance of ST11/OXA-48 and ST405/OXA-48 to the interregional spread of ST307/OXA-48 and ST512/KPC-3.[136]

1.3.3 *Enterococcus faecium*

Enterococcus spp are Gram-positive catalase-negative cocci that occur in pairs or short chains. Enterococci are facultative anaerobes with homofermentative metabolism.[72] They are considered lactic acid bacteria because their metabolism results in the production of lactic acid as a major product of glucose fermentation. Enterococci are commonly found as commensals of the human and animal gastrointestinal tracts, but they can also survive in the environment.[137] Enterococci often act as opportunistic pathogen in humans, being *Enterococcus faecalis* predominantly involved followed by *Enterococcus faecium*.

E. faecium is one of the six ESKAPE pathogens frequently involved in nosocomial infections.[57] This bacterium usually infects the urinary tract, the biliary tract, surgical site

wounds, and bloodstream. *E. faecium* may cause endocarditis and infections related to catheters and other implanted medical devices, and it is often involved in polymicrobial infections (i.e. pelvic infections and intra-abdominal infections).[138]

The genome size of *E. faecium* (2.7-3.2 Mb) varies among strains. This bacterial species has great genomic plasticity and high versatility to easily adapt to different niches. Pathogenicity islands (PAIs) are large chromosomal genetic elements that are horizontally transmitted. Located in specific genomic regions, some PAI play a key role in bacterial survival when environmental conditions are limiting.[139]

E. faecium specific healthcare-associated lineages have acquired a broad range of virulence factors that contribute to its pathogenicity by promoting colonization, tissue invasion, adhesion to inanimate surfaces and survival under stressful conditions. These factors include bacterial cell surface molecules (including capsule), stress response proteins, transport systems and specific gene regulators.[140,141] Virulence factors associated with tissue colonization are enterococcal surface protein (Esp), endocarditis- and biofilm-associated pili (Ebp), collagen-binding adhesin (Acm) and *E. faecium* antigen A (Afm). Cytolysin and gelatinase contribute to tissue invasion.[142]

E. faecium has natural resistance to a broad range of common antibiotics (e.g, cephalosporins, aminoglycosides, clindamycin, and trimethoprim-sulfamethoxazole).[138] Ampicillin resistance is an acquired trait in *E. faecium*, but it has become prevalent in clinical isolates due to clonal spread, especially in healthcare settings. Ampicillin resistance is mainly due to mutations in pbp5 gene or hyperproduction of PBP5, which has low affinity for beta-lactams.[143,144] This bacterium may acquire further antibiotic resistance by different mechanisms.

The acquisition of multiple antimicrobial resistance in *E. faecium* has been associated to some specific clonal complexes (CC) such as CC17, which is strongly involved with hospital outbreaks and invasive infections.[137] Characterized by ampicillin-resistance, CC17 has become a global high-risk clone, contributing to the spread of this antibiotic resistance. More recently horizontal acquisition of vancomycin resistance (VanA and VanB) has complicated the management and outcomes of *E. faecium* infections in many clinical settings.[145]

1.4 Antibiotic susceptibility testing

Antibiotic susceptibility testing (AST) of microorganisms is essentially performed to guide antimicrobial treatments. Beyond this use, AST results have several other applications in healthcare. AST results are useful for epidemiological surveillance by monitoring the prevalence and spread of AMR within populations. Infection control relies on AST results, and so does antimicrobial stewardship. Guidelines for empirical antimicrobial therapy are usually settled based on local epidemiological data.

The Clinical and Laboratory Standards Institute (CLSI) and the European Committee on Antimicrobial Susceptibility Testing (EUCAST) are the two main organizations that provide standard methods and guidelines for AST to ensure reliable and consistent results across different laboratories.[146] The CLSI Subcommittee on AST is an American

volunteer-led, multidisciplinary consensus body that has been publishing AST standards used internationally for over five decades.[147] EUCAST is an international AST committee founded in 1997 with the initial goal of harmonizing European breakpoints.[148] Currently EUCAST guidelines have been adopted by all countries in Europe and in other parts of the world.[149]

As previously mentioned, AST results are the basis for the selection of the most appropriate therapeutic option to treat bacterial infections.[150] AST can be performed by either conventional phenotypic methods or by genotypic methods (Figure 8). Phenotypic methods can predict antimicrobial susceptibility and resistance, whereas genotypic methods predict resistance only.[151]

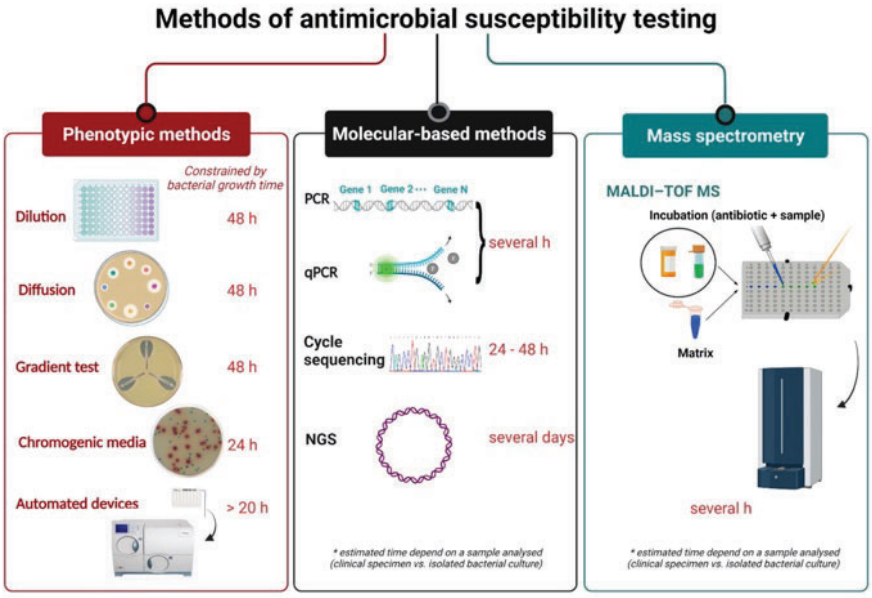

Figure 8. Current methods for antimicrobial susceptibility testing and turnaround time. PCR—polymerase chain reaction. qPCR—quantitative polymerase chain reaction. NGS—next-generation sequencing. MALDI-TOF MS—matrix-assisted laser desorption/ionization time-of-flight mass spectrometry.[150]

Conventional AST relies on phenotypic methods and assesses the bacterial response to antimicrobial agents, predicting susceptibility and resistance. AST results are usually obtained after an incubation of 18-24h. These culture-dependent techniques are the most used in clinical routine despite the delay of results. In contrast, molecular techniques entail a culture-independent AST approach with a shorter turnaround (circa 1-6h).[146] Based on the detection of specific ARG, molecular AST techniques can only predict resistance.[152] These molecular methods are expensive and can overestimate resistance as the detection of an ARG does not imply that it will always be expressed and lead to phenotypical resistance. Currently the combination of both genotypic and phenotypic methods is commonly used for AST in most Clinical Microbiology laboratories.

1.4.1 Phenotypic AST

The basis of all antibiotic susceptibility testing is the MIC, which corresponds to the lowest antibiotic concentration that inhibits the growth of the studied pathogen. Commonly known as antibiogram, phenotypical AST can be performed by either quantitative or semiquantitative methods.

1.4.2 Quantitative methods

AST quantitative methods determine the antibiotic MIC value. Antibiotic concentrations are usually tested at two-fold dilutions and expressed in micrograms per milliliter (µg /mL) or milligrams per liter (mg/L). The range of concentrations tested depends on the antimicrobial agent, the pathogen, and the site of infection.[152] This range should encompass those concentrations that define the clinical breakpoints used to categorize AST results.[153] AST quantitative methods include dilution testing and gradient diffusion.

Dilution testing can be performed either in liquid (broth) or on solid media (agar). Broth AST methods (microdilution and macrodilution) use two-fold dilutions of antibiotics in liquid medium-containing tubes that are later inoculated with a standardized bacterial suspension of 1–5×105 CFU/mL.[153] Broth microdilution (BMD) is currently considered the international reference standard AST.[153,154] BMD is usually performed using a dilution volume of 0.1mL in 96-well disposable plastic plates. BMD may be either in-house prepared, or most frequently performed using commercial panels that include dried antibiotic dilutions. Regarding macrodilution, this method is performed in test tubes usually containing a minimum dilution volume of 2mL. In contrast to broth dilution testing, agar dilution involves preparing agar plates with different antibiotic concentrations, followed by the application of a standardized bacterial inoculum onto the agar surface.[155]

Gradient diffusion is a quantitative technique based on the use of commercially prepared strips containing a range of antibiotic concentrations.[156] These plastic or high-quality paper strips are applied onto the agar plates previously inoculated with a standardized bacterial suspension and the antibiotic diffuses gradually on the agar. After overnight incubation, the MIC is determined by the intersection of the lower part of growth inhibition area with the printed gradient scale strip.[156]

1.4.3 Disk diffusion - semiquantitative method

The Kirby-Bauer Method, also known as disk diffusion, is the oldest AST and one of the most frequently used.[154] Both CLSI and EUCAST have similar standard methods for disk diffusion although they differ in the antibiotic content of disks and breakpoints and the media used for fastidious bacteria.[153] Disk diffusion is performed by applying antibiotic-containing disks onto an agar plate previously inoculated with a standardized bacterial suspension of 1–2 x 10^8 CFU/mL (McFarland 0.5 standard).[154] Once the disk is placed onto the surface, the antimicrobial agent diffuses through the agar. The pathogen grows except in the areas where the antibiotic inhibits its growth, resulting in zones of inhibition around each active drug. Disk diffusion does not allow to determine antimicrobial MICs but CLSI and EUCAST provide standardized charts that inversely correlate the inhibition zone diameters to MIC values. The diameter of the bacterial inhibition zone (measured in millimeters) is proportional to the antimicrobial susceptibility and it can be categorized following the breakpoint guidelines established by these committees.[152]

1.5 Therapeutic options against MDR bacteria

Optimization of the different strategies to combat MDR microorganisms is essential given the current limited therapeutic options. One of these strategies relies on the deployment of new antibiotics but the pharmaceutical pipeline has a slow turnaround for these drugs. This bottleneck is caused not only by scientific and technical challenges, but also due to regulatory and economic issues.[157] Although some new antibiotics have been recently commercialized (e.g. ceftazidime/avibactam, cefiderocol, etc), the arsenal of new antibiotics is still insufficient in the current scenario where infections due to pan-resistant isolates occur more and more often.

Another strategy against MDR bacteria relies on the reintroduction of old antibiotics that had been previously replaced by more effective and/or less toxic ones. This was the case of colistin use in human medicine.[23] Due to its high toxicity, this antibiotic had been put aside from the clinical practice when cephalosporines were introduced. Currently considered a last-resort antibiotic, colistin was reintroduced in the early 2000s due to the increase in MDR Gram-negative bacilli and the scarcity of new antibiotics to treat infections caused by these bacteria.[23] Given their ototoxicity and nephrotoxicity, the use of aminoglycosides also declined in parallel with the introduction of safer antibiotic classes.[158] However, a resurgent interest in this antibiotic class has emerged as MDR bacteria have spread worldwide. Moreover, aminoglycosides are recommended as part of combination therapy for empiric treatment of some difficult-to-treat infections.[158]

Combining antibiotics to obtain a synergistic effect has become another cornerstone strategy against MDR bacteria. Synergy refers to a more significant effect of the antibiotic combination than the sum of the individual effects.[155] Antibiotic combinations aim to improve outcomes by enhancing efficacy while potentially reducing antibiotic dosage and minimizing side effects.[159] The selection of an appropriate antibiotic, dose, and route of administration as well as potential associations with the other antibiotic are critical to achieve good clinical outcomes and reduce the risk of resistance and toxicity.[160]

Combinations may enhance bactericidal activity by targeting different resistance mechanisms. Early empirical combination treatment with two antibiotics of different mechanisms of action has been associated with better outcomes compared with monotherapy in bacterial septic shock.[161] Many reports support the practice of combining antibiotics, especially in patients with high risk of MDR Gram-negative bacilli.[162,163] Alternative therapies include the use of bacteriophages, antimicrobial peptides, nanoparticles, adjuvants and photodynamic light therapy.[3,164,165]

1.5.1 *In vitro* evaluation of antibiotic combinations

Different methods have been used to assess the activity of antibiotic combinations *in vitro* to predict synergy *in vivo*.[155] The microtiter checkerboard assay is a static microdilution method that evaluates antibiotic combinations in a grid pattern where different concentrations of the two drugs are tested.[155] Alternatively, a broth macrodilution method may also be used. Synergy between two antibiotics can also be detected using disk diffusion or by intersecting gradient diffusion strips.

Time-kill curves analyze bacterial death in the presence of fixed concentrations of antibiotic in relation to time.[155] A standardized inoculum is added to flasks with broth

supplemented with various concentrations of an antimicrobial agent and to a flask without the agent. An aliquot from each flask is taken at the beginning and several other times throughout the experiment, and the numbers of colony forming units (CFU) are determined by performing serial dilution and bacterial colony counts. This technique allows the analysis of each antibiotic alone as well as their combination to evaluate possible synergies.

The whole performance of time-kill curves to evaluate antibiotic combinations is a laborious technique. The turnaround in 24-hour time-kill experiments is about two days as results are usually obtained by viable cell counting.[155] All these technical issues have relegated time-kill curves mainly to research studies but a faster and less demanding methodology than the classical plate count method could make it easier for clinical laboratories to perform occasionally this type of studies.

Based on the results obtained in time-kill curves, more advanced PK/PD dynamic techniques can be performed to evaluate antibiotic combinations *in vitro*. These techniques include the one-compartment chemostat and the two-compartment Hollow fiber infection model.[166] These complex models are continuous culture systems with a controlled environment to evaluate bacterial growth and antibiotic efficacy over time. The Hollow fiber infection model simulates changes in antibiotic concentration over time as they would happen *in vivo*.[166]

1.5.2 Alternative methods for the evaluation of antibiotic combinations

Some bioluminescence-based methods used for bacterial quantification could be used as alternative means for the evaluation of antibiotic combinations. These methods correlate cell viability with metabolic activity by measuring nicotinamide adenine dinucleotide (NAD) or adenosine triphosphate (ATP). Detection of either of these molecules indicates the presence of living organisms.[167]

The bioluminescence-based ATP testing was described in 1968 by Chappelle *et al.*[168] Luminometers allow the quantification of bioluminescence produced by luciferase and relate it to the number of viable cells (Figure 9). The increase in bioluminescence is directly proportional to the amount of ATP, which in turn correlates with the living organisms present in the sample. These systems are widely used, especially in industry and in healthcare settings, to evaluate the effectiveness of cleaning and/or sterilization processes.[169–171] The potential use of this technique to evaluate antibiotic activity has been also reported.[170,172,173] These authors used the ATP assay to study the bactericidal effect of antibiotics. However, the pharmacodynamic parameter of synergy has not been determined before using this technique in time-kill curves. The present thesis aimed to assess the role of this ATP assay as a surrogate for traditional cell counting in time-kill experiments to evaluate antibiotic combinations. This methodology may offer the possibility of quick and high-throughput assessment of antibiotic combinations in Clinical Microbiology laboratories.

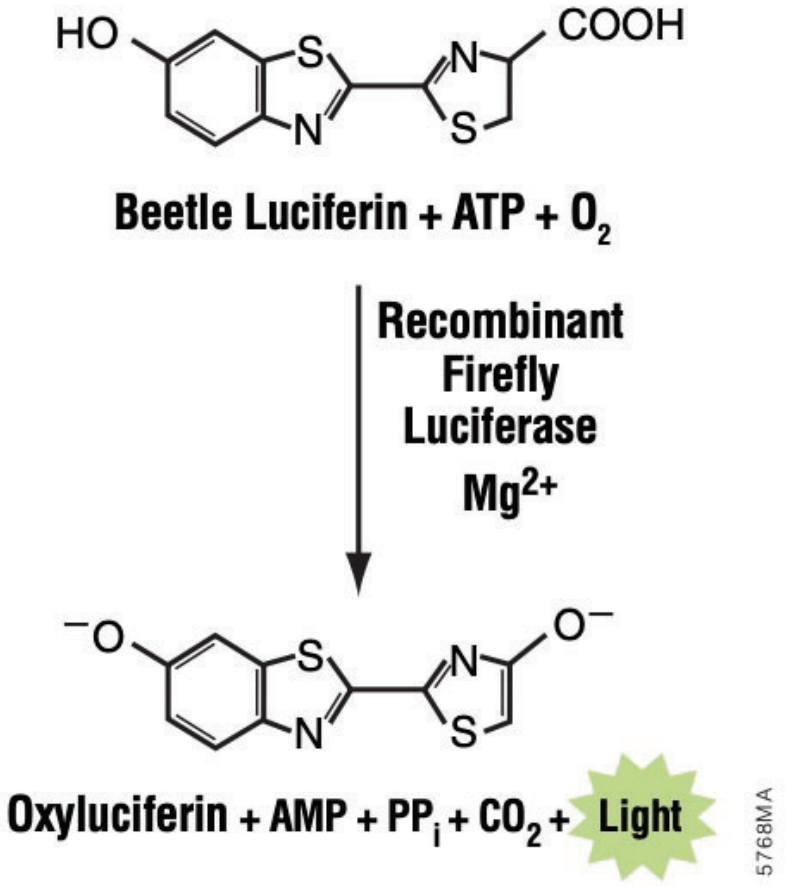

Figure 9. The luciferase reaction. Mono-oxygenation of luciferin is catalyzed by luciferase in the presence of Mg2+, ATP and molecular oxygen.[174]

1.6 Amikacin and meropenem in combination against *Klebsiella pneumoniae*

The acquisition of carbapenemases has complicated treatments of infections caused by *K. pneumoniae*. Currently new antibiotics like cefiderocol and newer β-lactam/β-lactamase inhibitors (BLBLI) such as ceftazidime/avibactam have improved the guided treatment options in CP-KP infections.[175] However, not long ago, the rise in infections caused by carbapenemase-producing isolates, coupled with the lack of effective antibiotics, led to the widespread use of antibiotic combinations aimed at achieving synergy. In this context, early empirical combined therapy with two antibiotics with different mechanism of action was associated with superior outcomes compared with monotherapy in septic shock.[161] The retrospective study INCREMENT also showed that combined antibiotic therapy was associated to improved survival in bloodstream infections caused by carbapenemase-producing *Enterobacterales* in patients with high mortality score risk.[175]

A common antibiotic combination was a β-lactam plus an aminoglycoside such as amikacin.[161] Aminoglycosides gained clinical interest with the emergence of MDR Gram-negative bacilli.[176,177] Aminoglycosides have been reported to bind to lipopolysaccharides and therefore disrupt the outer membrane. This permeabilizing effect may enhance the periplasmic target site penetration of β-lactam antibiotics such as meropenem.[178] The AMINOLACTAM study showed that including an aminoglycoside to the initial empirical antibiotic therapy with a broad-spectrum β-lactam significantly improved the outcome for Gram-negative bloodstream infections in haematological neutropenic patients.[179] The combination of meropenem and amikacin has been previously shown to be effective against some carbapenemase-producing *K. pneumoniae* (CP-KP) not only *in vitro* but also in murine models.[180] This antibiotic combination has been empirically used when a MDR Gram-negative infection is suspected.[181,182] However, the current guidelines of the Infectious Diseases Society of America (IDSA) do not recommend the use of carbapenems once a carbapenemase-carrying isolate is confirmed.[181] The European Society of Clinical Microbiology and Infectious Diseases (ESCMID) recommends avoiding carbapenem-based combination therapy for CRE infections unless the meropenem MIC is ≤ 8 mg/L. In such cases, high-dose extended-infusion meropenem may be considered as part of combination therapy, but only if the newer BLBLIs cannot be used.[183]

Both the choice of antibiotic and ensuring appropriate exposure at the site of infection are paramount in empirical treatments. The route of antibiotic administration and the dosing schedule may have an impact on clinical outcomes, especially in critically ill patients. The combination of meropenem plus amikacin is still commonly used for empirical treatment in patients with risk of severe infections by MDR Gram-negative bacilli although the newer BLBLI are currently preferred when available.[183,184] A recent systematic review analysed the evidence on the optimal duration of aminoglycoside therapy in combined regimens with β-lactam.[185] They concluded that a short duration of no more than 3 days should be used with β-lactam combinations, particularly in initial empirical treatments, and suggested that most of the synergistic bacterial killing in these combined regimens occurred during the initial phase of therapy. However, the timing of the first dose of amikacin in relation to the empirical administration of meropenem has never been defined in protocols or guidelines. The aminoglycoside may be given either together with the first dose of the β-lactam or in a staggered manner. The aim of the second part of this thesis was to evaluate the *in vitro* effect of these different dosing schedules of the meropenem/amikacin combination on the initial bacterial burden of selected CP-KP isolates and determine their impact in initial empirical treatments.

02

Hypothesis and objectives

2. Hypothesis and objectives

2.1 Hypothesis

The increase in antibiotic resistance has emerged as a global public health issue. Treating infections caused by multidrug-resistant (MDR) bacteria has become a clinical challenge. Combining antibiotics is one of the current strategies in the treatment of infections caused by MDR pathogens.

Antibiotic combinations can be evaluated by time-kill curves. The conventional colony count method in these experiments is laborious, which hampers their implementation in the routine of a clinical laboratory. The ATP bioluminescent measurement assay has already been used for quantification of viable bacteria in other biotechnological fields. This ATP assay may be useful for the evaluation of antibiotic combinations against Gram-positive and Gram-negative bacteria. Faster than the conventional colony count, this method would facilitate the implementation of time-kill studies to determine bactericidal effect and synergy of antibiotic combinations in clinical laboratories.

The combination of meropenem and amikacin has been empirically used against infections caused by Gram-negative bacilli, including extensively drug-resistant microorganism (XDR) *P. aeruginosa* and carbapenemase-producing *Klebsiella pneumoniae* (CP-KP). Regimens and dosages of this empirical antibiotic combination may be optimized

to achieve a better clinical outcome. The dosing schedule in the administration of amikacin and meropenem, either simultaneously or staggered, may influence the initial reduction of the bacterial load. In this study, the effect of dosage, combinations, and the administration schedule of amikacin and meropenem were analysed.

2.2 Objectives

1. To standardize the ATP assay to be further used in time-kill experiments. Standardization will be performed in two Gram-negative species *(Pseudomonas aeruginosa* and *Klebsiella pneumoniae*), and one Gram-positive species (*Enterococcus faecium*).

2. To evaluate the ATP assay as an alternative method for quantifying viable cells in time-kill experiments, in comparison to the conventional colony count technique, and using various antibiotic combinations against the two Gram-negative bacilli. Cut-off points for synergy and bactericidal effect will be determined using the ATP assay, with values equivalent to those obtained using the conventional method.

3. To assess the impact of simultaneous and staggered dosing regimens of the meropenem-amikacin combination on the initial bacterial load reduction in XDR *P. aeruginosa* and CP-KP, employing time-kill curves.

03
Materials and methods

3. Materials and Methods

3.1 Bacteria

Two Gram-negative bacterial species were used: *P. aeruginosa* and *K. pneumoniae*. *E. faecium* ATCC 19434 was also included in the luminometer standardization (section 3.7.3). Bacterial strains were preserved in a medium supplemented with 20% glycerol (Maim) at -80°C.

Twelve clinical isolates of XDR *P. aeruginosa* were selected. Additionally, Psd2209 isolate was included as a non-XDR control (amikacin-susceptible and susceptible increased exposure to meropenem). These clinical isolates had been collected from multicentric study that included nine Spanish hospitals.[182] They had been previously characterized at a phenotypical and molecular level Table 1.

Five carbapenemase-producing *K. pneumoniae* (CP-KP) clinical isolates (K1, K4, K10, K13 and K14) with different antimicrobial resistance profiles were selected. These clinical isolates had been previously isolated and characterized in *Laboratori de Referència de Catalunya* (El Prat de Llobregat, Barcelona) (Table 2). *K. pneumoniae* ATCC BAA-1706 was included as a bla_{KPC}-negative strain.

P. aeruginosa ISOLATE	ST	MECHANISMS OF RESISTANCE
10-009	**111**	VIM-2, AmpC hyperproduction, OprD deficiency
07-016	**175**	GES-5, OprD deficiency
10-023	**175**	AmpC hyperproduction, OprD deficiency
12-012	**175**	VIM-20, OXA-2, OprD deficiency, AacA4, AadA13, AadB
06-014	**179**	OXA-10, AmpC hyperproduction, OprD deficiency
07-004	**235**	GES-19, OXA-2, OprD deficiency, Aac(6')-33
12-003	**244**	AmpC hyperproduction, OprD deficiency
01-008	**253**	VIM-1, OprD deficiency, AadA1, AacC1
09-011	**274**	AmpC hyperproduction, OprD deficiency
10-019	**2221**	AmpC hyperproduction, OprD deficiency
10-021	**2533**	AmpC hyperproduction, OprD deficiency
06-025	**2534**	AmpC hyperproduction, OprD deficiency
06-027	**2535**	AmpC hyperproduction
06-001	**2536**	AmpC hyperproduction, OprD deficiency

Table 1. *Pseudomonas aeruginosa* isolates. The name of the isolate, the corresponding sequence type (ST) and the mechanisms of resistance are shown. Verona integron-encoded metallo-β-lactamases (VIM-1, VIM-2, VIM-20), oxacillinases (OXA-2, OXA-10), extended-spectrum β-lactamases (GES-5, GES-19), AmpC hyperproduction and porin deficency (OprD). Adapted from Oliver A. *et a.l*[62]

K. pneumoniae ISOLATE	MECHANISMS OF RESISTANCE
KP1	KPC
KP4	NDM-1, OXA-48
KP10	KPC
KP13	OXA-48, ESBL
K14	OXA-48, ESBL

Table 2. Mechanisms of resistance of *Klebsiella pneumoniae* clinical isolates. The phenotypic and/or genotypic characterization of these mechanisms of resistance was performed at the *Laboratori de Referència de Catalunya.* Klebsiella pneumoniae carbapenemase (KPC), New Delhi metallo- β -lactamase (NDM-1), OXA β -lactamases 48 (OXA-48) and extended-spectrum β -lactamase (ESBL).

3.2 Culture media

The solid culture media used were Columbia blood agar (COS) and Mueller-Hinton Agar (MH) (both from bioMérieux), and Trypticase Soy Agar Modified broth (TSA II) (Becton Dickinson). COS is a rich culture medium supplemented with 5% sheep blood. COS plates were used to routinely culture the isolates. MH is a non-selective nutrient culture medium that is mainly used for antimicrobial susceptibility testing. MH plates were used for the quantification of CFU/mL in time-kill curves. Trypticase Soy Agar Modified broth (TSA II) (Becton-Dickinson) was used for heteroresistance analysis. TSA II broth was prepared by dissolving 40 g TSA II in 1L of distilled water. This medium was sterilized in an autoclave (Matachana) at 121°C for 10 minutes.

Cation-adjusted Mueller-Hinton (CA-MH) broth (Becton-Dickinson) was the liquid culture medium used to perform time-kill curves. CA-MH broth is usually used in quantitative procedures for AST of rapidly growing aerobic and facultatively anaerobic bacteria. CA-MH broth is supplemented with divalent cations (Mg^{+2} and Ca^{+2}) according to the concentrations recommended by CLSI.[146] This medium was prepared by adding 22g CA-MH in 1L of distilled water; it was sterilized in the autoclave at 121°C for 10 minutes.

3.3 Antibiotics

The antibiotics used for the time-kill curve experiments were meropenem, aztreonam, colistin and amikacin (all from SIGMA-Aldrich®), and ceftolozane/tazobactam (Zerbaxa®, MSD). The antibiotic concentrations corresponded to the area under the concentration-time curve from 0 to 24 hours (AUC_{24}); the equivalent clinical dose is included in Table 3. Additional concentrations of 40 mg/L amikacin and 32 mg/L meropenem were also tested. The experimental design is detailed in section 3.8.

ANTIBIOTIC	CLINICAL DOSE	AUC_{24} (mg*h/L)	FLASK CONCENTRATION (mg/L)
Meropenem	2g q8H	425	17.71
Aztreonam	2g q8H	1050	43.75
Ceftolozane/tazobactam	3g q8H	912/150	36 / 6.25
Colistin	4.5UI q12H	50	2.08
Amikacin	1g q24H	196	8.17

Table 3. Concentration of the antipseudomonal antibiotics used in time-kill curves. Area under the concentration-time curve from 0 to 24 hours (AUC_{24}) concentrations and their equivalent clinical doses. IU: international units.

3.3.1 Preparation of the antibiotic stock

Antibiotic stocks were prepared according to Clinical and Laboratory Standards Institute (CLSI) using their correspondent solvent and dissolvent (Table 4).[146] The pharmacological characteristics of these antibiotics were obtained from the manufacturer and the support of the Pharmacy Department of Hospital del Mar (Barcelona). The product and batch numbers, solvent/dissolvent, molecular weight, water percentage and purity were obtained from the analytical certificate of each antibiotic batch. Based on these data, the power of each antibiotic was calculated through the formula:[186]

$$\%\ \text{Potency} = (\text{purity}) \cdot (1 - \text{water content}) \cdot (\text{active fraction})$$

Antibiotic stocks were prepared at a concentration of 2mg/mL, further aliquoted and preserved at -40°C. Stocks were prepared from the pure substance except for ceftolozane/tazobactam, for which clinical vials of Zerbaxa® (MSD) were used. The potency-weight ratio range accepted to commercialize a clinic vial is 95-105% in Europe and 90-110% in the US.[187] Minimum inhibitory concentrations (MIC) of each antibiotic (and for every new batch) were assessed in *E. coli* ATCC 25922 to have an internal quality control.

Pure substance required for each antibiotic stock was calculated through the following formula:[146]

$$\text{ATB (mg)} = (\text{total volume needed}) \cdot \left(\text{stock concentration } \frac{\text{mg}}{\text{ml}}\right) \cdot \frac{1}{\text{antibiotic power}}$$

	MEROPENEM	AZTREONAM	COLISTIN	AMIKACIN
SOLVENT	Water	Saturated solution sodium carbonate	Water	Water
DISSOLVENT	Water	Water	Water	Water
PRESERVATION OF PURE SUBSTANCE (°C)	2-8	-30	2-8	2-8

Table 4. Characteristics of the pure antibiotics used in the time kill curves.

3.4 Antibiotic susceptibility testing

Antibiotic susceptibility testing (AST) was performed to determine the antibiotic susceptibility profile of the studied isolates. AST was routinary accomplished by microdilution using MicroScan panels in a WalkAway system (Beckman Coulter). MIC values correspond to the lowest antibiotic concentration that inhibits growth of a given bacterial isolate. AST results were categorized following the 2023 clinical breakpoints from EUCAST.[188] The mechanisms of resistance were phenotypically characterized according to EUCAST guidelines.[176] Carbapenemase production was detected using immunochromatography CARBA (NG Biotech) and when necessary, molecularly confirmed by PCR using LightCycler® 480 II (Roche).

MIC values of amikacin and meropenem were further confirmed by broth microdilution following the recommendations of CLSI.[146] The broth microdilution procedure was performed as follows:

1. Plate preparation: 96-well plates were prepared with two-fold dilutions of meropenem or amikacin (ranging from 0.25 to 128 mg/L). Antibiotic dilutions were prepared from the stock using CA-MH; 90µL of each antibiotic dilution were added to the corresponding well. Sterility and growth controls were included in all plates.

2. Inoculum preparation: Isolates were cultured on COS plates at 37ºC for 18-24h. A bacterial suspension of 4-5x10^6 CFU/mL was prepared by diluting 0.4 mL of a 0.5 McFarland turbidity standard (10^8 CFU/mL) in 12.5 mL of CA-MH. From each starter culture, 10µL were inoculated into the corresponding wells. Inoculated plates were incubated 24h at 37°C.

3. Control of the inoculum: A control of the inoculated bacterial suspension was performed. Ten-fold dilutions of the samples were prepared using normal isotonic saline solution (B. BRAUN). 100µL of each dilution were inoculated onto MH plates and incubated at 37°C for 18-24h. CFU were counted after an overnight (O/N) incubation. Only plates with 30-300 colonies were considered.

3.5 Amikacin heteroresistance

Amikacin heteroresistance refers to a phenomenon where a bacterial isolate contains an isogenic subpopulation that exhibits lower susceptibility to amikacin compared to the main population.[189] These subpopulations with reduced susceptibility may selectively be amplified during amikacin exposure. Heteroresistance was assessed using the Population Analysis Profile (PAP), which is considered the gold standard method for its detection.[190] Amikacin heteroresistance was studied in *P. aeruginosa* isolates with MIC≤16 mg/L (Table 1). The PAP procedure was as follows:

1. Plates preparation:
Six-well plates (Thermo Scientific) were prepared with double-serial dilutions of amikacin ranging from 4-128 mg/L in TSA II agar. Each amikacin concentration was studied in duplicate. The preparation of the plates was performed in a biosafety cabinet class II (Thermo Scientific). Plates were left to dry and stored in the refrigerator until use. The concentrations tested were chosen according to the MIC values for each isolate (Table 3).

2. Inoculum preparation and inoculation:

- A starter culture using 30 mL of CA-MH broth was performed from an O/N culture on COS plate.
- The starter culture was incubated in a water bath shaker (Precision SWB-27, Thermo Scientific) at 37°C for 90 min to achieve early exponential growth.
- A normalized 0.5 McFarland turbidity standard bacterial suspension (108 CFU/mL) was prepared from this starter culture.
- Tenfold serial dilutions of the bacterial suspension were performed and 50 µL were inoculated to each well.
- Additional tenfold dilutions of the bacterial suspension were plated onto agar plates without antibiotics.
- Plates were incubated at 37°C for 48h.

3. Heteroresistance analysis:
The PAP value was calculated as the ratio of the CFU/mL on the plate with the highest amikacin concentration in relation to the control plate.[190]

$$\text{PAP value} = \frac{\text{(CFU on the antibiotic plate·Dilution factor)}}{\text{(CFU on the control plate·Dilution factor)}}$$

An isolate was considered heteroresistant to amikacin when the following two parameters were fulfilled: a) the subpopulation was at least four-fold above the MIC value of the isolate, and b) the PAP value was $\geq 10^{-7}$.

3.6 Time-kill curves

Time-kill curves allow the assessment of the activity of a fixed concentration of an antibiotic or a combination of antibiotics against a bacterial strain over time.[155] The performance of 24-hour time-kill curves was analyzed in parallel using the conventional

colony-count of viable cells and the ATP quantification method. The procedure for time-kill assays was as follows (Figure 11):[155]

1. Inoculum preparation:

- Bacterial isolates were grown in 30 mL CA-MH broth aerobically in a water bath shaker (Precision SWB-27, Thermo Scientific) at 37°C for 18-24h.
- A starter culture was prepared by inoculating the overnight (O/N) culture (1/30 inoculum and 30 mL CA-MH broth). This starter culture was incubated in a water bath shaker at 37°C for 90 minutes to achieve early exponential growth and the bacterial density required as starting inoculum.
- The starter culture was diluted with CA-MH according to the absorbance at 630 nm. The magnitudes of absorbance ranged from 0.2 to 0.4. The final bacterial inoculum was approximately 6 to 7 $\log_{10}$ CFU/mL per flask.[191]

2. Time-kill curve procedure:

Each erlenmeyer flask contained 30mL of CA-MH and it was supplemented with either one single antibiotic or an antibiotic combination (section 3.8). Each experiment included a flask without antibiotics as growth control. These flasks were inoculated with the corresponding volume of bacterial culture previously calculated to start the experiment with 10^6 CFU/mL.

- Erlenmeyer flasks were incubated in the water bath shaker at 37°C for 24h.
- Aliquots (1mL) were collected from each flask at different culture times.
- These aliquots were centrifugated (Centrifuge-5424, Eppendorf) to eliminate antibiotic from the medium.
- Supernatants were discarded and bacterial cells were resuspended with the same volume of neutral saline solution (NSS).

These aliquots were used to quantify viable cells. Each aliquot was analyzed in parallel using two methods: 1) conventional viable cell count (CFU/mL), and 2) ATP measurement assay (RLU/mL) (3.6.1 and 3.7.2, respectively).

3.6.1 Conventional viable cell count

The conventional viable cell count was performed by the colony-forming unit count method (CFU/mL) as follows:

- Decimal dilutions of aliquots were performed using NSS.
- 200 µL of each dilution were inoculated onto MH plates and incubated at 37°C for 18-24h.
- CFU were counted after an O/N incubation. Only plates with 30 to 300 colonies were considered.

3.6.2 Established pharmacodynamic parameters

Pharmacodynamic parameters are important for understanding the relationship between drug concentration and its therapeutic effect.[192] These parameters are essential for optimizing drug therapy, predicting clinical outcomes and minimizing adverse effects. These parameters are used to design drug regimens.

The pharmacodynamic parameters evaluated in our time-kill experiments were the bactericidal effect of antibiotics and synergy of antibiotic combinations. Bactericidal

effect is defined as a reduction of ≥3 log CFU/mL at 24h from the start of the time-kill curves.[155] Synergy is defined as a reduction of ≥2 log CFU/mL in the combination condition at 24h compared to the antibiotic condition with higher bactericidal effect on monotherapy at 24h.[193]

3.7 ATP quantification technique by bioluminescence (RLU/mL)

The ATP quantification technique was performed using the BacTiter-Glo™ Microbial Cell Viability Assay kit (Promega) and the GloMax®[96] Microplate Luminometer (Promega). This bioluminescent assay allows the quantification of viable cells by measuring ATP.[194] Following the lysis of bacterial cells, free ATP reacts with the Ultra-Glo Recombinant Luciferase enzyme, which induces a luminescent signal proportional to the quantity of viable cells. The luminometer results are given in relative light units (RLU).

The ATP quantification technique was evaluated as an alternative to the colony-count method in time-kill curves where antibiotic combinations were tested against XDR *P. aeruginosa* and CP-KP isolates. The validation of this system was performed in parallel with the conventional viable cell count (section 3.6.1).

3.7.1 Reagent preparation

BacTiter-Glo™ Microbial Cell Viability Assay kit has two separate components: BacTiter-Glo Substrate and BacTiter-Glo™ Buffer. Both were preserved at -20°C.

The BacTiter-Glo™ Reagent was obtained by transferring 10mL of BacTiter-Glo™ Buffer into the amber bottle containing BacTiter-GloTM Substrate to reconstitute the lyophilized enzyme/substrate mixture. This reagent was preserved at -20°C or at 4°C for 4 days maximum (Figure 10). Both components and the reagent were preserved from light. This reagent was left at room temperature for 15 minutes to temperate prior to its use.

3.7.2 ATP measurement

ATP measurement was performed using 96 opaque-walled multi-well plates (Costar). Each sample from time-kill curves was measured in triplicate, and samples from the linearity assay were measured five times. Each assay included background medium controls: three wells in time-kill curves and five wells in the linearity study.

The procedure was as follows:

- Addition of 100 µL sample per well.
- 100 µL BacTiter-Glo™ Reagent (equilibrated at room temperature) were added to each well. The content was briefly mixed.
- The opaque-walled plate was incubated at 37°C for 5 minutes.
- The plate was placed then into the luminometer at 1 second integration time. Bioluminescence results (RLU) were recorded.

Strict control of light and temperature was required during the preparation and measurement of bioluminescence.[174] The reagent and the plate were protected from light. NSS and CA-MH used as background controls were kept at 37°C so that temperature did not interfere with reading of RLU results.

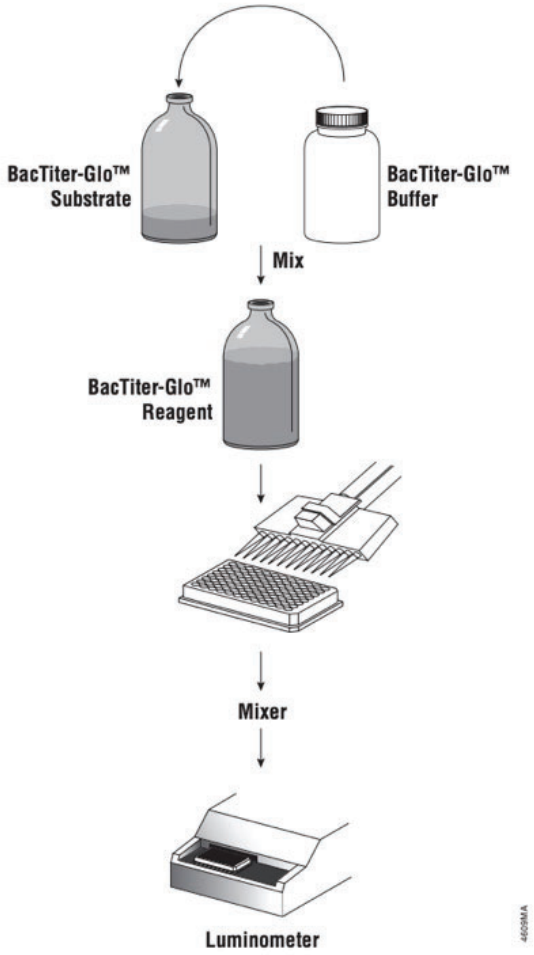

Figure 10. Diagram of the BacTiter-Glo™ Microbial Cell Viability Assay protocol.[174]

3.7.3 Luminometer standardization

The standardization of a laboratory new technique is paramount to ensure reliability, reproducibility and validity of clinical research and medical diagnostics. The standardization of this ATP quantification assay was required prior to its evaluation as an alternative to the colony-count method in time-kill curves. Background, linearity and limit of detection were analyzed for standardization of the luminometer for the evaluation of antibiotic combinations.

3.7.3.1 Background

Background refers to any signal detected by the luminometer not caused by the presence of microorganisms. The background was determined to control any significant oscillation.

Two different reading backgrounds were tested (CA-MH broth and NSS). Data used for this calculation was collected from the linearity assays (section 3.7.3.2); these

corresponded to the values obtained with CA-MH broth and NSS alone. Average and standard deviation (SD) were calculated.

3.7.3.2 Linearity

Linearity corresponded to the correlation between the bioluminescence signal (RLU/mL) and CFU/mL. This parameter was calculated at different time points (0, 8, and 24 hours) using the following strains: *P. aeruginosa* ST175 (10-023), *K. pneumoniae* ATCC BAA-1705 and *E. faecium* ATCC 19434. The procedure was performed as follows:

- The bacterial isolates were grown in 30 mL CA-MH broth aerobically in a water bath shaker at 37°C for 18-24h.
- A starter culture was obtained from the O/N culture, using a 1/30 inoculum and 30 mL CA-MH broth. This starter culture was incubated in a water bath shaker at 37°C for 90 minutes to achieve an early exponential growth and the density required as starting inoculum.
- Decimal dilutions of the bacterial culture were performed in CA-MH.
- Two 1mL-alliquot of each dilution were obtained to test the two different backgrounds (CA-MH and NSS).
- For NSS background, one aliquot was centrifugated at 5,000 rpm for 5 minutes. The supernatant was discarded, and bacterial cells were resuspended with 1 mL NSS. This step was performed twice to follow the same procedure as in time-kill assays.
- For CA-MH background, there were no additional steps prior to reading.

Each aliquot was analyzed in parallel using both the luminometer (five readings) and performing cultures onto MH plates in duplicate for the colony count method (section 3.8).

3.7.3.3 Limit of detection

The limit of detection is the smallest quantity of microorganisms that can be reliably detected by the luminometer. This limit was calculated from the linearity assay (section 3.7.3.2) using the following formula:[195]

Limit of detection = background average + 3 (background standard deviation)

3.7.4 Diagnostic performance

The diagnostic performance of a test is its ability to correctly categorize the analyzed samples. Cut-off points are used for this categorization. These correspond to established threshold values that allow the discrimination between positive and negative results.[196]

Sensitivity and specificity are the two basic parameters used to define the diagnostic performance of a test. Sensitivity determines the probability that a positive sample will yield a positive result, quantifying the ability to avoid false negative results. Specificity measures the probability that a negative sample yields a negative result, quantifying the ability to avoid false positives. Both parameters can be adjusted through the modification of the cut-off points depending on the aim and application of the test.

The diagnostic performance of the ATP assay was aimed to evaluate the effect of antibiotic combinations in time-kill curves. The bactericidal effect and synergy were

determined using the conventional colony-count method as the gold standard (sections 3.6.1 and 3.6.2).

3.7.4.1 Determination of the ATP-measurement assay cut-off points

There were no established cut-off points for synergy and bactericidal effect in RLU/mL. Receiver Operating Characteristic (ROC) curves and Youden Test were performed with Stata version 15 to establish these cut-off points.

The Youden index (sensibility + specificity – 1) is defined for all the points of a ROC curve.[196] All the cut-off points maximizers of Youden index were chosen. The unweighted accuracy (UA) of cut-off values was calculated using the following formula:[169]

$$UA = \frac{\text{sensitivity+specificity}}{2}$$

3.7.5 Comparative study: colony count method *versus* ATP assay

The comparative study between the conventional colony count method and the ATP assay included: 1) a correlation study of the growth curves, and 2) the establishment of the pharmacodynamic parameters.

The correlation between CFU and RLU along the 24-hour growth curves was studied with the values from the *P. aeruginosa* and *K. pneumoniae* growth controls (without antibiotic). A Shapiro-Wilk test for normal data was performed prior to calculating the Pearson correlation coefficient and the intraclass correlation coefficient (ICC), with Stata version 15. The pharmacodynamic parameters analyzed and compared between techniques were bactericidal effect and synergy (section 3.6.2).

3.8 Experimental design

The experimental design of the studies included in this thesis are shown below. These studies include the evaluation of the ATP assay as a tool for antibiotic combination analysis, and the evaluation of different dosing schedules of the empirical combination meropenem plus amikacin against CP-KP in time-kill curves.

3.8.1 Evaluation of the ATP measurement assay for antibiotic combination studies

The aim of the study was to validate the ATP assay GloMax 96 microplate (Promega) (section 3.7) as an alternative to the conventional colony count method (section 3.6.1) in studies of antibiotic combinations. Standardization of this assay was previously performed by determining the background, linearity, and the detection limit. These determinations were done for one strain of *P. aeruginosa*, *K. pneumoniae* and *E. faecium* (section 3.1)

Twenty-four-hour time-kill curves (section 3.6) were performed in parallel by both methods with 12 selected XDR *P. aeruginosa* clinical isolates and five CP-KP clinical isolates of *K. pneumoniae*. *K. pneumoniae* isolates corresponded to K1, K4, K10, K13 and K14. The antibiotics used against *P. aeruginosa* were meropenem, aztreonam, colistin, and amikacin and ceftolozane-tazobactam. The antibiotic concentrations used corresponded to the AUC serum levels (Table 3): meropenem 2 g every 8h (q8h) with an area under the concentration-time curve for 24 h (AUC24) of 425mg*h/L, aztreonam 2 g

q8h with an AUC_{24} of 1,050 mg*h/mL, ceftolozane/tazobactam 3g q8h with an AUC_{24} of 912/50[197], colistin, 4.5 MIU (million International units) q12h with an AUC_{24} of 50mg*h/L, and amikacin, 1 g q24h with an AUC_{24} of 196mg*h/L. The antibiotics used against *K. pneumoniae* were amikacin and meropenem. The final concentrations used are shown in section 3.8.

ANTIBIOTICS COMBINATIONS
Amikacin + meropenem
Aztreonam + ceftolozane/tazobactam
Aztreonam + amikacina
Aztreonam + colistin
Aztreonam + meropenem
Aztreonam + ceftolozane/tazobactam + colistin
Aztreonam + meropenem + colistin
Ceftolozane/tazobactam + colistin
Ceftolozane/tazobactam + amikacin
Ceftolozane/tazobactam + meropenem
Colistin + meropenem
Ceftolozane/tazobactam + colistin + meropenem

Table 5. Combinations of antipseudomonal antibiotics tested in time-kill curves. The antibiotic concentrations were amikacin (8.17 mg/L), aztreonam (43.75mg/L), colistin (2.08 mg/L), ceftolozane/tazobactam (38/6.25 mg/L), and meropenem (17.71 mg/L).

P. aeruginosa samples were collected at different times (0, 8, and 24 h) and centrifuged at 5,000 rpm for 5 min. After the supernatants were discarded, bacterial cells were resuspended twice with saline solution to eliminate the antibiotic from the medium. *K. pneumoniae* samples were collected at 0, 2, 4, 8 and 24h. Sampling collection time points for *K. pneumoniae* differed from those for *P. aeruginosa* due to the experimental design of the optimization of the dosing schedules (section 3.8). For this bacterial species, elimination of antibiotic from the medium was optimized by centrifuging at 14,000 rpm for 3min in and resuspending the bacterial cells only once. All samples were analyzed in parallel using two methods: 1) conventional viable cell count (CFU / mL) (section 3.6.1) and 2) the ATP measurement assay (RLU/mL) (section 3.7).

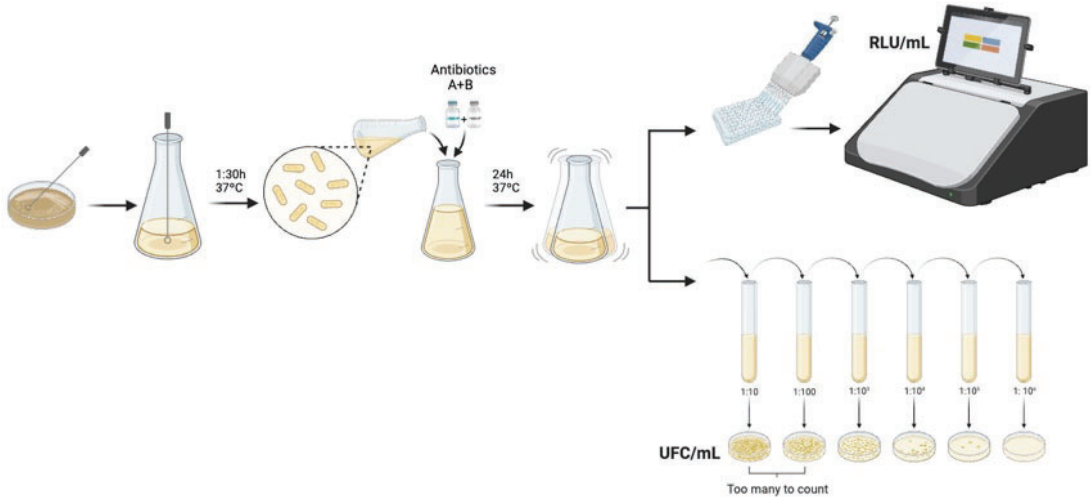

Figure 11. Time-kill curves procedure. Created with Biorender.com.

The cut-off points for synergy and for bactericidal effect were determined to categorize the results of antibiotic combinations in time-kill curves by using this ATP assay. These parameters were determined in *P. aeruginosa* and *K. pneumoniae* (section 3.7.4.1)

3.8.2 Optimization of amikacin plus meropenem dosing schedules

This study aimed to assess the optimal timing of amikacin (AK) when combined with meropenem (MEM) against XDR *P. aeruginosa* and CP-KP isolates by using time-kill curves. These experiments in *P. aeruginosa* were performed in seven clinical isolates [ST175 (12-012), ST179 (06-014), ST235 (07-004), ST244 (12-003), ST253 (01-008), ST274 (09-011), ST2536 (06-011)] and five clinical CP-KP isolates [K1, K4, K10, K13, and K14] (section 3.1). *K. pneumoniae* ATCC BAA-1706 (bla_{KPC}-negative strain) and a *P. aeruginosa* non-XDR isolate (Psd2209) were included as control.

Different dosing schedules of AK and MEM were tested against the previously mentioned Gram-negative isolates by 24-hour time-kill curves. The experimental conditions and different dosing schedules tested are shown in Table 6 . The concentrations for AK

and MEM corresponded to AK8 (8.17 mg/L) and MEM17 (17.71 mg/L). A higher dose of meropenem [MEM32 (32 mg/L)] was also assessed on all CP-KP isolates and four *P. aeruginosa* isolates [ST175 (12-012), ST179 (06-014), ST235 (07-004) and ST244 (12-003)]. A higher concentration of amikacin [AK40 (40 mg/L)] was evaluated against 1) *P. aeruginosa* ST179 (06-014), ST235 (07-004), ST253 (01-008), ST274 (09-011) and ST2536 (06-001), and 2) two high-level amikacin-resistant isolates (K1 and K4).

EXPERIMENTAL CONDITIONS	
AK8	MEM17 + AK8
AK40	MEM17 + AK40
MEM17	MEM32 + AK8
MEM32	MEM32 + AK40
AK8 + MEM17	AK8 = MEM17
AK8 + MEM32	AK8 = MEM32
AK40 + MEM17	AK40 = MEM17
AK40 + MEM32	AK40 = MEM32

Table 6. Experimental conditions used in time-kill curves. The different dosing schedules of amikacin (AK) and meropenem (MEM) are shown. The antibiotics were administered simultaneously (AK=MEM) and staggered. For staggered schedules, amikacin was added 2h after meropenem (MEM+AK) or conversely (AK+MEM). The antibiotic concentrations were MEM17=17.71mg/L and AK8=8.17mg/L. MEM32=32mg/L was added to test a concentration near the toxicity limit. A high AK concentration (AK40=40mg/L) was also tested in K1 and K4 to simulate the peak concentration.

The procedure was as follows:

Simultaneous schedules (AK=MEM) included both antibiotics at the start of the curve. In staggered schedules the second antibiotic was added two hours after the first antibiotic: AK after meropenem (MEM+AK) or conversely (AK+MEM).

- Samples (1mL) were collected at different times (0, 2, 4, 8 and 24h) and centrifuged at 14,000 rpm for 3 min.
- Supernatants were discarded and bacterial cells were resuspended with saline solution to eliminate the antibiotic from the medium.
- The viable cell count (logCFU/mL) was analyzed at each collection time. The initial bacterial load reduction was evaluated for each dosing schedule.

3.8.2.1 Analysis of antibiotic degradation

Antibiotic degradation throughout the curves was analyzed by measuring antibiotic levels at the end of the curve. Antibiotics levels were assessed by High Performance Liquid Chromatography (HPLC) by the Pharmacy service of Hospital del Mar.

The relevance of antibiotic degradation in the optimization of dosing schedules was also evaluated by refreshment experiments. These time-kill curves with medium and antibiotic refreshment were performed in two *P. aeruginosa* isolates [ST179 (06-014) and ST235 (07-001)]. The step of refreshment was performed at 12h as follows:

- The content of each flask was centrifuged at 8,000 rpm for 8 minutes.
- The supernatant was discarded, and the pellets were resuspended with CA-MH supplemented with the corresponding initial antibiotic concentration.
- Flasks were re-incubated in the bath shaker at 37°C up to 24h.
- Aliquots (1 mL) were collected from each flask at 12, 14, 16 and 24h. An additional 500 µL aliquot was taken from each experimental condition to determine meropenem levels by HPLC.

04
Results

4. Results

4.1 Antibiotic susceptibility testing (AST)

The antibiotic susceptibility profile of the K. pneumoniae clinical isolates obtained in our hospital was performed by automatized microdilution. The MIC values of meropenem and amikacin were further confirmed for both *P. aeruginosa* and *K. pneumoniae* isolates prior to the performance of the time-kill curves. The results are shown in Table 7 and Table 8. All XDR *P. aeruginosa* isolates from the multicentric study were categorized as resistant to meropenem; three of them were resistant to amikacin. All CP-KP isolates were resistant to meropenem except for K10, which was susceptible, increased exposure. Three *K. pneumoniae* isolates (K1, K4 and K10) were amikacin resistant.

***P. aeruginosa* ISOLATE**	**AMIKACIN MIC (mg/L)**	**AMIKACIN SC**	**MEROPENEM MIC (mg/L)**	**MEROPENEM SC**
Psd2209	1	S	8	**I**
ST175 (12-012)	32	R	64	**R**
ST179 (06-014)	16	S	32	**R**
ST235 (07-004)	128	R	32	**R**
ST244 (12-003)	16	S	32	**R**
ST253 (01-008)	16	S	>256	**R**
ST274 (09-011)	128	R	32	**R**
ST2536 (06-011)	8	S	32	**R**

Table 7. Amikacin and meropenem susceptibility profile of the Pseudomonas aeruginosa strains. Minimum inhibitory concentration (MIC) is expressed in mg/L. EUCAST clinical breakpoints (2024) were used. Susceptibility testing categorization (SC): R (Resistant), I (Susceptible, increased exposure) and S (Susceptible).

	K1		K4		K10		K13		K14	
	MIC	**SC**	**MIC**	**SC**	**MIC**	**SC**	**MIC**	**SC**	**MIC**	**SC**
AMC	>16/8	R	>8/4	R	>16/8	R	>32	R	>16	R
TZP	>8	R	>16	R	>64	R	>16	R	>64	R
AZT	-	-	>4	R	>16	R	-	-	-	-
CTX	>16	R	>16	R	>32	R	>32	R	>32	R
CAZ	>16	R	>8	R	>16	R	>32	R	16	R
FEP	-	-	>4	R	>16	R	>8	R	>32	R
ETP	-	-	>1	R	>1	R	>1	R	>4	R
IPM	>8	R	>8	R	>8	R	>8	R	>8	R
MEM	64	R	128	R	8	I	64	R	32	R
GEN	<=2	S	>4	R	<=2	S	<=2	S	>8	R
TOB	>4/76	R	>4	R	>8	R	<=2	S	-	-
AK	32	R	>128	R	32	R	1	S	4	S
CIP	>2	R	>1	R	>2	R	>1	R	>2	R
TGC	-	-	<=1	S	<1	S	-	-	-	-
CST	-	S	-	-	<=2	S	-	-	-	-
SXT	>4/76	R	>4/76	R	>4/76	R	>4/76	R	>160	R

Table 8. Antibiotic susceptibility profile of Klebsiella pneumoniae isolates. Minimum inhibitory concentration (MIC) is expressed in mg/L (left column). EUCAST clinical breakpoints (2024) were used. Susceptibility testing categorization (SC) (right column): R (resistant), I (susceptible, increased exposure) and S (susceptible, standard dosing regimen). Amikacin (AK), amoxicillin/clavulanate (AMC), aztreonam (AZT), cefotaxime (CTX), cefepime (FEP), ceftazidime (CAZ), ciprofloxacin (CIP), colistin (CST), ertapenem (ETP), gentamicin (GEN), imipenem (IPM), meropenem (MEM), piperacillin-tazobactam (TZP), tigecycline (TGC), tobramycin (TOB) and trimethoprim/sulfamethoxazole (SXT).

4.2 Heteroresistance

Amikacin heteroresistance was studied in *P. aeruginosa* isolates with amikacin MIC≤16 mg/L. PAP values of the studied isolates ranged from 4.38x10-7 to 4.14x10-6 (Table 9). The amikacin MIC values of the corresponding subpopulations were one or two-fold above the initial amikacin breakpoint. None of these isolates were considered heteroresistant by the PAP method.

P. aeruginosa ISOLATE	ISOLATE AK MIC (MG/L)	SUBPOPULATION AK MIC (MG/L)	PAP VALUE
PSD2209	1	4	$8X10^{-7}$
179 (06-014)	16	16	$4.14X10^{-6}$
244 (12-003)	16	32	$4.38X10^{-7}$
253 (01-008)	16	32	$2.14X10^{-6}$
2536 (06-011)	8	16	$8.7X10^{-7}$

Table 9. Analysis of amikacin heteroresistance by Population Analysis Profile (PAP) method. Amikacin (AK) minimum inhibitory concentrations (MIC), amikacin MIC values of the resistant subpopulations and the Population analysis profile (PAP) values obtained. PAP was performed in those isolates with MIC£16 mg/L. The control strain Psd2209 was included.

4.3 Evaluation of the ATP measurement assay for antibiotic combination studies

The initial standardization of the luminometer was required before evaluating antibiotic combinations. Once the different variables were set for accurate measurements using this method, time-kill curve experiments were performed to analyze different antibiotic combinations. A comparative analysis of the results from these experiments was done in parallel using the conventional method and the ATP measurement assay.

4.3.1 ATP measurement assay standardization

Background, linearity and limit of detection were analyzed for the standardization of the luminometer.

4.3.1.1 Background

The overall data included for this calculation were 20 readings for each media. The background average values obtained for both CA-MH broth and NSS were 10^3 and 10^2 RLU/mL, respectively. Bacterial RLU readings below these values were confounded with the corresponding medium RLU reading. Background oscillation was considered relevant enough to be removed in further assays. The mean value of background

was calculated for each reading time and subtracted from the corresponding ATP measurements.

4.3.1.2 Linearity and detection limit

Linearity assessment was conducted for each species at 0, 8 and 24 hours (Figure 12, Figure 13 and Figure 14). Two different backgrounds (CA-MH and NSS) were used for the experiments with the two Gram-negative species (*P. aeruginosa* and *K. pneumoniae*). The detection limit was calculated from the values obtained in the linearity assay.

Detection limits varied with the washing/dilution medium used. The calculated detection limits were 10^4 and 10^3 CFU/mL for CA-MH broth and NSS respectively. The range of linear relationship between log RLU/mL and log CFU/mL was 10^4-10^8 CFU/mL (r=0.98-1) in CA-MH and within of 10^3-10^9 CFU/mL in NSS (r=0.99-1). NSS was established as the washing and dilution medium in further studies due to its broader range. Once NSS was defined as the washing medium, linearity was also determined for a Gram-positive bacterium (*E. faecium*). No significant differences were observed at different times for the three evaluated species.

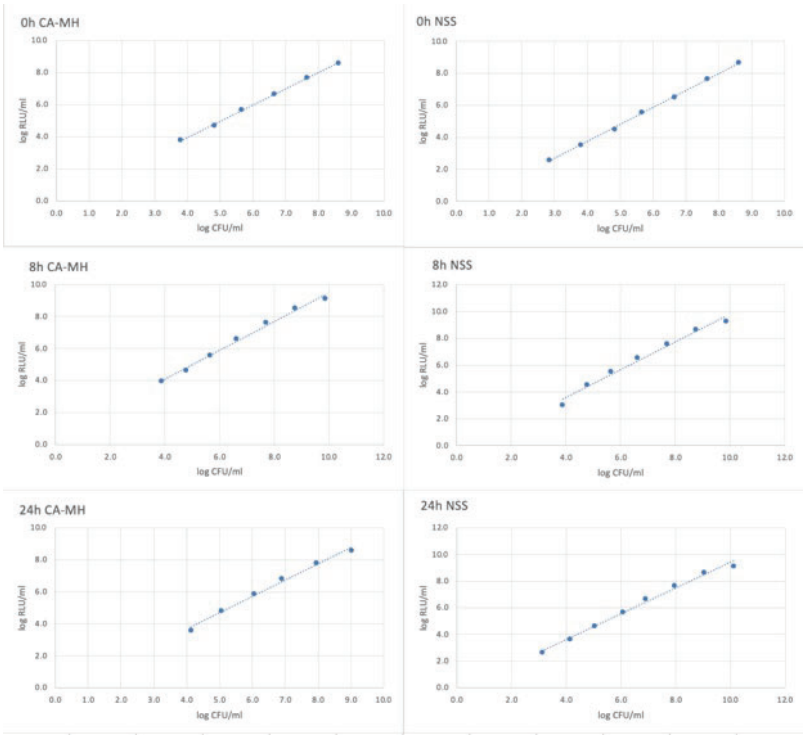

Figure 12. Linearity study of *Pseudomonas aeruginosa*. Samples were collected at 0, 8, and 24 h with cation-adjusted Mueller-Hinton broth (CA-MHB) (left) and normal saline solution (NSS) (right).

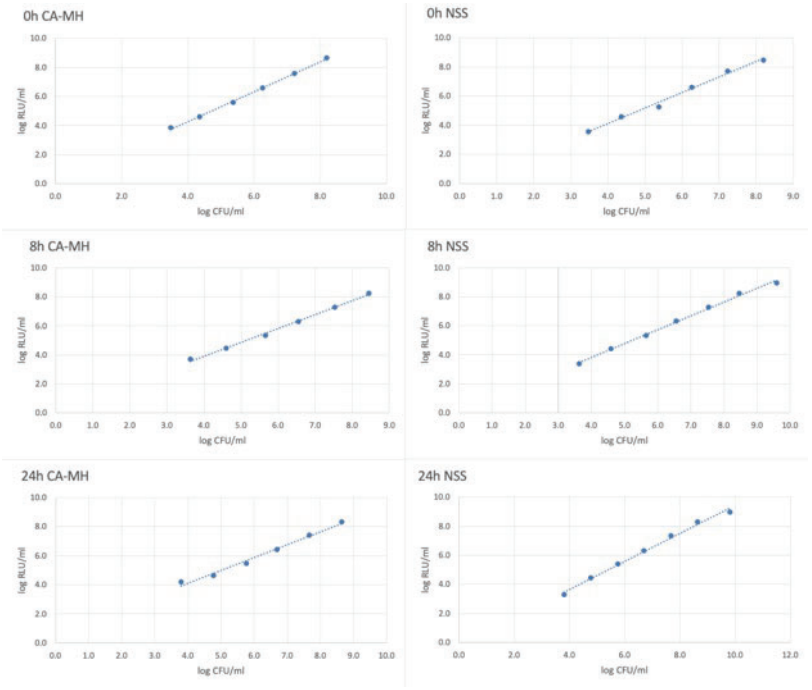

Figure 13. Linearity study of Klebsiella pneumoniae at 0, 8, and 24 h with cation-adjusted Mueller-Hinton broth (CA-MHB) (left) and normal saline solution (NSS) (right).

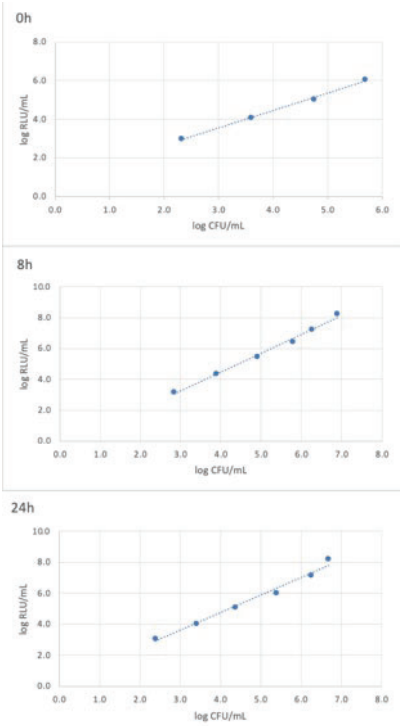

Figure 14. Linearity study of Enterococcus faecium at 0, 8, and 24 h with normal saline solution (NSS)

4.3.2 Comparative analysis

The comparative analysis between the conventional colony count method and the ATP assay aimed to study the correlation of units (CFU and RLU). This analysis was performed throughout the time-kill curves. The last part of this study included the establishment of the pharmacodynamic parameters in RLU so that the luminometer could be used to detect the bactericidal effect and synergy instead of the viable cell count.

Time-kill curves were performed for 24 hours. Aliquots were collected at three different times, and analyzed using both systems in parallel. The comparative analysis was done with *P. aeruginosa* (n=86) and *K. pneumoniae* (n=80). The comparison of the results for time-kill curves of the two species obtained by both systems are shown in Figure 15 and Figure 16, respectively. The average of results (CFU and RLU) was represented in log.

4.3.2.1 Growth curves

The growth curves study was performed from the values obtained in the experimental condition without antibiotic (negative control). The Pearson correlation coefficient (r) for *P. aeruginosa* was 0.93 and infraclass coefficient correlation (ICC) was 0.881 (95% IC 0.816-0.923). The Pearson correlation coefficient (r) for *K. pneumoniae* was 0.87 and intraclass correlation coefficient (ICC) was 0.79 (95% IC 0.696-0.863).

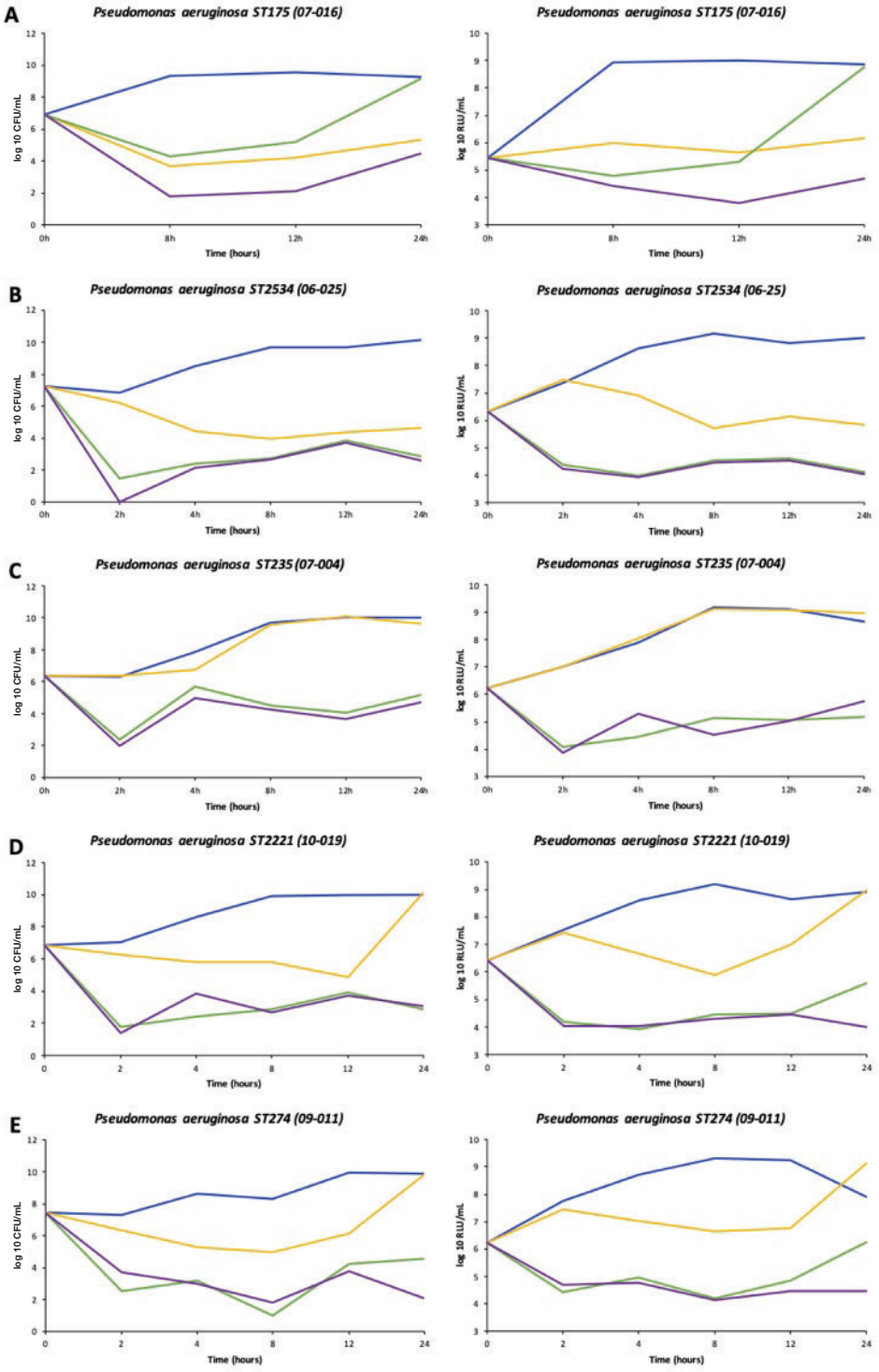

Figure 15. Time-kill curves for *P. aeruginosa* ST175 (07-016), ST235 (07-004), ST274 (09-011), ST2221 (10-016), ST2534 (06-025), and ST2536 (06-001). Results for the conventional colony count method (CFU per milliliter) (left) and ATP measurement assay (RLU per milliliter) (right) are shown. Four experimental conditions were studied: growth control (blue), meropenem alone (yellow), colistin alone (green), and meropenem plus colistin (purple). The antibiotic concentrations were 17.71 mg/L for meropenem and 2.08 mg/L for colistin.

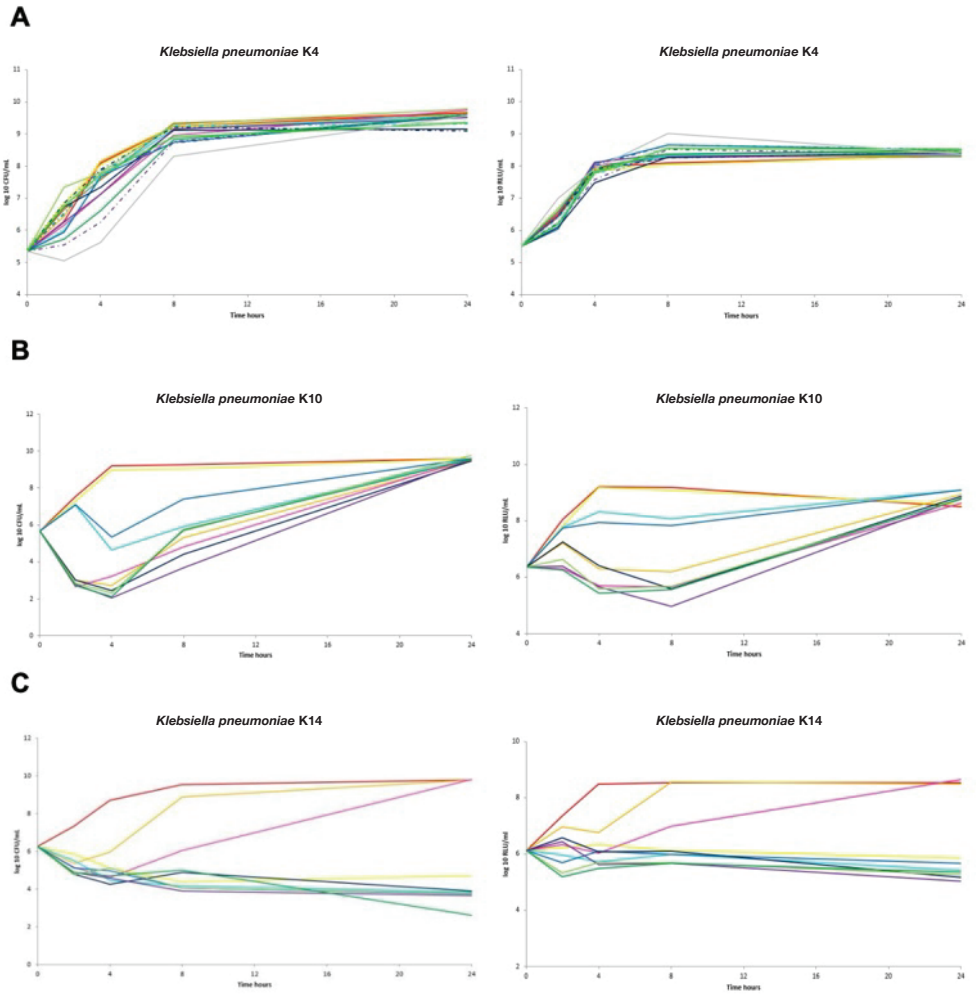

Figure 16. Time-kill curves for *K. pneumoniae* K4, K10 and K14. Results are shown for the conventional colony count method (CFU per milliliter) (left) and ATP measurement assay (RLU per milliliter) (right). Different dosing schedules of amikacin (AK) and meropenem (MEM) alone and in combination were tested. Simultaneous schedules (AK=MEM) included both antibiotics at the start of the curve. In staggered schedules the second antibiotic was added two hours after the first antibiotic: AK after MEM (MEM+AK) or conversely (AK+MEM). The chosen antibiotic concentrations for were AK8 (8.17 mg/L), AK40 (40 mg/L), MEM17 (17.71 mg/L) and MEM32 (32 mg/L). Growth control (red), amikacin alone (AK8 – yellow, AK40 – blue lines), meropenem alone (MEM17 – orange, MEM32 - pink), simultaneous schedules (AK8=MEM17 – light green, AK8=MEM32 – dark green, AK40=MEM17 – bright green, AK40=MEM32 - grey) and staggered schedules (AK8 + MEM17 – light blue, AK8 + MEM32 – dark blue, AK40 + MEM17 – light blue lines, AK40 + MEM32 – blue, MEM17 + AK8 – black, MEM17 + AK40 – olive green, MEM32 + AK8 – purple, MEM32 + AK40 – purple lines).

4.3.2.2 Cut-off point determination for the ATP-measurement assay

The cut-off points for the bactericidal effect and synergy were determined for the two species using paired data obtained in the time-kill curves. Each pair of data consisted of the values from the analysis of the same sample obtained in parallel by the conventional colony count method (CFU/mL) and the ATP assay (RLU/mL). Results obtained using the conventional colony-count method were used as a gold standard to determine the pharmacodynamic parameters in RLU/mL. ROC curves and the Youden Test were performed to establish these cut-off points.

4.3.2.3 Pharmacodynamic parameters

The values obtained from the experimental conditions of each antibiotic alone and antibiotic combinations were used to establish the cut-off point for bactericidal effect.

The sample size to establish the cut-off for bactericidal effect in *P. aeruginosa* was 257 paired data points. The value for the bactericidal effect cut-off was 1.348 log RLU/mL, with a sensitivity of 93%, and a specificity of 78.5%. The UA was 85.75% and the area under the curve (AUC) obtained was 0.929 (Figure 17). The cut-off point for synergy was established considering the values obtained from antibiotic combinations. The sample size included 105 paired data (CFU/mL-RLU/mL). The cut-off point for synergy was 0.9 log RLU/mL, with a sensitivity of 95% and a specificity of 88%. The UA was 91.5% and the area under the curve (AUC) obtained was 0.9430 (Figure 17). Specificity should be prioritized over sensitivity to avoid false positive results and maximize the therapeutic benefit of the antibiotic combinations. The cut-off was 2.199 (53% sensitivity) when considering a specificity of 100%.

The sample size to establish the cut-off for bactericidal effect in *K. pneumoniae* was 162 paired observations. The value for the bactericidal effect cut-off was 0.764 log RLU/mL, with a sensitivity of 100%, and a specificity of 76%. The UA was 88% and the area under the curve (AUC) obtained was 0.9384 (Figure 18). The sample size for synergy included 110 paired data (CFU/mL-RLU/mL). The cut-off point for synergy was 2.95 log RLU/mL, with a sensitivity of 78.6% and a specificity of 100%. The UA was 89.5% and the area under the curve (AUC) obtained was 0.9807 (Figure 18).

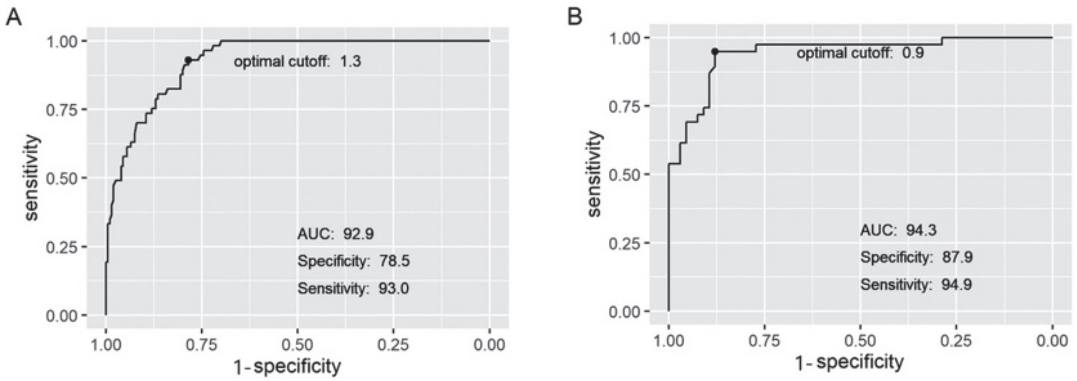

Figure 17. *Pseudomonas aeruginosa* ROC curves for bactericidal effect and synergy. High areas under the ROC curves (0.929 to 0.943) were observed in both pharmacodynamic parameters bactericidal effect (above) and synergy (below).

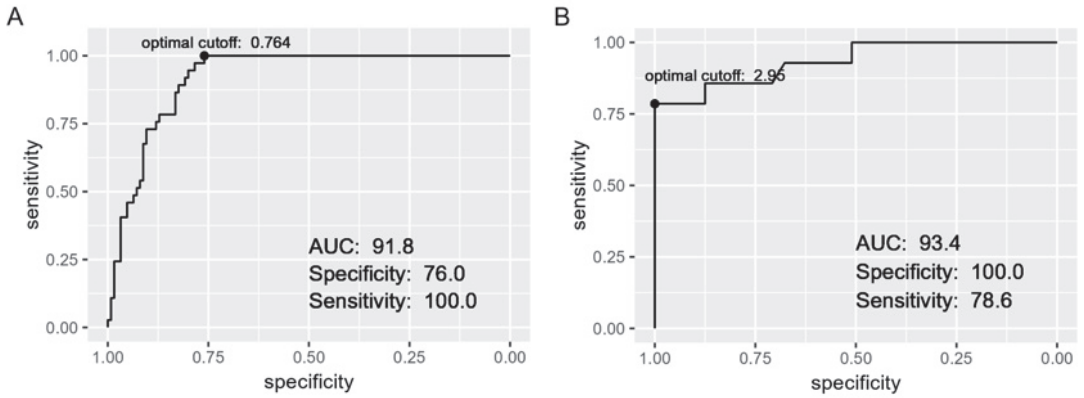

Figure 18. *Klebsiella pneumoniae* ROC curves for bactericidal effect and synergy. High areas under the ROC curves (0.9185 to 0.9342) were observed in both pharmacodynamic parameters bactericidal effect (above) and synergy (below).

4.4 Optimization of meropenem plus amikacin dosing schedules

The administration of meropenem plus amikacin may be optimized to improve the clinical outcome using this empirical combined therapy. These antibiotics given either simultaneously or staggered may influence the initial reduction of the bacterial load. The effect of the different dosing schedules on the initial bacterial load was analyzed by means of time-kill experiments.

The efficacy of this antibiotic combination was assessed in *P. aeruginosa* isolates (n=8) and in *K. pneumoniae* isolates (n=5). Different dosing schedules of meropenem and amikacin against XDR *P. aeruginosa* and CP-KP were studied. Samples were obtained at different times (0, 2, 4, 8, 24h) to determine the viable cell count. The bacterial load reduction (log CFU/mL) and bactericidal and synergistic effects were calculated.

4.4.1 Pseudomonas aeruginosa

Different dosing schedules of combined meropenem and amikacin were tested against seven XDR *P. aeruginosa* isolates and a non-XDR P. aeruginosa isolate (Psd2209). The bacterial load reduction (log10 CFU/mL) for each dosing schedule is shown in Table 10.

PSD2209

CONDITIONS	0-2H	0-4H	0-8H	0-24H	B	S
GC	0.97	1.31	2.08	4.14	NA	NA
AK40	-2.81	-3.46	-3.68	-5.18	+	NA
AK8	-2.68	-3.1	-3.48	-4.83	+	NA
MEM17	0.15	-0.97	-1.96	-4.03	+	NA
AK40+MEM17	-3.01	-3.54	-3.88	-4.27	+	-
AK8+MEM17	-2.35	-2.79	-3.61	-3.77	+	-
MEM17+AK40	0.159	-2.79	-3.38	-4.83	+	-
MEM17+AK8	0.03	-2.44	-2.96	-0.85	-	-
AK40=MEM17	-2.95	-3.22	-3.79	-5.18	+	-
AK8=MEM17	-2.37	-2.91	-3.72	-5.18	+	-

ST175 (12-012)

CONDITIONS	0-2H	0-4H	0-8H	0-24H	B	S
GC	0.33	1.26	3.78	4.35	NA	NA
AK8	0.21	1.09	3.22	4.44	-	NA
MEM32	-0.36	-1.24	-0.36	3.71	-	NA
MEM17	-0.03	-0.01	2.48	4.36	-	NA
AK8+MEM32	0.44	1.05	-0.77	0.84		+

Table 10 Bacterial load reduction (log_{10} CFU/mL) and bactericidal (B) and synergistic (S) effects in *Pseudomonas aeruginosa* isolates caused by each dosing schedule of meropenem (MEM) and amikacin (AK). Bacterial load reduction was calculated by deducting the initial viable cell count from the final viable cell count. It was calculated for each time, experimental condition and isolate. Positive values correspond to an increase in the bacterial load, and negative values to a reduction. Bacterial load was considered stable when the reduction was ≤1 log_{10} CFU/mL. Antibiotics were administered simultaneously (AK=MEM) and staggered. For staggered schedules, amikacin was added 2h after meropenem (MEM+AK) or conversely (AK+MEM). Antibiotic concentrations were MEM17=17.71mg/L, AK8=8.17mg/L, MEM32=32mg/L and AK40=40mg/L. Growth control (GC); positive (+); negative (-), not applicable (NA).

AK8+MEM17	0.64	0.50	0.72	4.19	-	-
MEM32+AK8	-0.26	-1.41	-1.72	0.67	-	+
MEM17+AK8	0.08	-0.60	-0.54	3.89	-	-
AK8=MEM32	-0.46	-1.42	-1.26	0.80	-	+
AK8=MEM17	-0.20	-0.57	-1.16	3.63	-	-

ST179 (06-014)

CONDITIONS	0-2H	0-4H	0-8H	0-24H	B	S
GC	0.28	1.57	3.26	3.78	NA	NA
AK40	-2.59	-3.42	-3.64	-1.92	-	NA
AK8	0.21	0.91	1.52	3.64	-	NA
MEM32	-2.61	-2.37	-3.60	2.99	-	NA
MEM17	-0.79	-1.99	-2.06	3.39	-	NA
AK40+MEM32	-2.44	-4.12	-2.89	-2.88	-	-
AK40+MEM17	-2.97	-3.76	-4.31	-2.66	-	-
AK8+MEM32	0.10	-1.07	-1.72	-1.90	-	+
AK8+MEM17	-0.74	-0.66	-3.17	0.07	-	+
MEM32+AK40	-1.83	-4.97	-4.91	-2.63	-	-
MEM32+AK8	-1.83	-3.43	-4.32	-1.25	-	+
MEM17+AK40	-0.97	-3.47	-4.68	-1.45	-	-

Table 10 Bacterial load reduction (log_{10} CFU/mL) and bactericidal (B) and synergistic (S) effects in *Pseudomonas aeruginosa* isolates caused by each dosing schedule of meropenem (MEM) and amikacin (AK). Bacterial load reduction was calculated by deducting the initial viable cell count from the final viable cell count. It was calculated for each time, experimental condition and isolate. Positive values correspond to an increase in the bacterial load, and negative values to a reduction. Bacterial load was considered stable when the reduction was ≤1 log_{10} CFU/mL. Antibiotics were administered simultaneously (AK=MEM) and staggered. For staggered schedules, amikacin was added 2h after meropenem (MEM+AK) or conversely (AK+-MEM). Antibiotic concentrations were MEM17=17.71mg/L, AK8=8.17mg/L, MEM32=32mg/L and AK40=40mg/L. Growth control (GC); positive (+); negative (-), not applicable (NA).(Continued)

MEM17+AK8	-1.33	-3.20	-4.06	-1.20	-	**+**
AK40=MEM32	-3.78	-5.38	-5.62	-2.72	-	-
AK40=MEM17	-3.44	-6.12	-4.90	-1.90	-	-
AK8=MEM32	-2.57	-4.94	-4.77	-1.36	-	**+**
AK8=MEM17	-1.54	-4.02	-4.76	-1.41	-	**+**

ST235 (07-004)

CONDITIONS	0-2H	0-4H	0-8H	0-24H	B	S
GC	0.14	1.47	3.69	4.64	NA	NA
AK40	-0.85	-1.48	-2.65	2.84	-	NA
AK8	0	1.37	3.38	4.61	-	NA
MEM32	-1.41	-1.71	-1.31	3.73	-	NA
MEM17	-1.45	-2.06	-1.29	4.33	-	NA
AK40+MEM32	-0.94	-2.62	-2.43	-1.71	-	**+**
AK40+MEM17	-1.12	-2.73	-1.86	-1.47	-	**+**
AK8+MEM32	-0.01	-1.59	-1.04	3.41	-	-
AK8+MEM17	-0.37	-0.57	-0.85	4.24	-	-
MEM32+AK40	-1.53	-2.79	-3.07	-1.32	-	**+**
MEM32+AK8	-1.38	-2.62	-2.13	-0.97	-	**+**
MEM17+AK40	-1.59	-2.60	-2.93	-1.80	-	**+**

Table 10 Bacterial load reduction (log_{10} CFU/mL) and bactericidal (B) and synergistic (S) effects in *Pseudomonas aeruginosa* isolates caused by each dosing schedule of meropenem (MEM) and amikacin (AK). Bacterial load reduction was calculated by deducting the initial viable cell count from the final viable cell count. It was calculated for each time, experimental condition and isolate. Positive values correspond to an increase in the bacterial load, and negative values to a reduction. Bacterial load was considered stable when the reduction was ≤1 log_{10} CFU/mL. Antibiotics were administered simultaneously (AK=MEM) and staggered. For staggered schedules, amikacin was added 2h after meropenem (MEM+AK) or conversely (AK+-MEM). Antibiotic concentrations were MEM17=17.71mg/L, AK8=8.17mg/L, MEM32=32mg/L and AK40=40mg/L. Growth control (GC); positive (+); negative (-), not applicable (NA).(Continued)

MEM17+AK8	-1.94	-2.39	-2.92	1.76	-	+
AK40=MEM32	-1.58	-2.39	-1.45	-1.29	-	+
AK40=MEM17	-1.60	-2.70	-2.02	-2.63	-	+
AK8=MEM32	-1.67	-2.07	-3.39	-2.02	-	+
AK8=MEM17	-1.82	-1.99	-2.96	1.82	-	+

ST244 (12-003)

CONDITIONS	0-2H	0-4H	0-8H	0-24H	B	S
GC	1.04	3.16	3.92	3.84	NA	NA
AK8	0.85	2.41	2.60	3.92	-	NA
MEM32	0.13	-1.40	-2.22	2.8	-	NA
MEM17	-0.14	1.05	1.91	3.56	-	NA
AK8+MEM32	1.32	-2.30	-2.43	-0.36	-	+
AK8+MEM17	2.28	-1.61	-1.29	0.13	-	+
MEM32+AK8	0.10	-1.81	-1.64	-0.37	-	+
MEM17+AK8	-0.41	-0.78	-1.46	-0.52	-	+
AK8=MEM32	-2.16	-3.17	-4.00	-1.62	-	+
AK8=MEM17	-0.78	-2.04	-2.24	-0.54	-	+

Table 10 Bacterial load reduction (log_{10} CFU/mL) and bactericidal (B) and synergistic (S) effects in *Pseudomonas aeruginosa* isolates caused by each dosing schedule of meropenem (MEM) and amikacin (AK). Bacterial load reduction was calculated by deducting the initial viable cell count from the final viable cell count. It was calculated for each time, experimental condition and isolate. Positive values correspond to an increase in the bacterial load, and negative values to a reduction. Bacterial load was considered stable when the reduction was ≤1 log_{10} CFU/mL. Antibiotics were administered simultaneously (AK=MEM) and staggered. For staggered schedules, amikacin was added 2h after meropenem (MEM+AK) or conversely (AK+-MEM). Antibiotic concentrations were MEM17=17.71mg/L, AK8=8.17mg/L, MEM32=32mg/L and AK40=40mg/L. Growth control (GC); positive (+); negative (-), not applicable (NA).(Continued)

ST253 (01-008)

CONDITIONS	0-2H	0-4H	0-8H	0-24H	B	S
GC	0.53	2.17	4.10	4.63	NA	NA
AK40	-2.72	-2.78	-2.00	4.37	-	NA
AK8	0.47	-0.16	-0.61	4.57	-	NA
MEM17	0.54	1.92	3.99	4.61	-	NA
AK40+MEM17	-3.26	-3.35	-3.50	4.00	-	-
AK8+MEM17	0.40	-0.59	-1.23	4.49	-	-
MEM17+AK40	0.70	-1.33	-1.87	4.09	-	-
MEM17+AK8	0.45	0.41	-0.61	4.15	-	-
AK40=MEM17	-2.57	-4.87	-2.61	4.02	-	-
AK8=MEM17	-0.24	-1.37	-1.88	3.43	-	-

ST274 (09-011)

CONDITIONS	0-2H	0-4H	0-8H	0-24H	B	S
GC	0.71	1.84	3.45	4.19	NA	NA
AK40	0.26	0.86	1.82	4.13	-	NA
AK8	1.05	1.6	3.81	4.27	-	NA
MEM17	-1.12	-1.70	-1.69	3.20	-	NA
AK40+MEM17	-0.02	-1	-1.30	2.39	-	-

Table 10 Bacterial load reduction (log_{10} CFU/mL) and bactericidal (B) and synergistic (S) effects in *Pseudomonas aeruginosa* isolates caused by each dosing schedule of meropenem (MEM) and amikacin (AK). Bacterial load reduction was calculated by deducting the initial viable cell count from the final viable cell count. It was calculated for each time, experimental condition and isolate. Positive values correspond to an increase in the bacterial load, and negative values to a reduction. Bacterial load was considered stable when the reduction was ≤1 log_{10} CFU/mL. Antibiotics were administered simultaneously (AK=MEM) and staggered. For staggered schedules, amikacin was added 2h after meropenem (MEM+AK) or conversely (AK+-MEM). Antibiotic concentrations were MEM17=17.71mg/L, AK8=8.17mg/L, MEM32=32mg/L and AK40=40mg/L. Growth control (GC); positive (+); negative (-), not applicable (NA).(Continued)

AK8+MEM17	0.94	-1.16	-0.46	1.62	-	**+**
MEM17+AK40	-1.31	-2.48	-2.46	1.81	-	-
MEM17+AK8	-1.55	-2.46	-2.34	2.29	-	**+**
AK40=MEM17	-2.95	-3.69	-2.69	1.59	-	-
AK8=MEM17	-1.03	-2.30	-2.40	2.70	-	**+**

ST2536 (06-001)

CONDITIONS	0-2H	0-4H	0-8H	0-24H	B	S
GC	0.31	1.40	3.51	4.35	NA	NA
AK40	-2.77	-3.22	-4.58	-1.45	-	NA
AK8	-2.71	-3.45	-2.12	2.46	-	NA
MEM17	-0.57	-0.42	-0.38	3.74	-	NA
AK40+MEM17	-3.14	-4.43	-2.70	-2.36	-	-
AK8+MEM17	-2.52	-4.27	-3.69	-0.21	-	**+**
MEM17+AK40	-0.49	-4.34	-4.76	-0.92	-	-
MEM17+AK8	-0.47	-2.61	-3.09	-0.56	-	**+**
AK40=MEM17	-4.16	-4.42	-4.31	-1.66	-	-
AK8=MEM17	-3.18	-3.69	-4.26	-1.80	-	**+**

Table 10 Bacterial load reduction (log_{10} CFU/mL) and bactericidal (B) and synergistic (S) effects in *Pseudomonas aeruginosa* isolates caused by each dosing schedule of meropenem (MEM) and amikacin (AK). Bacterial load reduction was calculated by deducting the initial viable cell count from the final viable cell count. It was calculated for each time, experimental condition and isolate. Positive values correspond to an increase in the bacterial load, and negative values to a reduction. Bacterial load was considered stable when the reduction was ≤1 log_{10} CFU/mL. Antibiotics were administered simultaneously (AK=MEM) and staggered. For staggered schedules, amikacin was added 2h after meropenem (MEM+AK) or conversely (AK+-MEM). Antibiotic concentrations were MEM17=17.71mg/L, AK8=8.17mg/L, MEM32=32mg/L and AK40=40mg/L. Growth control (GC); positive (+); negative (-), not applicable (NA).(Continued)

4.4.1.1 Monotherapies

Both meropenem and amikacin were assessed alone i*P. aeruginosa* isolates. The results of MEM and AK monotherapies are shown in Figure 19.

The two amikacin concentrations tested were 8.17µg/mL (AK8) and 40 µg/mL (AK40). AK8 did not cause any effect against the amikacin-resistant isolates [ST175 (12-012), ST235 (07-004), ST274 (09-011)] and against two out of three amikacin-susceptible isolates with an MIC of 16 mg/L [ST179 (06-014), ST244 (12-003)]. The bacterial load of the third isolate [ST253 (01-008)] showed a lag phase, followed by regrowth starting at 8h. The remaining isolate [ST2536 (06-011)], which had an amikacin MIC of 8 mg/L, presented an initial bacterial load reduction [3.45 $\log_{10}$ CFU/mL at 4h], followed by regrowth.

The highest concentration of amikacin (AK40) achieved a reduction of over a 2-$\log_{10}$ in ST179 (06-014) and ST253 (01-008) at 2h [2.59 and 2.72 $\log_{10}$ CFU/mL, respectively] and in ST235 (07-004) at 8h [2.65 $\log_{10}$ CFU/mL]. The largest bacterial load decrease achieved with AK40 was observed in ST2536 (06-011) [4.58 $\log_{10}$ CFU/mL at 8h]. All XDR isolates had final regrowth using AK40 monotherapy. Psd2209 isolate reached final log reductions of 4.83 $\log_{10}$ CFU/mL and 5.18 $\log_{10}$ CFU/mL using AK8 and AK40, respectively.

Two meropenem concentrations were tested, 17.71 µg/mL (MEM17) and 32 µg/mL (MEM32). MEM17 alone was assessed against all XDR isolates. This concentration of meropenem had no effect against the isolate with the highest meropenem MIC [ST253 (01-008)] whereas it caused a 4-hour lag in two isolates [ST244 (12-003), ST175 (12-012)] and an 8-hour lag in another [ST2536 (06-011)], followed by regrowth in the three of them. The remaining XDR isolates [ST179 (06-014), ST235 (07-004), ST274 (09-011)] showed an initial bacterial load reduction [1.7-2 $\log_{10}$ CFU/mL at 4h] after which bacterial regrowth was observed. The non-XDR Psd2209 isolate reached a final log reduction of 4.03 $\log_{10}$ CFU/mL using MEM17 monotherapy.

The highest concentration of meropenem (MEM32) was assessed against four XDR isolates. The isolate ST235 (07-004) had the same behaviour with MEM32 as with MEM17 monotherapy. MEM32 caused an initial 1-$\log_{10}$ bacterial reduction [1.24 $\log_{10}$ CFU/mL at 4h] in ST175 (12-012). This concentration of meropenem caused a further bacterial load decrease in isolates ST179 (06-014) and ST244 (12-003) [3.60 and 2.22 $\log_{10}$ CFU/mL at 8h, respectively]. All isolates reached a final bacterial load like the growth control.

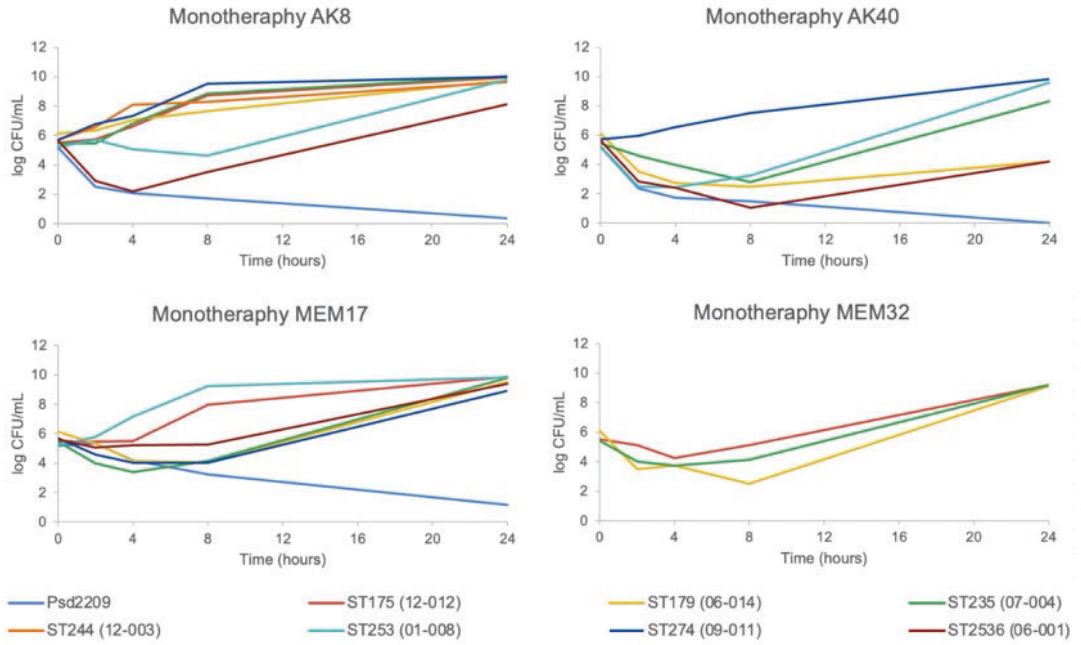

Figure 19 Time-kill curves with amikacin (AK) and meropenem (MEM) monotherapies against *Pseudomonas aeruginosa* clinical isolates. Amikacin concentrations were 8.17 mg/L (AK8) and 40 mg/L (AK40). Meropenem concentrations were 17.71 mg/L (MEM17) and 32 mg/L (MEM32). Data were expressed as the logarithm with the base 10 of CFU/mL (log_{10} CFU/mL).

4.4.1.2 Simultaneous schedules of the antibiotic combination

Simultaneous schedules of amikacin and meropenem (AK=MEM) were studied against the *P. aeruginosa* isolates by adding both antibiotics at the beginning of time-kill curve (Figure 20).

The simultaneous dosing schedule AK8=MEM17 resulted in an initial bacterial load decrease in all the XDR *P. aeruginosa* isolates. The meropenem-resistant amikacin-susceptible isolates ST179 (06-014) and ST2536 (06-011) showed the steepest initial bacterial load decline, achieving 4.76 and 4.26 log_{10} CFU/mL at 8h, respectively. All XDR isolates showed final regrowth whereas the control strain Psd2209 reached a final log decrease of 5.18 log_{10} CFU/mL.

The simultaneous dosing schedule AK8=MEM32 had a similar effect to AK8=MEM17 on the initial bacterial load reduction of the four XDR isolates tested [ST175 (12-012), ST179 (06-014), ST235 (07-004) and ST244 (12-003)]. An enhanced reduction in the initial bacterial load of the isolate ST244 (12-003) [4 log_{10} CFU/mL at 8h] was observed. The simultaneous schedule AK40=MEM17 had the same effect against ST235 and ST2536 (06-011) as AK8=MEM17. An improvement in the initial bacterial load reduction was observed in ST179 (06-014), ST253 (01-008) and ST274 (09-011) [6.12, 4.87 and 3.69 log_{10} CFU/mL at 4h, respectively]. No regrowth was observed in ST235 with the highest amikacin concentration. Psd2209 reached a final log_{10} decrease of 5.18 CFU/mL for both simultaneous dosing schedules (AK8=MEM32 and AK40=MEM17).

The simultaneous schedule with high concentration of both antibiotics AK40=MEM32 had a similar effect against the two XDR isolates tested [ST179 (06-014) and ST235] compared to AK8=MEM32.

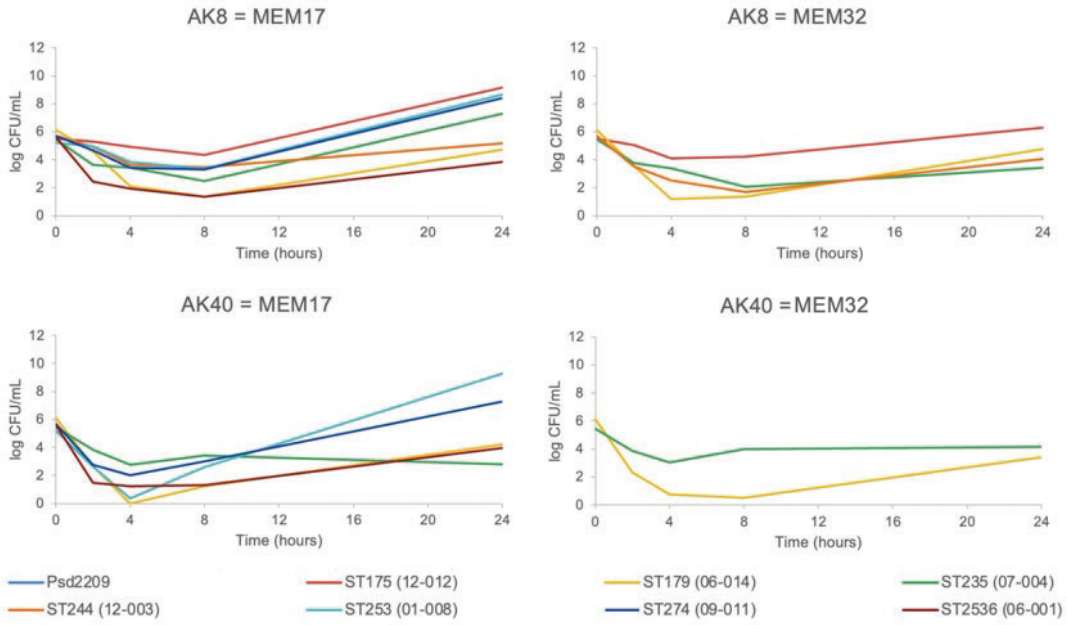

Figure 20 Time-kill curves with simultaneous dosing schedules of meropenem (MEM) and amikacin (AK) against *Pseudomonas aeruginosa* isolates. Amikacin concentrations were 8.17 mg/L (AK8) and 40 mg/L (AK40). Meropenem concentrations were 17.71 mg/L (MEM17) and 32 mg/L (MEM32). Data were expressed as the logarithm with the base 10 of CFU/mL (log_{10} CFU/mL).

4.4.1.3 Staggered schedules of the antibiotic combination

The staggered schedules of this antibiotic combination against the *P. aeruginosa* isolates were performed by adding amikacin 2 hours after meropenem (MEM+AK) or coanversely (AK+MEM) (Figure 21).

The staggered schedule AK8+MEM17 achieved the highest initial bacterial load reduction against ST2536 (06-011) [4.27 log_{10} CFU/mL at 4h] and ST179 (06-014) [3.17 log10 CFU/mL at 8h]. The initial increase in the bacterial load of ST244 (12-003) and ST274 (09-011) was reverted after adding MEM17. Final regrowth was present in all XDR isolates. Three of them [ST175, ST235 (07-004), ST253 (01-008)] achieved a final bacterial load similar to the growth control while the other four isolates [ST179 (06-014), ST244 (12-003), ST274 (09-011), ST2536 (06-011)] reached similar values to the initial load at the end of the curves.
The staggered MEM17+AK8 schedule caused the highest initial reduction in the bacterial

load of ST274 (09-011) [2.46 log_{10} CFU/mL at 4h], ST2536 (06-011) [2.61 log_{10} CFU/mL at 4h], ST179 (06-014) [4.06 log_{10} CFU/mL at 8h] and ST235 [2.92 log_{10} CFU/mL at 8h]. A lag was observed in the remaining two XDR isolates [ST175 (12-012) and ST253 (01-008)] for the first eight hours. All XDR isolates showed final regrowth with this schedule. The final bacterial load of ST175 (12-012) and ST253 (01-008) was similar to that of the growth control. ST274 (09-011) and ST235 (07-004) had a final increase in the bacterial load of 2.29 and 1.76 log10 CFU/mL, respectively.

The highest amikacin concentration (AK40) in the staggered AK40+MEM17 schedule was tested against five XDR isolates [ST179 (06-014), ST235 (07-004), ST253 (01-008), ST274 (09-011) and ST2536 (06-011)]. The greatest initial reduction in the bacterial load was achieved against the three amikacin susceptible isolates: ST2536 (06-011) [4.43 log_{10} CFU/mL at 4h], ST179 (06-014) [4.31 log_{10} CFU/mL at 8h], and ST253 (01-008) [3.35 log10 CFU/mL at 4h]. This dosing schedule produced no difference against one of the two amikacin-resistant isolates [ST274 (09-011)] compared to the same staggered schedule with AK8. An initial reduction was observed using this dosing schedule against the remaining isolate ST235 (07-004) [2.73 log_{10} CFU/mL at 4h], without final regrowth. These isolates had a similar behaviour when MEM17 was added prior to AK40 (MEM17+AK40).

The highest meropenem concentration (MEM32) in staggered schedules was tested against four isolates [ST175 (12-012), ST179 (06-014), ST235 (07-004) and ST244 (12-003)]. The initial response of these isolates to MEM32+AK8 was similar to that observed with MEM17+AK8. When AK8 was added prior to MEM32 (AK8+MEM32), the two isolates with the lowest amikacin MIC (16 mg/L) showed a larger bacterial load reduction at 8h than AK8+MEM17. Three of the four isolates had reduced final regrowth when MEM32 was used.

Schedules with the highest concentrations of the two antibiotics (AK40 and MEM32) were tested in two isolates [ST179 (06-014) and ST235 (07-004)]. The staggered schedule AK40+MEM32 achieved a decrease in the initial bacterial load [>2 log_{10} CFU/mL] that was not observed with AK8+MEM17. The reverse staggered schedule MEM32+AK40 did not achieve any improvement compared to MEM17+AK8.

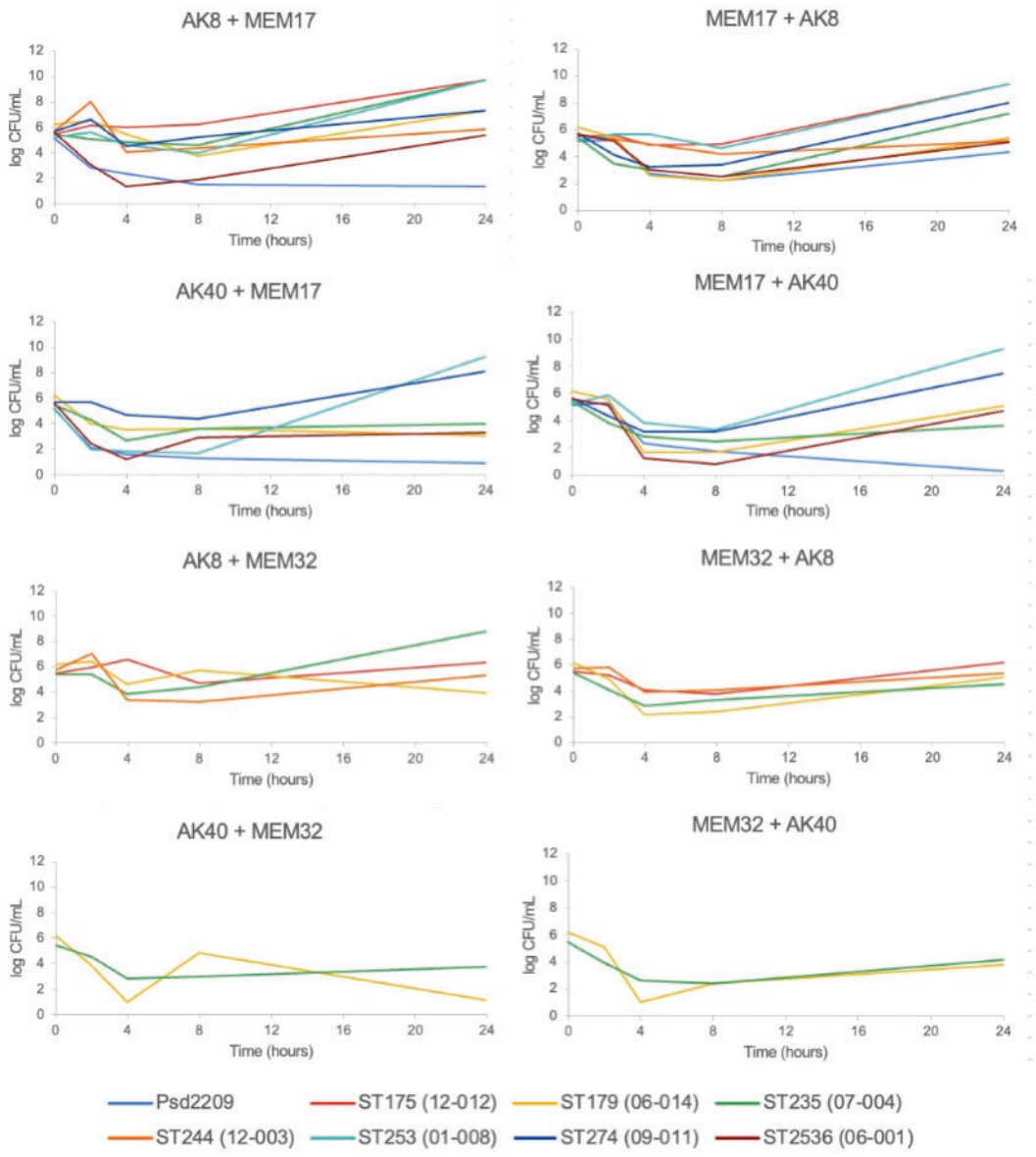

Figure 21. Time-kill curves with simultaneous dosing schedules of meropenem (MEM) and amikacin (AK) against *Pseudomonas aeruginosa* isolates. Amikacin concentrations were 8.17 mg/L (AK8) and 40 mg/L (AK40). Meropenem concentrations were 17.71 mg/L (MEM17) and 32 mg/L (MEM32). Data were expressed as the logarithm with the base 10 of CFU/mL (log_{10} CFU/mL).

4.4.1.4 Bactericidal effect and synergy

The bactericidal effect and synergy of this antibiotic combination were evaluated in seven XDR *P. aeruginosa* isolates (Table 10). No bactericidal effect was observed for any of the schedules in these isolates. All dosing schedules with AK8 and MEM17 concentrations and MEM32 combined with AK8 caused synergy in four of these isolates [ST179 (06-014), ST244 (12-003), ST274 (09-011), ST2536 (06-011)]. Synergy was detected in ST175 using the three dosing schedules with MEM32. Synergy was detected in ST235 (07-004) in all dosing schedules except when AK8 was given first. Schedules with the highest concentrations of the two antibiotics were tested in isolates ST179 (06-014) and ST235 (07-004); synergy was achieved only in the latter.

4.4.1.5 Antibiotic refreshment

Antibiotic refreshment experiments assessed the role of antibiotic degradation in time-kill results. Time-kill curves with nine experimental conditions corresponding to AK8 and MEM17/32 and their combined dosing schedules were performed with antibiotic refresh against two XDR *P. aeruginosa* isolates [ST179 (06-014) and ST235 (07-004)]. The replacement of the flask content was performed at 12h to minimize the impact of the antibiotic degradation effect. Bacterial killing at 24h was analysed (Table 11) and compared to the results from the standard time-kill curves (Table 12).

No differences in regrowth at 24h were observed for isolate ST179 (06-014) compared to the standard time-kill curves. Regarding ST235 (07-004), final regrowth was diminished in six out of nine experimental conditions compared to the standard curves. This improvement corresponded to a reduction exceeding 3 $\log_{10}$ CFU/mL in three of the dosing schedules (MEM32, AK8 + MEM32 and AK8 + MEM17).

No differences in bactericidal effect and synergy in isolate ST179 (06-014) was observed when the refreshment of the antibiotics was performed at 12 hours (Table 13). ST235 (07-004) had the same behaviour except for two dosing schedules (MEM32+AK8 and MEM32=AK8). The synergy observed with these schedules in time-kill curves without refreshment was not observed in this isolate when the refreshment was performed.

ST179 (06-014) WITH REFRESHMENT OF ANTIBIOTICS AT 12H

CONDITIONS	0-2H	0-4H	0-8H	0-12H	0-14H	0-16H	0-24H
GC	1.09	2.38	4.23	4.60	4.47	4.59	**4.86**
AK8	0.97	1.49	1.83	2.10	2.63	3.06	**4.46**
MEM32	-0.80	-2.52	-3.14	-1.26	-1.63	-1.19	**2.41**
MEM17	-0.28	-0.31	-1.85	-0.35	-0.20	0.84	**4.19**
AK8+MEM32	0.81	-1.08	-2.29	-2.89	-3.14	-2.85	**-2.08**
AK8+MEM17	0.68	-0.52	-1.71	-1.92	-0.90	-2.78	**0.21**
MEM32+AK8	-2.18	-2.83	-4.40	-4.15	-4.42	-4.77	**-1.47**
MEM17+AK8	-0.87	-3.04	-4.57	-3.95	-3.89	-4.77	**-1.47**
AK8=MEM32	-1.94	-3.10	-3.16	-3.95	-3.43	-3.66	**-1.71**
AK8=MEM17	-1.23	-1.21	-0.79	-0.76	-1.07	-3.61	**0.12**

ST235 (07-004) WITH REFRESHMENT OF ANTIBIOTICS AT 12H

CONDITIONS	0-2H	0-4H	0-8H	0-12H	0-14H	0-16H	0-24H
GC	0.3	2.04	3.81	4.50	4.50	4.67	**5.02**
AK8	0.87	1.87	3.73	4.43	4.52	4.68	**4.91**
MEM32	-1.52	-2.28	-2.79	-2.99	-3.23	-3.62	**0.53**
MEM17	-1.29	-1.58	-1.98	-1.05	-0.26	-1.14	**2.59**
AK8+MEM32	0.46	-0.76	-1.73	-1.35	-2.55	-3.83	**-1.03**

Table 11 Bacterial load reduction (log_{10} CFU/mL) in *Pseudomonas aeruginosa* isolates caused by each dosing schedule of meropenem (MEM) and amikacin (AK) in the time-kill curves with refreshment of the antibiotics. Bacterial load reduction was calculated by deducting the initial viable cell count from the final viable cell count. It was calculated for each time, experimental condition and isolate. Positive values correspond to an increase in the bacterial load, and negative values to a reduction. Bacterial load was considered stable when the reduction was ≤1 log_{10} CFU/mL. Antibiotics were administered simultaneously (AK=MEM) and staggered. For staggered schedules, amikacin was added 2h after meropenem (MEM+AK) or conversely (AK+MEM). Antibiotic concentrations were: MEM17 (17.71mg/L), AK8(8.17mg/L), MEM32 (32mg/L) and AK40 (40mg/L). GC: Growth control.

AK8+MEM17	0.26	-0.38	-0.97	-0.93	-0.86	-1.75	**0.67**
MEM32+AK8	-1.81	-2.43	-2.77	-3.17	-3.74	-4.59	**-0.87**
MEM17+AK8	-1.58	-2.61	-2.19	-2.07	-2.70	-2.55	**-0.26**
AK8=MEM32	-2.12	-2.70	-3.15	-2.76	-3.89	-4.59	**-1.39**
AK8=MEM17	-1.69	-1.97	-2.46	-1.70	-1.85	-3.08	**-0.12**

Table 11 Bacterial load reduction (log_{10} CFU/mL) in *Pseudomonas aeruginosa* isolates caused by each dosing schedule of meropenem (MEM) and amikacin (AK) in the time-kill curves with refreshment of the antibiotics. Bacterial load reduction was calculated by deducting the initial viable cell count from the final viable cell count. It was calculated for each time, experimental condition and isolate. Positive values correspond to an increase in the bacterial load, and negative values to a reduction. Bacterial load was considered stable when the reduction was ≤1 log_{10} CFU/mL. Antibiotics were administered simultaneously (AK=MEM) and staggered. For staggered schedules, amikacin was added 2h after meropenem (MEM+AK) or conversely (AK+MEM). Antibiotic concentrations were: MEM17 (17.71mg/L), AK8(8.17mg/L), MEM32 (32mg/L) and AK40 (40mg/L). GC: Growth control. (Continued)

DOSING SCHEDULE

		GC	AK8	MEM32	MEM17	AK8+ MEM32	AK8+ MEM17	MEM32 +AK8	MEM17 +AK8	AK8 = MEM32	AK8 = MEM17
ST179 (06-	no refreshment	3.78	3.64	2.99	3.39	-1.9	0.07	-1.25	-1.2	-2.02	**1.82**
014)	refreshment	4.86	4.46	2.41	4.19	-2.08	0.21	-1.47	-1.47	-1.71	**0.12**
ST235 (07-	no refreshment	4.64	4.61	3.73	4.33	3.41	4.24	-0.97	1.76	-2.02	**1.82**
004)	refreshment	5.02	4.91	0.53	2.59	-1.03	0.67	-0.87	-0.26	-1.39	**-0.12**

Table 12. Final bacterial load decrease in 24h-time-kill curves with and without antibiotic refreshment. Dosing schedules of amikacin (AK) and meropenem (MEM) were simultaneous (AK=MEM) and staggered. For staggered schedules, AK was added 2h after MEM (MEM+AK) or conversely (AK+MEM). Antibiotic concentrations were MEM32=32 mg/L and AK8=8.17 mg/L. Antibiotic refreshment was performed at 12 hours. GC: growth control without antibiotic.

TIME-KILL CURVES WITH REFRESHMENT OF ANTIBIOTICS AT 12H

CONDITION	BACTERICIDAL EFFECT		SYNERGY AT 24H	
	ST179 (06-014)	ST235 (07-004)	ST179 (06-014)	ST235 (07-004)
AK8=MEM17	NO	NO	YES	**YES**
AK8+MEM17	NO	NO	YES	**NO**
MEM17+AK8	NO	NO	YES	**YES**
AK8=MEM32	NO	NO	YES	**NO**
AK8+MEM32	NO	NO	YES	**NO**
MEM32+AK8	NO	NO	YES	**NO**

Table 13. PK/PD parameters in time-kill curves with antibiotic refreshment. Bactericidal (B) and synergistic (S) effect of simultaneous and staggered dosing schedules of amikacin and meropenem in combination against XDR *Pseudomonas aeruginosa* isolates. Amikacin (AK) and meropenem (MEM) were administered simultaneously (AK=MEM) and staggered. For staggered schedules, amikacin was added 2h after meropenem (MEM+AK) or conversely (AK+MEM). Amikacin concentration was 8.17 mg/L (AK8) and meropenem concentrations were 17.71 mg/L (MEM17) and 32 mg/L (MEM32). Antibiotic refreshment was performed at 12h.

4.4.1.6 Analysis of antibiotic degradation

Antibiotic concentration was assessed to evaluate the possible contribution of antibiotic degradation to bacterial regrowth at the end of time-kill curves. Samples were taken during the refreshed time-kill curves at 0h, twice at 12h (before and after refreshment) and at 24h. Meropenem presented an average degradation rate of 21.3% at 12h (Table 14). No degradation of amikacin was detected throughout the 24h time-kill curves.

CONDITION	CONCENTRATION (mg/L)	MEAN (mg/L)	ANTIBIOTIC RATE (%)	DEGRADATION (%)
MEM AT 0H	22	25.47±4.11	100	**0**
MEM+AK AT 0H	30			
MEM=AK AT 0H	24.4			
MEM AT 12H	15.4	20.78±3.96	81.58	**18.42**
AK+MEM AT 12H	23.7			
MEM+AK AT 12H	23.8			
MEM=AK AT 12H	20.2			
MEM AT 12H (post-refreshment)	31.1	31.9±2.07	100	**0**
AK+MEM AT 12H (post-refreshment)	35			
MEM+AK AT 12H (post-refreshment)	30.8			
MEM=AK AT 12H (post-refreshment)	30.7			
MEM AT 24H	24	24.23±0.25	75.97	**24.03**
AK+MEM AT 24H	24.2			
MEM+AK AT 24H	24.5			
MEAN VALUE AT 12H	-	-	**78.77**	**21.23**

Table 14. Average degradation rate of meropenem in refreshed time-kill curves. Dosing schedules of amikacin (AK) and meropenem (MEM) were simultaneous (AK=MEM) and staggered. For staggered schedules, AK was added 2h after MEM (MEM+AK) or conversely (AK+-MEM). Antibiotic concentrations were MEM32=32 mg/L and AK8=8.17 mg/L.

4.4.2 *Klebsiella pneumoniae*

Different dosing schedules of combined meropenem and amikacin were tested against five CP-KP isolates. The bacterial load reduction (log_{10} CFU/mL) for each dosing schedule is shown in Table 15.

	K1					
EXPERIMENTAL CONDITION	**0-2H**	**0-4H**	**0-8H**	**0-24H**	**B**	**S**
GROWTH CONTROL	1.50	2.83	3.16	3.36	NA	NA
AK8	1.37	2.42	3.09	3.35	-	NA
AK40	-2.60	-3.17	-2.42	2.86	-	NA
MEM17	0.62	1.22	2.96	3.36	-	NA
MEM32	-0.65	0.05	2.56	3.36	-	NA
AK8 + MEM17	1.30	1.81	2.83	3.27	-	-
AK8 + MEM32	1.29	1.58	2.41	3.19	-	-
AK40 + MEM17	-2.90	-3.77	-4.43	-5.75	**+**	**+**
AK40 + MEM32	-3.12	-3.89	-3.61	-5.25	**+**	**+**
MEM17 + AK8	0.48	1.02	2.55	3.40	-	-
MEM17 + AK40	0.21	-1.99	-2.06	3.19	-	-
MEM32 + AK8	-1.04	-0.81	1.90	3.37	-	-
MEM32 + AK40	-1.22	-3.10	-2.63	1.14	-	-
AK8 = MEM17	0.54	0.00	2.43	3.35	-	-
AK8 = MEM32	-0.96	-1.64	0.32	3.32	-	-

Table 15. Bacterial load reduction of *Klebsiella pneumoniae* isolates (log_{10} CFU/mL) and bactericidal (B) and synergistic (S) effect caused by each dosing schedules of meropenem (MEM) and amikacin (AK). Bacterial load reduction was calculated by deducting the final viable cell count from the initial viable cell count. It was calculated for each time, experimental condition and isolate. Positive values correspond to an increase in the bacterial load, and negative values to a reduction. Bacterial load was considered stable when the reduction was ≤1 log_{10} CFU/mL. The antibiotics were administered simultaneously (AK=MEM) and staggered. For staggered schedules, amikacin was added 2h after meropenem (MEM+AK) or conversely (AK+-MEM). Antibiotic concentrations were MEM17=17.71mg/L, AK8=8.17mg/L, MEM32=32mg/L and AK40=40mg/L. Growth control (GC); positive (+); negative (-), not applicable (NA).

AK40 = MEM17	-1.96	-3.86	-3.25	-2.87	-	**+**
AK40 = MEM32	-1.04	-3.19	-3.07	-2.54	-	**+**

K4

EXPERIMENTAL CONDITION	0-2H	0-4H	0-8H	0-24H	B	S
GROWTH CONTROL	1.28	2.76	3.82	4.08	NA	NA
AK8	1.57	2.72	3.71	4.08	-	NA
AK40	1.42	2.44	3.69	4.07	-	NA
MEM17	1.34	2.82	3.74	4.07	-	NA
MEM32	1.55	2.30	3.54	4.13	-	NA
AK8 + MEM17	1.48	2.52	3.69	4.06	-	-
AK8 + MEM32	1.45	2.57	3.43	4.07	-	-
AK40 + MEM17	1.60	2.53	3.69	3.89	-	-
AK40 + MEM32	1.26	2.62	3.44	4.07	-	-
MEM17 + AK8	1.55	2.42	3.67	3.87	-	-
MEM17 + AK40	1.55	2.66	3.72	3.81	-	-
MEM32 + AK8	1.68	2.25	3.68	4.00	-	-
MEM32 + AK40	1.27	1.85	3.44	4.03	-	-

Table 15. Bacterial load reduction of *Klebsiella pneumoniae* isolates (log_{10} CFU/mL) and bactericidal (B) and synergistic (S) effect caused by each dosing schedules of meropenem (MEM) and amikacin (AK). Bacterial load reduction was calculated by deducting the final viable cell count from the initial viable cell count. It was calculated for each time, experimental condition and isolate. Positive values correspond to an increase in the bacterial load, and negative values to a reduction. Bacterial load was considered stable when the reduction was ≤1 log_{10} CFU/mL. The antibiotics were administered simultaneously (AK=MEM) and staggered. For staggered schedules, amikacin was added 2h after meropenem (MEM+AK) or conversely (AK+MEM). Antibiotic concentrations were MEM17=17.71mg/L, AK8=8.17mg/L, MEM32=32mg/L and AK40=40mg/L. Growth control (GC); positive (+); negative (-), not applicable (NA). (Continued)

AK8 = MEM17	1.83	2.64	3.76	4.16	-	-
AK8 = MEM32	1.37	2.07	3.50	4.00	-	-
AK40 = MEM17	1.52	2.56	3.56	3.93	-	-
AK40 = MEM32	1.03	1.55	3.17	3.98	-	-

K10

EXPERIMENTAL CONDITION	0-2H	0-4H	0-8H	0-24H	B	S
GROWTH CONTROL	1.24	3.19	3.52	3.83	NA	NA
AK8	1.39	3.12	3.35	3.76	-	NA
MEM17	-2.99	-3.00	0.04	3.66	-	NA
MEM32	-3.58	-2.84	-0.28	3.78	-	NA
AK8 + MEM17	1.33	-0.79	0.45	3.70	-	NA
AK8 + MEM32	1.26	-0.47	1.94	3.71	-	-
MEM17 + AK8	-2.56	-2.97	-0.57	3.68	-	-
MEM32 + AK8	-3.24	-3.44	-1.09	3.63	-	-
AK8 = MEM17	-3.05	-3.26	0.11	3.81	-	-
AK8 = MEM32	-3.09	-3.45	-0.72	3.71	-	-

Table 15. Bacterial load reduction of *Klebsiella pneumoniae* isolates (log_{10} CFU/mL) and bactericidal (B) and synergistic (S) effect caused by each dosing schedules of meropenem (MEM) and amikacin (AK). Bacterial load reduction was calculated by deducting the final viable cell count from the initial viable cell count. It was calculated for each time, experimental condition and isolate. Positive values correspond to an increase in the bacterial load, and negative values to a reduction. Bacterial load was considered stable when the reduction was ≤1 log_{10} CFU/mL. The antibiotics were administered simultaneously (AK=MEM) and staggered. For staggered schedules, amikacin was added 2h after meropenem (MEM+AK) or conversely (AK+MEM). Antibiotic concentrations were MEM17=17.71mg/L, AK8=8.17mg/L, MEM32=32mg/L and AK40=40mg/L. Growth control (GC); positive (+); negative (-), not applicable (NA). (Continued)

K13

EXPERIMENTAL CONDITION	0-2H	0-4H	0-8H	0-24H	B	S
GROWTH CONTROL	1.56	2.72	3.65	3.83	NA	NA
AK8	-4.26	-4.52	-3.28	-2.62	-	NA
MEM17	1.39	2.81	3.58	3.81	-	NA
MEM32	1.09	2.67	3.44	3.78	-	NA
AK8 + MEM17	-3.77	-3.96	-4.14	-2.93	-	NA
AK8 + MEM32	-2.25	-4.67	-4.46	-3.44	+	-
MEM17 + AK8	0.96	-3.52	-3.41	-1.91	-	-
MEM32 + AK8	1.19	-1.62	-4.59	-2.71	-	-
AK8 = MEM17	-3.59	-4.63	-5.11	-3.45	+	-
AK8 = MEM32	-4.13	-4.57	-5.46	-3.32	+	-

Table 15. Bacterial load reduction of *Klebsiella pneumoniae* isolates (log_{10} CFU/mL) and bactericidal (B) and synergistic (S) effect caused by each dosing schedules of meropenem (MEM) and amikacin (AK). Bacterial load reduction was calculated by deducting the final viable cell count from the initial viable cell count. It was calculated for each time, experimental condition and isolate. Positive values correspond to an increase in the bacterial load, and negative values to a reduction. Bacterial load was considered stable when the reduction was ≤1 log_{10} CFU/mL. The antibiotics were administered simultaneously (AK=MEM) and staggered. For staggered schedules, amikacin was added 2h after meropenem (MEM+AK) or conversely (AK+MEM). Antibiotic concentrations were MEM17=17.71mg/L, AK8=8.17mg/L, MEM32=32mg/L and AK40=40mg/L. Growth control (GC); positive (+); negative (-), not applicable (NA). (Continued)

K14

EXPERIMENTAL CONDITION	0-2H	0-4H	0-8H	0-24H	B	S
GROWTH CONTROL	1.49	2.97	3.64	3.77	NA	NA
AK8	-1.15	-1.50	-1.71	-2.18	-	NA
MEM17	-1.08	-0.84	1.57	3.74	-	NA
MEM32	-1.65	-2.06	0.02	3.76	-	NA
AK8 + MEM17	-1.17	-1.88	-2.16	-3.56	+	-
AK8 + MEM32	-1.32	-1.72	-2.83	-3.57	+	-
MEM17 + AK8	-1.23	-2.31	-2.37	-3.28	+	-
MEM32 + AK8	-1.72	-2.08	-2.03	-2.05	-	-
AK8 = MEM17	-1.36	-1.30	-2.71	-2.33	-	-
AK8 = MEM32	-1.96	-2.48	-1.78	-4.17	+	-

Table 15. Bacterial load reduction of *Klebsiella pneumoniae* isolates (log_{10} CFU/mL) and bactericidal (B) and synergistic (S) effect caused by each dosing schedules of meropenem (MEM) and amikacin (AK). Bacterial load reduction was calculated by deducting the final viable cell count from the initial viable cell count. It was calculated for each time, experimental condition and isolate. Positive values correspond to an increase in the bacterial load, and negative values to a reduction. Bacterial load was considered stable when the reduction was ≤1 log_{10} CFU/mL. The antibiotics were administered simultaneously (AK=MEM) and staggered. For staggered schedules, amikacin was added 2h after meropenem (MEM+AK) or conversely (AK+MEM). Antibiotic concentrations were MEM17=17.71mg/L, AK8=8.17mg/L, MEM32=32mg/L and AK40=40mg/L. Growth control (GC); positive (+); negative (-), not applicable (NA). (Continued)

4.4.2.1 Monotherapies

Both meropenem and amikacin were assessed alone in all *K. pneumoniae* isolates. The results of MEM and AK monotherapies are shown in Figure 22.

Monotherapy of amikacin with a concentration of 8.17 µg/mL (AK8) did not cause any effect against the three amikacin-resistant isolates [K1, K4, K10]. Regarding the amikacin-susceptible isolates, K13 had an initial reduction [4.26 $\log_{10}$ CFU/mL at 2h], followed by regrowth of 1.64 $\log_{10}$ CFU/mL, and K14 had an overall bacterial load reduction of 2.18 $\log_{10}$ CFU/mL. The highest concentration of amikacin (AK40) was assessed against two amikacin-resistant isolates [K1, K4]. AK40 caused an initial decrease [2.6 $\log_{10}$ CFU/mL at 2h] in K1 but regrowth reached a final bacterial load like the growth control. The high-level amikacin-resistant K4 isolate had the same behaviour as the growth control, reaching a similar final bacterial load.

Monotherapy of meropenem caused final regrowth against the five *K. pneumoniae* isolates. The meropenem concentration of 17.17 µg/mL (MEM17) did not cause any effect against three out of the four meropenem-resistant isolates [K1, K4, K13]. A final bacterial load like the growth control was reached both in the other meropenem-resistant isolate [K14] and in the isolate with susceptibility increased exposure to meropenem [K10], despite their initial bacterial load reduction [1.08 $\log_{10}$ CFU/mL and 2.99 $\log_{10}$ CFU/mL at 2h, respectively]. MEM32 had a similar effect to MEM17 against four isolates [K4, K10, K13, K14]. Compared to MEM17, the remaining isolate [K1] showed an increase in the bacterial load after a 4-hour lag, reaching a similar final bacterial load. The highest initial reduction in the bacterial load [3.58 $\log_{10}$ CFU/mL at 2h] was observed in K10, which had the lowest meropenem MIC (8 mg/L).

4.4.2.2 Simultaneous schedules of the antibiotic combination

Simultaneous schedules (AK=MEM) were studied by adding both meropenem and amikacin at the same time in the beginning of the time-kill experiments (Figure 23).

The simultaneous schedule AK8=MEM17 had no effect against the two isolates that were resistant to both antibiotics [K1, K4]. The amikacin-resistant isolate K10, which was susceptible to meropenem with increased exposure, had an initial reduction in the bacterial load [3.05 log10 CFU/mL at 2h], followed by an increase that reached the growth control value at the end of the experiment. The decrease in the bacterial load of the two meropenem-resistant amikacin-susceptible isolates K13 and K14 [5.11 and 2.71 $\log_{10}$ CFU/mL at 8h, respectively] was followed by no regrowth.

The simultaneous schedule with a higher concentration of meropenem (AK8=MEM32) had the same effect as AK8=MEM17 against K4, K10 and K13. Regarding K14, a further decrease in the bacterial load of 2.39 $\log_{10}$ CFU/mL was achieved compared to AK8=MEM17, corresponfing to a final reduction of 4.17 $\log_{10}$ CFU/mL. Despite the initial decrease in K1 [1.64 $\log_{10}$ CFU/mL], the final bacterial load was similar to the growth control.

The highest concentration of amikacin (AK40) was tested against the two isolates that were resistant to both antibiotics [K1, K4]. Compared to AK8=MEM17, no differences

were observed in K4 using AK40=MEM17 whereas there was a higher reduction in the bacterial load of K1 [3.86 $\log_{10}$ CFU/mL at 4h] without further regrowth. No differences were observed when the highest concentration of meropenem (MEM32) was simultaneously added to AK40 (AK40=MEM32).

4.4.2.3 Staggered schedules of the antibiotic combination

For staggered schedules, amikacin was added 2h after meropenem (MEM+AK) or conversely (AK+MEM) (Figure 24).

The staggered schedule AK8+MEM17 did not cause any effect against the two isolates [K1, K4] that were resistant to both antibiotics. The initial bacterial load increase in the amikacin-resistant isolate K10, which was susceptible to meropenem with increased exposure, was followed by a 2-log decrease [2.12 $\log_{10}$ CFU/mL] when MEM17 was added. Regarding the two meropenem-resistant amikacin-susceptible isolates, K13 achieved a 3-$\log_{10}$ decrease [3.77 $\log_{10}$ CFU/mL] before the administration of MEM17 and K14 had a decrease of 1.88 $\log_{10}$ CFU/mL 2h after adding MEM17. No regrowth was observed for these two isolates [K13, K14] whereas K10 reached a final bacterial load similar to the growth control.

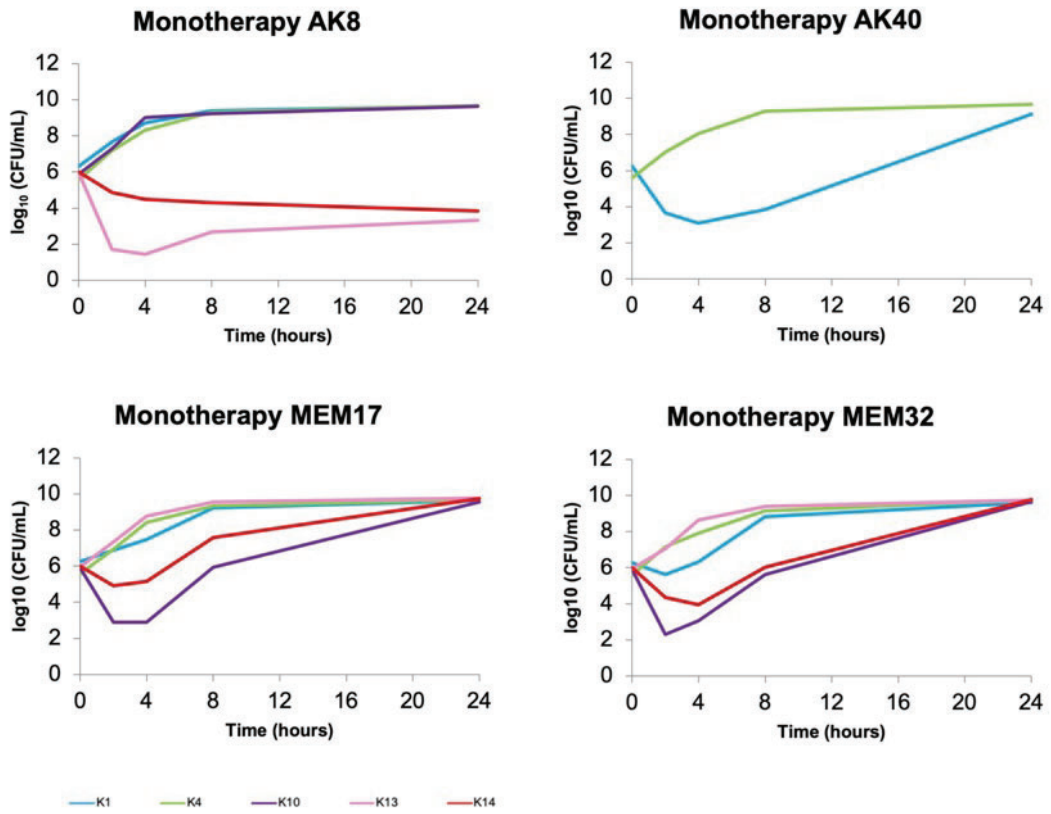

Figure 22. Time-kill curves of *Klebsiella pneumoniae* isolates in amikacin (AK) and meropenem (MEM) monotherapies. The antibiotic concentrations tested were AK8=8.17 mg/L, AK40=40 mg/L, MEM17=17.71 mg/L and MEM32=32 mg/L. Data were expressed as the logarithm with the base 10 of CFU/mL ($\log_{10}$ CFU/mL).

The staggered schedule MEM17+AK8 caused the opposite initial effect in K10 and K13 compared to the schedule AK8+MEM17. The bacterial load of K10 started decreasing from the beginning of the experiment when meropenem was given alone. The initial increase in the bacterial load of the meropenem-resistant K13, which had an amikacin of MIC 1 mg/L, was followed by -4.48 log_{10} CFU/mL decrease when amikacin was added. No differences between both schedules were observed against the isolates that were resistant to both antibiotics [K1, K4] and the meropenem-resistant isolate K14 with an amikacin MIC of 4 mg/L.

The highest amikacin concentration (AK40) in the staggered schedules caused no difference against K4 compared to AK8. The schedule AK40+MEM17 caused an initial bacterial decrease in the other isolate with resistance to both antibiotics [K1], reaching a final overall reduction >5.5 log_{10} CFU/mL, whereas regrowth was observed using the reverse schedule (MEM17+AK40). The highest meropenem concentration (MEM32) in the staggered schedules caused no differences in the behaviour of the five isolates compared to MEM17. The only exception was MEM32+AK8 against K1, with an initial 1-log10 reduction [1.08 log_{10} CFU/mL] that was followed by regrowth. The staggered

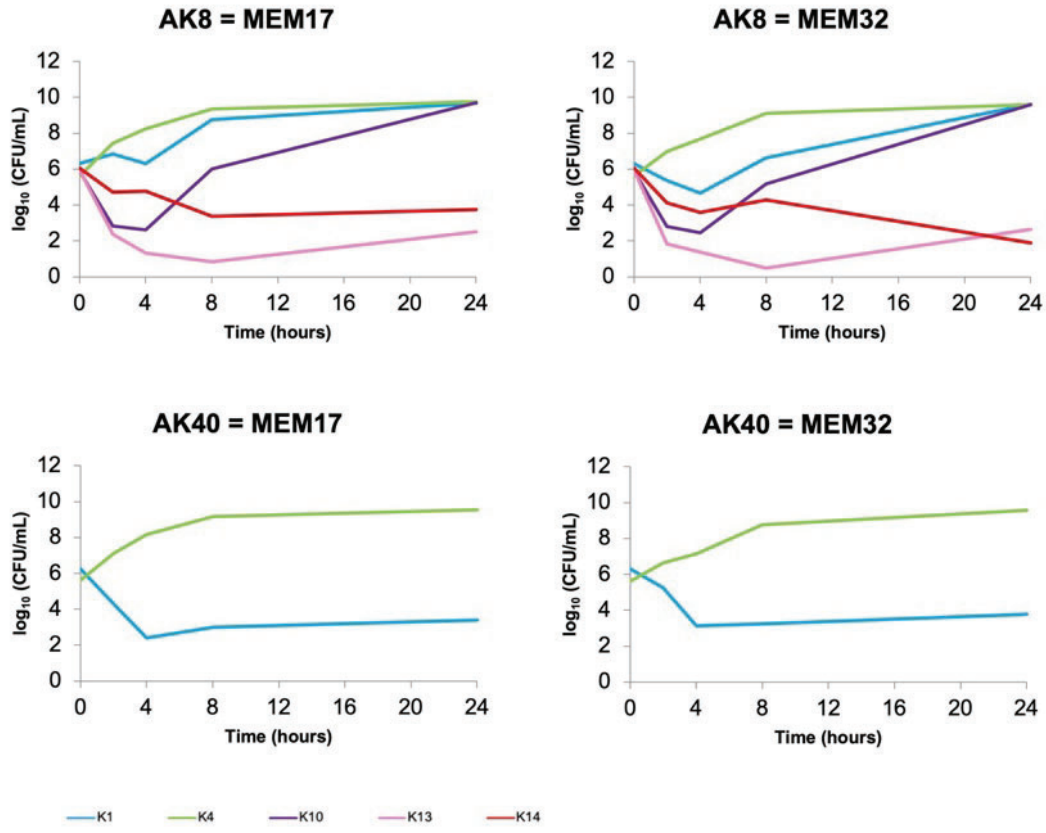

Figure 23. Time-kill curves of Klebsiella pneumoniae isolates performed using simultaneous administration (AK=MEM) of amikacin (AK) and meropenem (MEM). Antibiotic concentrations were AK8=8.17 mg/L, AK40=40 mg/L, MEM17=17.71 mg/L and MEM32=32 mg/L. Data were expressed as the logarithm with the base 10 of CFU/mL (log_{10} CFU/mL).

schedules with the high concentration of the two antibiotics had no effect against K4. Both staggered schedules with high concentrations caused an initial bacterial load reduction [>3 $\log_{10}$ CFU/mL] in K1 but final regrowth was observed when meropenem was given first (MEM32+AK40).

4.4.2.4 Bactericidal effect and synergy

Bactericidal and synergistic effects of the different dosing schedules of meropenem and amikacin in these five *K. pneumoniae* isolates (Table 16). No synergy was detected with any of the schedules using either the lower concentrations (AK8 or MEM17) or MEM32 combined with AK8. Bactericidal effect was observed in the two meropenem-resistant amikacin-susceptible isolates [K13, K14] when the staggered schedules started with AK8 or when using these simultaneous schedules; the only exception was AK8=MEM17 against K14.

These pharmacodynamic parameters were also assessed using dosing schedules with AK40 against the isolates with resistance to both antibiotics [K1, K4]. Synergy using these simultaneous schedules or when the staggered schedules started with AK40 was detected in K1. A bactericidal effect when using these staggered schedules starting with AK40 was detected against K1.

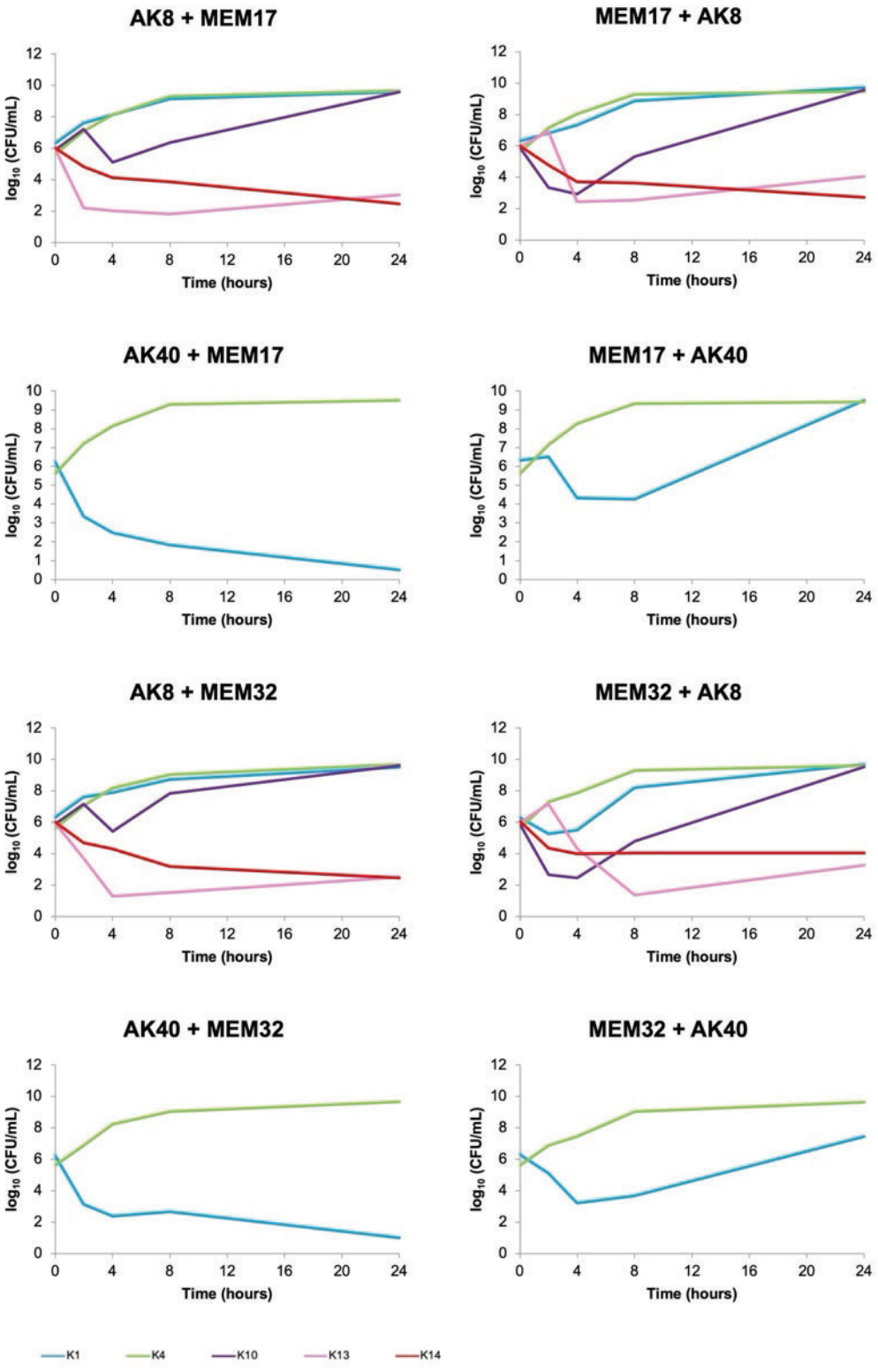

Figure 24. Time-kill curves of *Klebsiella pneumoniae* isolates performed using staggered regimen of amikacin (AK) and meropenem (MEM). Meropenem was added 2h after amikacin (AK+MEM) or conversely (MEM+AK). Antibiotic concentrations were: AK8 (8.17 mg/L), AK40 (40 mg/L), MEM17(17.71 mg/L) and MEM32 (32 mg/L). Data were expressed as $\log_{10}$ CFU/mL.

05
Discussion

5. Discussion

Infections caused by MDR bacteria are difficult to treat and often require the use of antibiotic combinations. In this context, the present doctoral thesis aimed to both validate an ATP measurement assay as an alternative to the colony count method for the study of antibiotic combinations in time-kill curves and compare the efficacy of different dosing schedules of the antibiotic combination meropenem plus amikacin against XDR *P. aeruginosa* and MDR CP-KP.

5.1 ATP-Measurement assay

Antibiotic combinations are often administered to treat in infections caused by MDR microorganisms. However, the evaluation of antibiotic combinations is too laborious to be included in the clinical laboratory workflow. The use of a quick and easy-to-perform ATP measurement assay to evaluate the performance of antibiotic combinations in time-kill curves would avoid an additional overnight culture for viable cell count.

The standardization of the ATP assay was performed for the set-up of this equipment to evaluate antibiotic combinations. Background, linearity, and detection limit were studied for the standardization of the ATP assay. These parameters were initially studied in two different Gram-negative species (*P. aeruginosa* and *K. pneumoniae*) using two

different media for antibiotic washing and reading, i.e. neutral saline solution (NSS) and cation-adjusted Mueller-Hinton (CA-MHB). The performance of NSS was compared to CA-MHB, which was the medium recommended by the manufacturer and used in previous studies.[173,174,198] Background oscillation for both media was considered relevant enough to be removed from the assay results. Therefore, the mean value of the background was calculated and subtracted at each reading time. Linearity showed similar Pearson's correlation coefficients for both CA-MH and NSS. However, given the lower detection limit and the broader range of linearity determined for NSS, this was established as the optimal medium instead of CA-MH. The detection limit obtained using NSS was considered adequate to evaluate bactericidal effect and synergy.

The standardization was also performed using *E. faecium*. Background, linearity and detection limit were studied in this Gram-positive species using NSS given the wider linear range observed with this medium in the previous experiments with Gram-negative bacteria. The detection limit and the range of linearity obtained with this species were the same as those obtained with Gram-negative bacteria. No significant differences in the performance of the ATP assay were observed between Gram-negative and Gram-positive species. This was an unexpected finding because *E. faecium* relies strictly on fermentative metabolism, which is less efficient than aerobic respiration, therefore producing lower amounts of ATP than the two Gram-negative bacilli.[72] Furthermore, high correlation between CFU and RLU was also observed in a recent study where the ATP assay was used to evaluate oral cleaning by quantifying levels of streptococci, which have the same type of metabolism as enterococci.[199]

Bioluminescence can be affected by external factors. Therefore, control of these variables affecting the bioluminescence reaction is essential for reliable results. The composition of the reading medium is one of these variables. Several ions have been reported to quench the bioluminescence reaction catalyzed by the firefly luciferase.[200] Cations should be strictly controlled while performing the assay, not only because of this potential quenching effect, but also because magnesium is required for the activity of this enzyme.[174,196] The cation concentration in CA-MHB medium may interfere with the RLU signal, consistent with our standardization results that support usingNSS instead. Additionally, extracellular ATP may also influence the signal as previously reported by Cai *et al.*[198] These authors used enzymatic methods to remove extracellular ATP from the reading medium. In contrast, ATP removal in our study may have been achieved during the washing step that involved centrifugation to eliminate antibiotics, which simplifies the process compared to the enzymatical procedure.

Two methods for measuring viable bacterial cells in time-kill assays were compared. The correlation between CFU using the conventional cell count and RLU using the ATP-assay was previously reported to diminish at 24 hours due to metabolic differences between growth phases.[201] However, these authors included readings above the upper limit of their linearity range which may have contributed to this result. In contrast, in the present study no differences in the correlation between CFU and RLU were found throughout the time-kill curve at different growth phases, probably because the readings were always within the linearity range.

Establishing the cut-off points in the ATP measurement assay for synergy and bactericidal effect was required. The results obtained in the evaluation of antibiotic combinations

using the ATP measurement assay were equivalent to those results obtained with the conventional method. Given that specificity should be prioritized over sensitivity when considering a therapeutic benefit of a combination, 100% specificity cutoff points for synergy should be used to avoid false positives and unnecessary side effects. Synergy should be confirmed by the colony count method when the bacterial load decrease is between the cutoff with maximum sensitivity and specificity and the 100% specificity cutoff point. In this situation, the same aliquot could be further evaluated by the conventional method.

The evaluation of the ATP assay for the study of antibiotic combinations included only *P. aeruginosa* and *K. pneumoniae*. Other Gram-negative bacilli and Gram-positive bacteria should also be evaluated to validate its use in other species. One of the strengths of our study was the large sample size of paired readings to establish the cutoff points for synergy and bactericidal effect, especially for *P. aeruginosa*. Another strength was the number of different antibiotic combinations included, which supports its potential in clinical backgrounds.

In conclusion, the ATP measurement assay used to determine the viable cell count in time-kill curves was a robust technique as the RLU signal correlated with CFU count when the assay was performed within the linear range. This easy-to-perform assay was adequate for antibiotic combination studies in *P. aeruginosa* and *K. pneumoniae*, defining cutoff points for synergy and bactericidal effect.

5.2 Optimization of dosing schedules of meropenem plus amikacin

The combination of meropenem plus amikacin is commonly used for empirical treatment of severe infections to minimize the risk of inadequate initial therapy when Gram-negative bacilli are suspected.[202] However, dosing schedules of this antibiotic combination are not clearly established in guidelines.[181,203] The timing of amikacin administration relative to the initiation of meropenem may have an impact on the initial reduction in the bacterial load, which in turn may be relevant in empirical treatments. The present work evaluated both simultaneous and staggered schedules of meropenem plus amikacin, mainly focusing on this initial impact.

5.2.1 *Pseudomonas aeruginosa*

Achieving an initial bacterial load decline is especially relevant in high inoculum infections caused by *P. aeruginosa*.[204] Current guidelines include aminoglycosides in combination with β-lactam antibiotics as initial empirical therapy for serious infections.[184,205] Otherwise, patients should receive β-lactam antibiotic monotherapy, always considering previous organisms identified from the patient, previous antibiotic exposure, and the local AST patterns for the most likely pathogens.[184,205] The combination of meropenem plus amikacin is one of the empirical options for serious *P. aeruginosa* infections, being its initial use reported to provide some bacterial killing against carbapenem-resistant isolates in dynamic models.[181,205] This combined therapeutic option may be optimized to achieve the best clinical outcome in these pseudomonal infections.

Monotherapy with amikacin may be used as an alternative to treat low-inoculum DTR *P.*

aeruginosa infections like urinary tract infections.[87,184] In our study, an initial bacterial load reduction was observed in most of the XDR isolates when the antibiotic concentration (either amikacin or meropenem in monotherapy) was close to or above the MIC. However, this reduction was followed by final regrowth in most of cases and no bactericidal effect was observed. The development of resistance using a single-agent therapy has been reported in pseudomonal isolates, especially highlighting amikacin.[205,206] Antibiotic combinations have been considered to reduce the risk of resistance emerging during treatment.[87,205,207]

Simultaneous and staggered conditions of amikacin and meropenem were compared to evaluate the influence of the dosing schedules against XDR *P. aeruginosa*. Simultaneous administration achieved the highest initial reduction in the bacterial load of all strains, regardless of the antibiotic concentration tested and their MIC values. Our results are consistent with a previous study using a combination of ciprofloxacin and azlocillin, where simultaneous administration was more effective than staggered dosing.[208] Additionally, the order of the first antibiotic given in the staggered administration was important. We found that the staggered schedules AK8+MEM17 and MEM17+AK8 were less effective when isolates had a high MIC value of the antibiotic given first. Accordingly, the antibiotic with lower MIC should be given first to avoid a two-hour monotherapy with the less effective antibiotic. A delay in giving an active antimicrobial therapy to treat *P. aeruginosa* infections has been associated with increased mortality.[209] According to our results, a simultaneous administration of meropenem and amikacin may be more effective for empirical treatments than staggered dosing schedules given that AST results are not available yet.

The effect of high concentrations of each antibiotic in this combination was also evaluated. On one hand, aminoglycosides are known to have a concentration-dependent killing and post-antibiotic effect.[210] These pharmacodynamic properties may justify the use of a once-daily higher-dose to optimize bacterial killing without greater toxicity compared to its fractionated administration. A single dose of 15 mg/kg/day amikacin would often reach a peak concentration of 25-35 mg/L, although higher doses may be required in critically ill patients and other clinical situations, achieving higher peak concentrations.[211] The PK/PD target for amikacin is the maximum concentration (Cmax)/CMI ratio ≥ 8, which would be very difficult to reach *in vivo* against our XDR *P. aeruginosa* isolates.[212] In our time-kill curves, we found a larger initial reduction in the bacterial load of most isolates using the higher amikacin concentration (AK40) that simulated a peak concentration during the first hours. However, the concentration of amikacin remained constant throughout these 24-hour static experiments, which is not a realistic scenario. On the other hand, meropenem is known to have a time-dependent activity, which means that its effectivity depends on the amount of time that the antibiotic concentration is above the MIC value.[213] In our study, no relevant differences were observed with the two meropenem concentrations (MEM17 and MEM32) in most isolates. Both concentrations were either below or equal to the MIC of the isolates and were considered suboptimal. Additionally, we found that the simultaneous dosing schedule with MEM32 achieved reduction in the bacterial load two hours earlier than with MEM17. As mentioned before, an early reduction in the bacterial load in XDR *P. aeruginosa* infections may result in better clinical outcomes, especially in high inoculum infections.[207] Reiterated above, the simultaneous dosing schedule of this antibiotic combination might be more suitable than staggered schedules in the treatment of these

infections. However, this is an *in vitro* observation that should be further validated by means of dynamic studies and clinical studies.

Antibiotic combination therapies aim to achieve a synergistic effect.[214] Synergy with the combination meropenem and amikacin has been reported in several MDR Gram-negative bacilli, including *P. aeruginosa*.[215–217] All dosing schedules including AK8 and MEM17 achieved synergy in isolates with meropenem MIC of 32 mg/L. The only exception was AK8+MEM17 in the high-level amikacin-resistant isolate ST235 (07-004). Remarkably, the other isolate [ST274 (09-011)] with the same amikacin MIC (128 mg/L) presented synergy using this schedule. The different behaviour between both amikacin-resistant isolates could be partially explained by the presence of an aminoglycoside-modifying enzyme (AME) in ST235 (07-004).[218] When increasing the concentration of amikacin (AK40) synergy was observed for all the dosing schedules only in the AME-carrying isolate. Compared to the MEM17-containing schedules, no differences were observed using the higher concentration of meropenem (MEM32) except for ST175 (12-012), where there was synergy in all dosing schedules. Those isolates with a meropenem MIC of 32 mg/L achieved synergy using schedules with low concentrations, whereas the forementioned isolate ST175 (12-012) (MIC of 64 mg/L) required the combination with MEM32 for synergy. Drug combinations can enhance efficacy and may allow to lower the individual drug doses.[219] Our results suggest that a meropenem concentration of half the MIC value combined with AK8 may be useful to achieve a synergistic effect against these isolates although this should be further assessed in dynamic assays.

Combination therapies should be bactericidal against the pathogen that causes the infection. The bactericidal effect is calculated at 24 hours allowing to detect the emergence of resistant subpopulations.[155] In our study, none of the schedules presented bactericidal effect against the isolates but the control isolate Psd2209. The abscence of bactericidal effect resulted from late bacterial regrowth, a phenomenon previously described due to the inherently static nature of time-kill curves.[220] Bacterial regrowth could be attributable to antibiotic degradation, heteroresistance or the emergence of resistance via mutational or adaptive mechanisms.[221,222]

Antibiotic degradation over time could influence the results of the time-kill curves. Amikacin remained stable throughout these curves, whereas the degradation of meropenem (21.23% at 12h) could have had an impact on the results. Therefore, an approach where time-kill curves refreshing antibiotics at 12 hours were performed in two isolates and compared to the standard time-kill curves. A decrease in final regrowth was observed in some of the dosing schedules for isolate ST235 (07-004) whereas no differences were observed for isolate ST179 (06-014). Both isolates had the same meropenem MIC but different amikacin MIC (128 mg/L and 16 mg/L, respectively), which may partially explain the different impact of meropenem degradation on regrowth. The loss of synergy observed in ST235 (07- 004) in two dosing schedules might be explained by the aforementioned decrease in final regrowth. Hence, meropenem degradation may negatively impact *in vitro* results for this antibiotic combination. Further studies using the Hollow-fiber technique should be performed to simulate antibiotic dosing schedules *in vivo*.[223]

Heteroresistance has been previously contribute to treatment failure.[224] The analysis of this phenomenon is complex and cannot be detected by the routine antibiotic-

susceptibility assays employed in clinical laboratories. Carbapenem heteroresistance has been previously described in *P. aeruginosa* but there is little information on this phenomenon for aminoglycosides. To our knowledge, amikacin heteroresitance in *P. aeruginosa* has only been described in one recent study.[225] Out of a collection of 170 isolates these authors found 66.5% of heteroresistance to amikacin. The selection of heteroresistant subpopulations may have contributed to regrowth in our time-kill curve experiments. Heteroresistance testing was limited to amikacin considering the antibiotic susceptibility profiles of our isolates. None of these isolates was heteroresistant to amikacin according to PAP evaluation criteria.[226] Nevertheless, all isolates but ST179 (06-014) had subpopulations with a two-fold increase in the amikacin MIC value, which could have been easily selected.

The emergence of resistant mutants may contribute to the final regrowth in time-kill curve experiments. Resistant subpopulations are known to emerge due to spontaneous mutations after an exposition to suboptimal antibiotic concentrations.[227] These resistant mutants can be selected within the range between the MIC and the mutant prevention concentration (MPC), which is the lowest antibiotic concentration that is able to prevent the emergence of these mutants.[227] The antibiotic concentrations tested in our time-kill experiments were close to MIC values for each antibiotic in most of the pseudomonal isolates. Therefore, the use of suboptimal concentrations may have contributed to the selection of mutants and to the final regrowth.

5.2.2 *Klebsiella pneumoniae*

The combination of meropenem plus amikacin has been used for empirical treatment of infections caused by *Enterobacterales*, including *K. pneumoniae*.[202] However, the current guidelines do not recommend the use of carbapenems when their susceptibility is not confirmed or a carbapenemase-producing isolate is detected.[175] Before the deployment of the newer beta-lactam antibiotics, the administration of extended-infusion meropenem in combination with a second agent like an aminoglycoside was considered a standard practice to treat infections caused by *Enterobacterales* isolates with meropenem MIC values of 8-16 mg/L.[175] Previously reported time-kill experiments showed synergy and enhanced bactericidal activity of combining meropenem plus amikacin against *K. pneumoniae* with reduced susceptibility to carbapenems.[228] These types of experiments are usually performed with fixed concentration of simultaneous antibiotic combinations. To our knowledge, there were no previous studies about the effect of different dosing schedules of this antibiotic combination on the early decrease in the bacterial load of CP-KP isolates.

The early killing dynamics of the combination meropenem plus amikacin against CP-KP differed depending on the dosing schedule. The simultaneous schedule AK8=MEM17 caused an initial reduction in the bacterial load of the two amikacin-susceptible meropenem-resistant isolates (K13 and K14), and the amikacin-resistant isolate that was susceptible increased exposure to meropenem (K10). Staggered administration of this combination also caused an initial decline in these three isolates, but the reduction differed depending on the first antibiotic added. Accordingly, the bacterial load started decreasing earlier in K10 and in K13 when using MEM17+AK8 and AK8+MEM17, respectively. This behaviour suggests that the corresponding first antibiotic in staggered schedules should be given at a concentration above the MIC to ensure a larger initial reduction in the bacterial load. These results in CP-KP isolates support our previous

observation in XDR P. aeruginosa isolates, suggesting that simultaneous schedules of meropenem plus amikacin may be safer and more effective approach than staggered schedules when given empirically as AST results are still unknown.

Suboptimal concentrations of antibiotics are associated with treatment failure.[229] *In vivo* beta-lactam efficacy depends on the duration that the free drug concentration remains above the MIC during the dosing interval.[230] The concentration MEM17 in the time-kill experiments was suboptimal for most CP-KP isolates based on their MIC. Considered suboptimal for most isolates as well, a higher concentration of meropenem (MEM32) that was closer to the toxicity limit was also evaluated in these experiments.[230] Compared to MEM17, an enhanced initial reduction in the bacterial load or a delay in growth was observed in some CP-KP isolates when MEM32 was used, either alone or in combination. Our results suggest that a high concentration of meropenem could have an additional benefit in the early dynamics, but this *in vitro* finding should be further assessed *in vivo*, and clinical toxicity should be monitored.

Aminoglycosides are concentration-dependent antibiotics with short half-life and a narrow therapeutic index due to its nephrotoxicity.[231] As mentioned before, a daily single high-dose of amikacin can be administered to ensure PK/PD targets, to decrease renal toxicity and to extend the post antibiotic effect.[232] We evaluated the effect of meropenem combined with a peak concentration of amikacin (40 mg/L) against the two high-level amikacin-resistant isolates. As expected, K4 (amikacin MIC>128 mg/L) had the same behaviour as the growth control with AK40. In contrast, meropenem combined with AK40 caused an initial reduction in the bacterial load of K1 (amikacin MIC=32 mg/L) except when MEM17+AK40 was used.

MIC values of meropenem and amikacin were more relevant in the initial bacterial reduction than the specific mechanism of resistance. The impact of meropenem MIC value in the clinical outcome of patients infected by KPC-*Klebsiella pneumoniae* has been previously reported.[233] This observational study showed that combining an aminoglycoside with a carbapenem was associated with lower mortality rates provided that meropenem was not resistant (MIC≤8 mg/L). In the present study, the two KPC-carrying isolates differed in their behaviour, probably due to their different MIC values. This combination had no effect in K1 (high-level of resistance to both antibiotics) whereas it caused an initial reduction in K10 (meropenem MIC 8 mg/L, amikacin MIC 16 mg/L) using the simultaneous schedule and only when meropenem was first added in the staggered schedule. The differences in the initial reduction in the bacterial load observed between K13 and K14 (both OXA-48- and ESBL-carriers) may also be attributable to their respective MICs. Our results showed that a higher initial reduction in the bacterial load was achieved when the concentration of the first antibiotic was above the MIC. When this was considered in the staggered schedule, the reduction in the bacterial load was similar to the simultaneous schedule. These findings in CP-KP are similar to those we observed in XDR *P. aeruginosa*. Therefore, simultaneous schedules of meropenem and amikacin rather than staggered should be used in empirical treatments given that MICs are unknown.

Combining aminoglycosides with β-lactams in the empirical treatment can broaden the spectrum and expedite bacterial clearance.[232] However, the impact of these schedules on the initial bacterial reduction of these CP-KP isolates was not translated into final

bactericidal and synergy effects in our time-kill experiments due to bacterial regrowth. Time-kill curves are typically performed over 24 hours to confirm bacterial eradication but the data collected at that time may not always be clinically relevant for assessing synergy, as the fixed concentrations used do not reflect standard antibiotic administration regimens and some antibiotics may also degrade over time.[234] Therefore, we suggest that calculating synergy at an earlier timepoint such as at 8 hours instead of 24 hours may provide a more accurate reflection of *in vivo* conditions.

As previously mentioned, final regrowth in time-kill curves could be attributable to meropenem degradation, the emergence of antibiotic resistance or heteroresistance.[235,236] Given the time-dependent nature of meropenem, an optimal concentration above the MIC should be maintained *in vivo* by extended or continuous perfusion to ensure PK/PD targets. An increase in meropenem and amikacin MIC values has been reported *in vivo* in a mice model with an infection caused by a CP-KP isolate with heteroresistance to both drugs after the exposure to these antibiotics.[237] Resistant subpopulations may become enriched during antibiotic treatment, driving a shift from heteroresistance to homogeneous resistance. Further studies employing a dynamic model should be conducted to assess the behavior of these resistant subpopulations under simulated clinical dosing.

The evaluation of the different dosing schedules of this antibiotic combination had some limitations. The study was performed only in *P. aeruginosa* and *K. pneumoniae*. A larger sample size including different resistant phenotypes should be assessed and other Gram-negative bacilli included. We assessed two different concentrations for each antibiotic, which were selected based on achievable plasma levels with clinical dosages. However, a time-kill curve is a fixed-concentration static model that cannot replicate the dynamic pharmacokinetics that occur *in vivo* following antibiotic administration.

In conclusion, the combination of meropenem plus amikacin effectively reduced the bacterial load in most XDR *P. aeruginosa* and CP-KP isolates during the first hours. Staggered dosing of this combination was more effective when the concentration of the first agent exceeded the MIC, whereas simultaneous administration achieved reductions comparable to the most effective staggered schedules. As MIC values are unknown in empirical treatments, simultaneous dosing of meropenem plus amikacin may offer a more reliable approach for initial reduction in the bacterial load. This proposed empirical simultaneous strategy warrants further investigation using dynamic *in vitro* models and *in vivo* validation.

05
Conclusions

6 Conclusions

1. The ATP measurement assay was a robust technique to determine the cell count in time-kill curves. The RLU signal correlated with CFU count when the assay was performed within the linear range in *Pseudomonas aeruginosa, Klebsiella pneumoniae* and *Enterococcus faecium*. Neutral saline solution yielded a wider range of linearity than cation-adjusted Mueller-Hinton and was further established as washing and dilution medium.

2. The ATP assay was adequate for evaluating antibiotic combinations against *P. aeruginosa* and *K. pneumoniae* by means of time-kill curves. The categorization of bactericidal effect and synergy using this technique was equivalent to that using the conventional colony count method.

3. Time-kill results of antibiotic combinations can be obtained within the same day when using the ATP measurement assay as no overnight incubation is required. The simplicity of this technique may facilitate the implementation of antibiotic combinations studies within the work-flow of clinical laboratories.

4. The combination of meropenem plus amikacin achieved a reduction in the initial bacterial load of most extensively drug-resistant *P. aeruginosa* and carbapenemase-producing *Klebsiella pneumoniae* isolates.

5. Staggered schedules of meropenem plus amikacin were more effective in reducing the initial bacterial load when the concentration of the first agent was above the MIC of the isolates.

6. Simultaneous schedules of this antibiotic combination resulted in an initial bacterial load reduction comparable to that achieved by the most effective staggered schedules. Since MICs are unknown in empirical treatments, simultaneous administrationof meropenem plus amikacin may reduce the initial bacterial load more effectively than staggered dosing schedules.

7. The combined schedules with a higher concentration of meropenem caused similar reductions in the initial bacterial load the mean concentration derived from the AUC_{24}. An earlier bacterial load reduction was additionally observed using the highest concentration of meropenem simultaneously. Combining a peak amikacin concentration of 40 mg/L with meropenem achieved a larger initial reduction in the bacterial load than the lower concentration in most isolates.

8. The finding that the empirical combination of meropenem plus amikacin would benefit from simultaneous administration should be further validated by means of an *in vitro* dynamic model or *in vivo* models.

06
Bibliography

1. Hutchings, M., Truman, A. & Wilkinson, B. Antibiotics: past, present and future. *Current Opinion in Microbiology* vol. 51 72–80 Preprint at https://doi.org/10.1016/j.mib.2019.10.008 (2019).

2. da Cunha, B. R., Fonseca, L. P. & Calado, C. R. C. Antibiotic discovery: Where have we come from, where do we go? *Antibiotics* **8**, (2019).

3. Aslam, B. *et al.* Antibiotic resistance: a rundown of a global crisis. *Infection and Drug Resistance* vol. 11 1645–1658 Preprint at https://doi.org/10.2147/IDR.S173867 (2018).

4. Marquardt, R. R. & Li, S. Antimicrobial resistance in livestock: Advances and alternatives to antibiotics. *Animal Frontiers* **8**, 30–37 (2018).

5. Aloke, C. & Achilonu, I. Coping with the ESKAPE pathogens: Evolving strategies, challenges and future prospects. *Microb Pathog* **175**, 105963 (2023).

6. Hibbing, M. E., Fuqua, C., Parsek, M. R. & Peterson, S. B. Bacterial competition: Surviving and thriving in the microbial jungle. *Nature Reviews Microbiology* vol. 8 15–25 Preprint at https://doi.org/10.1038/nrmicro2259 (2010).

7. Bottery, M. J., Pitchford, J. W. & Friman, V.-P. Ecology and evolution of antimicrobial resistance in bacterial communities. *ISME* J **15**, 939–948 (2021).

8. Aslam, B. et al. Antibiotic Resistance: One Health One World Outlook. *Frontiers in Cellular and Infection* Microbiology vol. 11 Preprint at https://doi.org/10.3389/fcimb.2021.771510 (2021).

9. Clatworthy, A. E., *Pierson*, E. & Hung, D. T. Targeting virulence: a new paradigm for antimicrobial therapy. *Nat Chem Biol* **3**, 541–548 (2007).

10. Kim, D.-W. & Cha, C.-J. Antibiotic resistome from the One-Health perspective: understanding and controlling antimicrobial resistance transmission. *Exp Mol Med* **53**, 301–309 (2021).

11. Willmann, M. & Peter, S. Translational metagenomics and the human resistome: confronting the menace of the new millennium. *J Mol Med* **95**, 41–51 (2017).

12. McEwen, S. A. & Collignon, P. J. Antimicrobial Resistance: a One Health Perspective. *Microbiol Spectr* **6**, (2018).

13. Zhu, Y.-G. et al. Soil biota, antimicrobial resistance and planetary health. *Environ Int* **131**, 105059 (2019).

14. United Nations Environment Programme. *Bracing for Superbugs : Strengthening Environmental Action in the One Health Response to Antimicrobial Resistance.* (United Nations Environment Programme, 2023).

15. Udaondo, Z. & Huertas, M. J. Fighting the enemy: one health approach against microbial resistance. *Microb Biotechnol* **13**, 888–891 (2020).

16. Cantón, R., González-Alba, J. M. & Galán, J. C. CTX-M enzymes: Origin and diffusion. *Frontiers in Microbiology* vol. 3 Preprint at https://doi.org/10.3389/fmicb.2012.00110 (2012).

17. Uluseker, C. *et al.* A Review on Occurrence and Spread of Antibiotic Resistance in Wastewaters and in Wastewater Treatment Plants: Mechanisms and Perspectives. *Frontiers in Microbiology* vol. 12 Preprint at https://doi.org/10.3389/fmicb.2021.717809 (2021).

18. Baran, A., Kwiatkowska, A. & Potocki, L. Antibiotics and Bacterial Resistance—A Short Story of an Endless Arms Race. *International Journal of Molecular Sciences* vol. 24 Preprint at https://doi.org/10.3390/ijms24065777 (2023).

19. Cho, H., Uehara, T. & Bernhardt, T. G. Beta-Lactam Antibiotics Induce a Lethal Malfunctioning of the Bacterial Cell Wall Synthesis Machinery. *Cell* **159**, 1300–1311 (2014).

20. El-Gamal, M. I. *et al.* Recent updates of carbapenem antibiotics. *Eur J Med Chem* **131**, 185–195 (2017).

21. Morrisette, T. *et al.* On- and off-label utilization of dalbavancin and oritavancin for Gram-positive infections. *Journal of Antimicrobial Chemotherapy* **74**, 2405–2416 (2019).

22. McCarthy, M. W. *et al.* Dalbavancin Reduces Hospital Stay and Improves Productivity for Patients with Acute Bacterial Skin and Skin Structure Infections: The ENHANCE Trial. *Infect Dis Ther* **9**, 53–67 (2020).

23. Falagas, M. E., Kasiakou, S. K. & Saravolatz, L. D. Colistin: The Revival of Polymyxins for the Management of Multidrug-Resistant Gram-Negative Bacterial Infections. *Clinical Infectious Diseases* **40**, 1333–1341 (2005).

24. Trimble, M. J., Mlynárčik, P., Kolář, M. & Hancock, R. E. W. Polymyxin: Alternative Mechanisms of Action and Resistance. *Cold Spring Harb Perspect Med* **6**, a025288 (2016).

25. Yin, J. *et al.* Mechanisms of bactericidal action and resistance of polymyxins for Gram-positive bacteria. *Appl Microbiol Biotechnol* **104**, 3771–3780 (2020).

26. Anderson, V. & Osheroff, N. Type II Topoisomerases as Targets for Quinolone Antibacterials Turning Dr. Jekyll into Mr. Hyde. *Curr Pharm Des* **7**, 337–353 (2001).

27. Bush, N. G., Diez-Santos, I., Abbott, L. R. & Maxwell, A. Quinolones: Mechanism, Lethality and Their Contributions to Antibiotic Resistance. *Molecules* **25**, 5662 (2020).

28. Ho, M. X., Hudson, B. P., Das, K., Arnold, E. & Ebright, R. H. Structures of RNA polymerase–antibiotic complexes. *Curr Opin Struct Biol* **19**, 715–723 (2009).

29. Reid, P. & Speyer, J. Rifampicin Inhibition of Ribonucleic Acid and Protein Synthesis in Normal and Ethylenediaminetetraacetic Acid-Treated Escherichia coli. *J Bacteriol* **104**, 376–389 (1970).

30. Arenz, S. & Wilson, D. N. Bacterial Protein Synthesis as a Target for Antibiotic Inhibition. *Cold Spring Harb Perspect Med* 6, a025361 (2016).

31. Chopra, I., Hawkey, P. M. & Hinton, M. Tetracyclines, molecular and clinical aspects. *Journal of Antimicrobial Chemotherapy* **29**, 245–277 (1992).

32. Henry, R. Etymologia: Streptomycin. *Emerg Infect Dis* **25**, 450–450 (2019).

33. Durante-Mangoni, E., Grammatikos, A., Utili, R. & Falagas, M. E. Do we still need the aminoglycosides? *Int J Antimicrob Agents* **33**, 201–205 (2009).

34. Clark, J. A. & Burgess, D. S. Plazomicin: a new aminoglycoside in the fight against antimicrobial resistance. *Ther Adv Infect Dis* **7**, 204993612095260 (2020).

35. Krause, K. M., Serio, A. W., Kane, T. R. & Connolly, L. E. Aminoglycosides: An Overview. *Cold Spring Harb Perspect Med* **6**, a027029 (2016).

36. Chopra, S. & Reader, J. tRNAs as Antibiotic Targets. *Int J Mol Sci* **16**, 321–349 (2014).

37. Schwarz, S. et al. Lincosamides, Streptogramins, Phenicols, and Pleuromutilins: Mode of Action and Mechanisms of Resistance. *Cold Spring Harb Perspect Med* **6**, a027037 (2016).

38. Patel, P. H. & Hashmi, M. F. Macrolides. in *StatPearls* (ed. StatPearls) (2023).

39. Connor, E. E. Sulfonamide antibiotics. *Prim Care Update Ob Gyns* **5**, 32–35 (1998).

40. C Reygaert, W. An overview of the antimicrobial resistance mechanisms of bacteria. *AIMS Microbiol* **4**, 482–501 (2018).

41. Leclercq, R. et al. EUCAST expert rules in antimicrobial susceptibility testing. *Clinical Microbiology and Infection* **19**, 141–160 (2013).

42. Munita, J. M. & Arias, C. A. Mechanisms of Antibiotic Resistance. *Microbiol Spectr* **4**, (2016).

43. Venter, H., Arzanlou, M. & Chai, W. C. Intrinsic, adaptive and acquired antimicrobial resistance in Gram-negative bacteria. *Essays in Biochemestry* (2017).

44. Belay, W. Y. et al. Mechanism of antibacterial resistance, strategies and next-generation antimicrobials to contain antimicrobial resistance: a review. *Front Pharmacol* **15**, (2024).

45. Porse, A., Jahn, L. J., Ellabaan, M. M. H. & Sommer, M. O. A. Dominant resistance and negative epistasis can limit the co-selection of de novo resistance mutations and antibiotic resistance genes. *Nat Commun* **11**, 1199 (2020).

46. Nouri, R., Ahangarzadeh Rezaee, M., Hasani, A., Aghazadeh, M. & Asgharzadeh, M. The role of gyrA and parC mutations in fluoroquinolones-resistant *Pseudomonas aeruginosa* isolates from Iran. *Braz J Microbiol* **47**, 925–930 (2016).

47. Zapun, A., Contreras-Martel, C. & Vernet, T. Penicillin-binding proteins and β-lactam resistance. *FEMS Microbiol Rev* **32**, 361–385 (2008).

48. Chevalier, S. *et al.* Structure, function and regulation of *Pseudomonas aeruginosa* porins. *FEMS Microbiol Rev* **41**, 698–722 (2017).

49. Lorusso, A. B., Carrara, J. A., Barroso, C. D. N., Tuon, F. F. & Faoro, H. Role of Efflux Pumps on Antimicrobial Resistance in *Pseudomonas aeruginosa. Int J Mol Sci* **23**, (2022).

50. Bush, K. Classification for β-lactamases: historical perspectives. *Expert Rev Anti Infect Ther* **21**, 513–522 (2023).

51. R P Ambler. The structure of β-lactamases. *Philosophical Transactions of the Royal Society of London. B, Biological Sciences* **289**, 321–331 (1980).

52. Bush, K. & Jacoby, G. A. Updated Functional Classification of β-Lactamases. *Antimicrob Agents Chemother* **54**, 969–976 (2010).

53. Egorov, A. M., Ulyashova, M. M. & Rubtsova, M. Y. Bacterial Enzymes and Antibiotic Resistance. *Acta Naturae* **10**, 33–48 (2018).

54. Magiorakos, A. P. *et al.* Multidrug-resistant, extensively drug-resistant and pandrug-resistant bacteria: An international expert proposal for interim standard definitions for acquired resistance. *Clinical Microbiology and Infection* **18**, 268–281 (2012).

55. Kadri, S. S. *et al.* Difficult-to-treat resistance in gram-negative bacteremia at 173 US hospitals: Retrospective cohort analysis of prevalence, predictors, and outcome of resistance to all first-line agents. *Clinical Infectious Diseases* **67**, 1803–1814 (2018).

56. Cosentino, F., Viale, P. & Giannella, M. MDR/XDR/PDR or DTR? Which definition best fits the resistance profile of *Pseudomonas aeruginosa*? *Curr Opin Infect Dis* **36**, 564–571 (2023).

57. Rice, L. B. Federal Funding for the Study of Antimicrobial Resistance in Nosocomial Pathogens: No ESKAPE. *J Infect Dis* **197**, 1079–1081 (2008).

58. Sirijan, S. & Nitaya, I. Mechanisms of antimicrobial resistance in bacteria in ESKAPE pahogens. *Control* **2016**, (2006).

59. World Health Organization. WHO publishes list of bacteria for which new antibiotics are urgently needed. https://www.who.int/news/item/27-02-2017-who-publishes-list-of-bacteria-for-which-new-antibiotics-are-urgently-needed (2017).

60. World Health Organization. *WHO Bacterial Priority Pathogens List, 2024: Bacterial Pathogens of Public Health Importance to Guide Research, Development and Strategies to Prevent and Control Antimicrobial Resistance. (2024).*

61. Baquero, F. & Coque, T. M. Multilevel population genetics in antibiotic resistance. *FEMS Microbiol Rev* **35**, 705–706 (2011).

62. Oliver, A., Mulet, X., López-Causapé, C. & Juan, C. The increasing threat of *Pseudomonas aeruginosa* high-risk clones. *Drug Resistance Updates* **21–22**, 41–59 (2015).

63. Moore, N. M. & Flaws, M. L. Introduction: *Pseudomonas aeruginosa*. *American Society for Clinical Laboratory Science* **24**, 41–42 (2011).

64. Peirano, G., Chen, L., Kreiswirth, B. N. & Pitout, J. D. D. Emerging Antimicrobial-Resistant High-Risk *Klebsiella pneumoniae* Clones ST307 and ST147. *Antimicrob Agents Chemother* **64**, (2020).

65. Mathers, A. J., Peirano, G. & Pitout, J. D. D. The role of epidemic resistance plasmids and international high- risk clones in the spread of multidrug-resistant Enterobacteriaceae. *Clin Microbiol Rev* **28**, 565–591 (2015).

66. Breidenstein, E. B. M., de la Fuente-Núñez, C. & Hancock, R. E. W. *Pseudomonas aeruginosa*: All roads lead to resistance. *Trends Microbiol* **19**, 419–426 (2011).

67. Banerjee, R. & Johnson, J. R. A new clone sweeps clean: The enigmatic emergence of Escherichia coli sequence type 131. *Antimicrob Agents Chemother* **58**, 4997–5004 (2014).

68. Diggle, S. P. & Whiteley, M. Microbe Profile: *Pseudomonas aeruginosa*: opportunistic pathogen and lab rat. *Microbiology (N Y)* **166**, 30–33 (2020).

69. Pang, Z., Raudonis, R., Glick, B. R., Lin, T. J. & Cheng, Z. Antibiotic resistance in *Pseudomonas aeruginosa*: mechanisms and alternative therapeutic strategies. *Biotechnol Adv* **37**, 177–192 (2019).

70. Wood, S. J., Kuzel, T. M. & Shafikhani, S. H. Pseudomonas aeruginosa: Infections, Animal Modeling, and Therapeutics. *Cells* **12**, (2023).

71. Qin, S. *et al*. *Pseudomonas aeruginosa*: pathogenesis, virulence factors, antibiotic resistance, interaction with host, technology advances and emerging therapeutics. *Signal Transduct Target Ther* **7**, 199 (2022).

72. Patrick R. Murray, Ken Rosenthal & Michael A. Pfaller. *Medical Microbiology.* (Elsevier, 2016).

73. King, J. D., Kocíncová, D., Westman, E. L. & Lam, J. S. Review: Lipopolysaccharide biosynthesis in Pseudomonas aeruginosa. Innate Immun **15**, 261–312 (2009).

74. Jurado-Martín, I., Sainz-Mejías, M. & McClean, S. *Pseudomonas aeruginosa*: An Audacious Pathogen with an Adaptable Arsenal of Virulence Factors. *Int J Mol Sci* **22**, 3128 (2021).

75. Sendra, E. *et al*. Impact of multidrug resistance on the virulence and fitness of *Pseudomonas aeruginosa*: a microbiological and clinical perspective. *Infection* **52**, 1235–1268 (2024).

76. Ozer, E. *et al*. An inside look at a biofilm: *Pseudomonas aeruginosa* flagella biotracking. *Sci Adv* 7, (2021).

77. Rocha, A. J. *et al. Pseudomonas aeruginosa*: Virulence factors and antibiotic resistance Genes. *Brazilian Archives of Biology and Technology* **62**, 1–15 (2019).

78. Cornelis, P. & Dingemans, J. *Pseudomonas aeruginosa* adapts its iron uptake strategies in function of the type of infections. *Front Cell Infect Microbiol* **3**, (2013).

79. Meletis, G., Exindari, M., Vavatsi, N., Sofianou, D. & Diza, E. Mechanisms responsible for the emergence of carbapenem resistance in *Pseudomonas aeruginosa*. *Hippokratia* **16**, 303–307 (2012).

80. Fazeli, H. *et al*. *Pseudomonas aeruginosa* infections in patients, hospital means, and personnel's specimens. *J Res Med Sci* **17**, 332–7 (2012).

81. Kung, V. L., Ozer, E. A. & Hauser, A. R. The Accessory Genome of *Pseudomonas aeruginosa* . *Microbiology and Molecular Biology Reviews* **74**, 621–641 (2010).

82. Lister, P. D., Wolter, D. J. & Hanson, N. D. Antibacterial-Resistant *Pseudomonas aeruginosa*: Clinical Impact and Complex Regulation of Chromosomally Encoded Resistance Mechanisms. *Clin Microbiol Rev* **22**, 582–610 (2009).

83. Sathe, N. *et al*. Pseudomonas aeruginosa: Infections and novel approaches to treatment "Knowing the enemy" the threat of Pseudomonas aeruginosa and exploring novel approaches to treatment. *Infectious Medicine* **2**, 178–194 (2023).

84. Horcajada, J. P. *et al*. Epidemiology and Treatment of Multidrug-Resistant and Extensively Drug-Resistant Pseudomonas aeruginosa Infections. *Clin Microbiol Rev* **32**, (2019).

85. Plasencia, V. *et al*. Influence of high mutation rates on the mechanisms and dynamics of in vitro and in vivo resistance development to single or combined antipseudomonal agents. *Antimicrob Agents Chemother* **51**, 2574–2581 (2007).

86. Vila, J. & Marco, F. [Interpretive reading of the non-fermenting gram-negative bacilli antibiogram]. *Enferm Infecc Microbiol Clin* **28**, 726–736 (2010).

87. Mensa, J. *et al.* Antibiotic selection in the treatment of acute invasive infections by pseudomonas aeruginosa: Guidelines by the Spanish society of chemotherapy. *Revista Espanola de Quimioterapia* **31**, 78–100 (2018).

88. Juan, C., Torrens, G., González-Nicolau, M. & Oliver, A. Diversity and regulation of intrinsic β-lactamases from non-fermenting and other Gram-negative opportunistic pathogens. *FEMS Microbiol Rev* **41**, 781–815 (2017).

89. Oliver, A. *et al. Pseudomonas aeruginosa* antimicrobial susceptibility profiles, resistance mechanisms and international clonal lineages: update from ESGARS-ESCMID/ISARPAE Group. *Clinical Microbiology and Infection* **30**, 469–480 (2024).

90. Xie, X. *et al.* Molecular epidemiology and carbapenem resistance mechanisms of Pseudomonas aeruginosa isolated from a hospital in Fujian, China. *Front Microbiol* **15**, (2024).

91. Thacharodi, A. & Lamont, I. L. Aminoglycoside-Modifying Enzymes Are Sufficient to Make Pseudomonas aeruginosa Clinically Resistant to Key Antibiotics. *Antibiotics* **11**, 884 (2022).

92. Pelegrin, A. C. *et al. Pseudomonas aeruginosa*: a clinical and genomics update. *FEMS Microbiol Rev* **45**, (2021).

93. del Barrio-Tofiño, E., López-Causapé, C. & Oliver, A. *Pseudomonas aeruginosa* epidemic high-risk clones and their association with horizontally-acquired β-lactamases: 2020 update. *Int J Antimicrob Agents* **56**, 106196 (2020).

94. Sastre-Femenia, M. À. *et al.* Pseudomonas aeruginosa antibiotic susceptibility profiles, genomic epidemiology and resistance mechanisms: a nation-wide five-year time lapse analysis. *The Lancet Regional Health - Europe* **34**, 100736 (2023).

95. del Barrio-Tofiño, E. et al. Genomics and Susceptibility Profiles of Extensively Drug-Resistant *Pseudomonas aeruginosa* Isolates from Spain. *Antimicrob Agents Chemother* **61**, (2017).

96. Kocsis, B., Gulyás, D. & Szabó, D. Diversity and Distribution of Resistance Markers in *Pseudomonas aeruginosa* International High-Risk Clones. *Microorganisms* **9**, (2021).

97. Kocsis, B., Gulyás, D. & Szabó, D. Diversity and Distribution of Resistance Markers in *Pseudomonas aeruginosa* International High-Risk Clones. *Microorganisms* **9**, 359 (2021).

98. Ashurst, J. V. & Dawson, A. *Klebsiella Pneumonia.* (2023).

99. Adeolu, M., Alnajar, S., Naushad, S. & S. Gupta, R. Genome-based phylogeny and taxonomy of the 'Enterobacteriales': proposal for Enterobacterales ord. nov. divided into the families Enterobacteriaceae, Erwiniaceae fam. nov., Pectobacteriaceae fam. nov., Yersiniaceae fam. nov., Hafniaceae fam. nov., Morganellaceae fam. nov., and Budviciaceae fam. nov. *Int J Syst Evol Microbiol* **66**, 5575–5599 (2016).

100. Navon-Venezia, S., Kondratyeva, K. & Carattoli, A. *Klebsiella pneumoniae*: A major worldwide source and shuttle for antibiotic resistance. *FEMS Microbiology Reviews* vol. 41 252–275 Preprint at https://doi.org/10.1093/femsre/fux013 (2017).

101. Mancuso, G., Midiri, A., Gerace, E. & Biondo, C. Bacterial antibiotic resistance: the most critical pathogens. *Pathogens* vol. 10 Preprint at https://doi.org/10.3390/pathogens10101310 (2021).

102. Chung, P. Y. The emerging problems of *Klebsiella pneumoniae* infections: Carbapenem resistance and biofilm formation. *FEMS Microbiology Letters* vol. 363 Preprint at https://doi.org/10.1093/femsle/fnw219 (2016).

103. Wyres, K. L., Lam, M. M. C. & Holt, K. E. Population genomics of *Klebsiella pneumoniae*. *Nat Rev Microbiol* **18**, 344–359 (2020).

104. Riwu, K. H. P., Effendi, M. H., Rantam, F. A., Khairullah, A. R. & Widodo, A. A review: Virulence factors of Klebsiella pneumonia as emerging infection on the food chain. *Vet World* **15**, 2172–2179 (2022).

105. Gomes, A. É. I. et al. Functional Insights From KpfR, a New Transcriptional Regulator of Fimbrial Expression That Is Crucial for Klebsiella pneumoniae Pathogenicity. *Front Microbiol* **11**, (2021).

106. Bryant, C. E., Spring, D. R., Gangloff, M. & Gay, N. J. The molecular basis of the host response to lipopolysaccharide. *Nat Rev Microbiol* **8**, 8–14 (2010).

107. Paczosa, M. K. & Mecsas, J. Klebsiella pneumoniae: Going on the Offense with a Strong Defense. *Microbiology and Molecular Biology Reviews* **80**, 629–661 (2016).

108. Wick, R. R., Heinz, E., Holt, K. E. & Wyres, K. L. Kaptive Web: User-Friendly Capsule and Lipopolysaccharide Serotype Prediction for *Klebsiella* Genomes. *J Clin Microbiol* **56**, (2018).

109. Li, B., Zhao, Y., Liu, C., Chen, Z. & Zhou, D. Molecular pathogenesis of *Klebsiella pneumoniae*. *Future Microbiol* **9**, 1071–1081 (2014).

110. Clarke, B. R. *et al*. Molecular basis for the structural diversity in serogroup O2-antigen polysaccharides in Klebsiella pneumoniae. *Journal of Biological Chemistry* **293**, 4666–4679 (2018).

111. Brisse, S. *et al.* wzi Gene Sequencing, a Rapid Method for Determination of Capsular Type for *Klebsiella* Strains. *J Clin Microbiol* **51**, 4073–4078 (2013).

112. Pan, Y.-J. *et al*. Genetic analysis of capsular polysaccharide synthesis gene clusters in 79 capsular types of *Klebsiella* spp. *Sci Rep* **5**, 15573 (2015).

113. Rodrigues, C., Sousa, C., Lopes, J. A., Novais, Â. & Peixe, L. A Front Line on *Klebsiella pneumoniae* Capsular Polysaccharide Knowledge: Fourier Transform Infrared Spectroscopy as an Accurate and Fast Typing Tool. *mSystems* **5**, (2020).

114. Guerra, M. E. S. *et al. Klebsiella pneumoniae* Biofilms and Their Role in Disease Pathogenesis. *Front Cell Infect Microbiol* **12**, (2022).

115. Li, Y. & Ni, M. Regulation of biofilm formation in *Klebsiella pneumoniae*. *Front Microbiol* **14**, (2023).

116. Kocsis, B. Hypervirulent *Klebsiella pneumoniae:* An update on epidemiology, detection and antibiotic resistance. *Acta Microbiol Immunol Hung* **70**, 278–287 (2023).

117. Osama, D. M. *et al.* Occurrence and Molecular Study of Hypermucoviscous/ Hypervirulence Trait in Gut Commensal *K. pneumoniae* from Healthy Subjects. *Microorganisms* **11**, (2023).

118. Russo, T. A. & Marr, C. M. Hypervirulent *Klebsiella pneumoniae*. *Clin Microbiol Rev* **23**, (2019).

119. Cubero, M. *et al.* Hypervirulent Klebsiella pneumoniae clones causing bacteraemia in adults in a teaching hospital in Barcelona, Spain (2007-2013). *Clinical Microbiology and Infection* **22**, 154–160 (2016).

120. Fang, C.-T., Chuang, Y.-P., Shun, C.-T., Chang, S.-C. & Wang, J.-T. A Novel Virulence Gene in *Klebsiella pneumoniae* Strains Causing Primary Liver Abscess and Septic Metastatic Complications. *J Exp Med* **199**, 697–705 (2004).

121. Ecdc. *Emergence of Hypervirulent Klebsiella Pneum Oniae ST23 Carrying Carbapenemase Genes in EU/EEA Countries.* (2021).

122. European Centre for Disease Prevention and Control (ECDC). Increase of hypervirulent carbapenem-resistant Klebsiella pneumoniae in the EU/EEA. https://www.ecdc.europa.eu/en/news-events/increase-hypervirulent-carbapenem-resistant-klebsiella-pneumoniae-eueea (2023).

123. Wyres, K. L. & Holt, K. E. *Klebsiella pneumoniae* as a key trafficker of drug resistance genes from environmental to clinically important bacteria. *Current Opinion in Microbiology* vol. 45 131–139 Preprint at https://doi.org/10.1016/j.mib.2018.04.004 (2018).

124. De Oliveira, D. M. P. *et al*. Antimicrobial Resistance in ESKAPE Pathogens. (2020) doi:10.1128/CMR.

125. Navarro, F., Miró, E. & Mirelis, B. Lectura interpretada del antibiograma de enterobacterias. *Enferm Infecc Microbiol Clin* **28**, 638–645 (2010).

126. Martin, R. M. & Bachman, M. A. Colonization, Infection, and the Accessory Genome of Klebsiella pneumoniae. *Front Cell Infect Microbiol* **8**, (2018).

127. European Centre for Disease Prevention and Control (ECDC). EARS-Net data. https://www.ecdc.europa.eu/en/about-us/networks/disease-networks-and-laboratory-networks/ears-net-data (2024).

128. Cantón, R. *et al.* Prevalence and spread of extended-spectrum β-lactamase-producing *Enterobacteriaceae* in Europe. *Clinical Microbiology and Infection* **14**, 144–153 (2008).

129. Rivera-Izquierdo, M. *et al*. OXA-48 Carbapenemase-Producing Enterobacterales in Spanish Hospitals: An Updated Comprehensive Review on a Rising Antimicrobial Resistance. *Antibiotics* **10**, 89 (2021).

130. Hansen, G. T. Continuous Evolution: Perspective on the Epidemiology of Carbapenemase Resistance Among Enterobacterales and Other Gram-Negative Bacteria. *Infect Dis Ther* **10**, 75–92 (2021).

131. European Centre for Disease Prevention and Control. *Interim Report of a Rapid Risk Assessment of the Spread of Carbapenemase-Producing Klebsiella Pneumoniae in Greece.* https://www.ecdc.europa.eu/sites/default/files/documents/k-pneumoniae-greece-report-november-2023.pdf (2023).

132. Argente, M. *et al.* Molecular characterization of OXA-48 carbapenemase-producing Klebsiella pneumoniae strains after a carbapenem resistance increase in Catalonia. *Enferm Infecc Microbiol Clin* **37**, 82–88 (2019).

133. Moya, C. & Maicas, S. Antimicrobial Resistance in Klebsiella pneumoniae Strains: Mechanisms and Outbreaks. in 11 (MDPI AG, 2020). doi:10.3390/proceedings2020066011.

134. Ruiz, J., Pons, M. J. & Gomes, C. Transferable mechanisms of quinolone resistance. *Int J Antimicrob Agents* **40**, 196–203 (2012).

135. Cain, A. K. *et al.* Morphological, genomic and transcriptomic responses of Klebsiella pneumoniae to the last-line antibiotic colistin. *Sci Rep* **8**, 9868 (2018).

136. Cañada-García, J. E. *et al.* CARB-ES-19 Multicenter Study of Carbapenemase-Producing Klebsiella pneumoniae and Escherichia coli From All Spanish Provinces Reveals Interregional Spread of High-Risk Clones Such as ST307/OXA-48 and ST512/KPC-3. *Front Microbiol* **13**, (2022).

137. Lee, T., Pang, S., Abraham, S. & Coombs, G. W. Antimicrobial-resistant CC17 Enterococcus faecium: The past, the present and the future. *J Glob Antimicrob Resist* **16**, 36–47 (2019).

138. García-Solache, M. & Rice, L. B. The Enterococcus: a Model of Adaptability to Its Environment. *Clin Microbiol Rev* **32**, (2019).

139. Farahani, A. State of globe: Enterococci: Virulence factors and biofilm formation. *J Glob Infect Dis* **8**, 1 (2016).

140. Gao, W., Howden, B. P. & Stinear, T. P. Evolution of virulence in Enterococcus faecium, a hospital-adapted opportunistic pathogen. *Curr Opin Microbiol* **41,** 76–82 (2018).

141. Upadhyaya, P. G., Ravikumar, K. & Umapathy, B. Review of virulence factors of enterococcus: an emerging nosomical pathogen. *Indian J Med Microbiol* **27**, 301–305 (2009).

142. Ramos, S., Silva, V., Dapkevicius, M. de L. E., Igrejas, G. & Poeta, P. Enterococci, from Harmless Bacteria to a Pathogen. *Microorganisms* **8**, (2020).

143. Cattoir, V. & Giard, J.-C. Antibiotic resistance in Enterococcus faecium clinical isolates. *Expert Rev Anti Infect Ther* **12**, 239–48 (2014).

144. Jureen, R. et al. Molecular characterization of ampicillin-resistant Enterococcus faecium isolates from hospitalized patients in Norway. *J Clin Microbiol* **41**, 2330–6 (2003).

145. Guzman Prieto, A. M. et al. Global Emergence and Dissemination of Enterococci as Nosocomial Pathogens: Attack of the Clones? *Front Microbiol* 7, 788 (2016).

146. CLSI. Performance Standards for Antimicrobial Susceptibility Testing. *33rd ed. CLSI supplement M100.* (2023).

147. Humphries, R., Bobenchik, A. M., Hindler, J. A. & Schuetz, A. N. *Overview of Changes to the Clinical and Laboratory Standards Institute Performance Standards for Antimicrobial Susceptibility Testing, M100, 31st Edition*. https://www.fda.gov/drugs/development-resources/antibacterial-susceptibility-test-interpretive-criteria (2021).

148. Giske, C. G., Turnidge, J., Cantón, R. & Kahlmeter, G. Update from the European Committee on Antimicrobial Susceptibility Testing (EUCAST). *J Clin Microbiol* **60**, (2022).

149. Giske, C. G., Turnidge, J., Cantón, R. & Kahlmeter, G. *Update from the European Committee on Antimicrobial Susceptibility Testing (EUCAST) on Behalf of the EUCAST Steering Committee*. https://mic.eucast.org/. (2022).

150. Gajic, I. *et al*. Antimicrobial Susceptibility Testing: A Comprehensive Review of Currently Used Methods. *Antibiotics* vol. 11 Preprint at https://doi.org/10.3390/antibiotics11040427 (2022).

151. Kahlmeter, G. Defining antibiotic resistance-towards international harmonization. *Upsala Journal of Medical Sciences* vol. 119 78–86 Preprint at https://doi.org/10.3109/03009734.2014.901446 (2014).

152. Jenkins, S. G. & Schuetz, A. N. Current concepts in laboratory testing to guide antimicrobial therapy. in *Mayo Clinic Proceedings* vol. 87 290–308 (Elsevier Ltd, 2012).

153. Blanton, L. S., Walker, D. H. & Bouyer, D. H. *Manual of Clinical Microbiology.* vol. 13th (ASM Press, Washington DC, USA, 2019).

154. Matuschek, E., Brown, D. F. J. & Kahlmeter, G. Development of the EUCAST disk diffusion antimicrobial susceptibility testing method and its implementation in routine microbiology laboratories. *Clinical Microbiology and Infection* **20,** O255–O266 (2014).

155. Leber, A. L. *Clinical Microbiology Procedures Handbook*. (American Society for Microbiology, 2016).

156. Jorgensen, J. H. & Ferraro, M. J. Antimicrobial Susceptibility Testing: A Review of General Principles and Contemporary Practices. *Clinical Infectious Diseases* **49**, 1749–1755 (2009).

157. Cook, M. A. & Wright, G. D. The past, present, and future of antibiotics. *Sci Transl Med* **14**, (2022).

158. Serio, A. W., Keepers, T., Andrews, L. & Krause, K. M. Aminoglycoside Revival: Review of a Historically Important Class of Antimicrobials Undergoing Rejuvenation. *EcoSal Plus* **8**, (2018).

159. Zhu, M., Tse, M. W., Weller, J., Chen, J. & Blainey, P. C. The future of antibiotics begins with discovering new combinations. *Ann N Y Acad Sci* **1496**, 82–96 (2021).

160. Mensa, J. *et al.* Antibiotic Selectiom Treatment Acute *Pseudomonas Aeruginosa* Guidelines. *Rev Esp Quimioter* **31**, 78–100 (2018).

161. Kumar, A. *et al*. Early combination antibiotic therapy yields improved survival compared with monotherapy in septic shock: A propensity-matched analysis*. *Crit Care Med* **38**, 1773–1785 (2010).

162. Vergara-López, S., Domínguez, M. C., Conejo, M. C., Pascual, Á. & Rodríguez-Baño, J. Lessons from an outbreak of metallo-β-lactamase-producing Klebsiella oxytoca in an intensive care unit: the importance of time at risk and combination therapy. *Journal of Hospital Infection* **89**, 123–131 (2015).

163. Schmid, A. *et al.* Monotherapy versus combination therapy for multidrug-resistant Gram-negative infections: Systematic Review and Meta-Analysis. *Sci Rep* **9**, 15290 (2019).

164. Mulani, M. S., Kamble, E. E., Kumkar, S. N., Tawre, M. S. & Pardesi, K. R. Emerging strategies to combat ESKAPE pathogens in the era of antimicrobial resistance: A review. *Front Microbio*l **10**, (2019).

165. Ronit, A. *et al*. Bacteriophages for the treatment of pseudomonas-infected vascular prosthesis. *Ugeskr Laeger* **186**, 1–3 (2024).

166. Montero, M. M. *et al.* Comparison of Ceftolozane/Tazobactam Infusion Regimens in a Hollow-Fiber Infection Model against Extensively Drug-Resistant *Pseudomonas aeruginosa* Isolates. *Microbiol Spectr* **10**, (2022).

167. Shama, G. & Malik, D. J. International Journal of Hygiene and The uses and abuses of rapid bioluminescence-based ATP assays. *Int J Hyg Environ Health* **216**, 115–125 (2013).

168. Chappelle, E. W. & Levin, G. V. Use of the firefly bioluminescent reaction for rapid detection and counting of bacteria. *Biochem Med* **2,** 41–52 (1968).

169. Cai, Y. *et al*. Using an adenosine triphosphate bioluminescent assay to determine effective antibiotic combinations against carbapenem-resistant gram negative bacteria within 24 hours. *PLoS One* **10**, 1–15 (2015).

170. Aragonès, L., Escudé, C., Visa, P., Salvi, L. & Mocé-Llivina, L. New insights for rapid evaluation of bactericidal activity: A semi-automated bioluminescent ATP assay. *J Appl Microbiol* **113**, 114–125 (2012).

171. Tang, Y. *et al.* Comparison of coliform paper test and ATP bioluminescence assay for monitoring the disinfection of kitchen utensils in canteens of hebei, China. *Heliyon* **9**, (2023).

172. Ivančić, V. *et al.* Rapid antimicrobial susceptibility determination of uropathogens in clinical urine specimens by use of ATP bioluminescence. *J Clin Microbiol* **46**, 1213–1219 (2008).

173. Cai, Y. *et al.* Rapid Antibiotic Combination Testing for Carbapenem-Resistant Gram-Negative Bacteria within Six Hours Using ATP Bioluminescence. *Antimicrob Agents Chemother* 1–10 (2018).

174. Promega. *BacTiter-Glo™ Microbial Cell Viability Assay Instructions for Use of Products G8230, G8231, G8232 and G8233*. www.promega.com (2021).

175. Tamma, P. D. *et al.* Infectious Diseases Society of America 2023 Guidance on the Treatment of Antimicrobial Resistant Gram-Negative Infections. *Clinical Infectious Diseases* (2023) doi:10.1093/cid/ciad428.

176. Skov, R. & Skov, G. EUCAST guidelines for detection of resistance mechanisms and specific resistances of clinical and / or epidemiological importance. 1–47 (2022).

177. Becker, B. & Cooper, M. A. Aminoglycoside antibiotics in the 21st century. *ACS Chem Biol* **8**, 105–115 (2013).

178. Yadav, R. *et al.* Aminoglycoside concentrations required for synergy with carbapenems against Pseudomonas aeruginosa determined via mechanistic studies and modeling. *Antimicrob Agents Chemother* **61**, 1–16 (2017).

179. Albasanz-Puig, A. *et al.* Impact of the Inclusion of an Aminoglycoside to the Initial Empirical Antibiotic Therapy for Gram-Negative Bloodstream Infections in Hematological Neutropenic Patients: a Propensity-Matched Cohort Study (AMINOLACTAM Study). *Antimicrob Agents Chemother* **65**, (2021).

180. Ota, K., Kaku, N. & Yanagihara, K. Efficacy of meropenem and amikacin combination therapy against carbapenemase-producing *Klebsiella pneumoniae* mouse model of pneumonia. *Journal of Infection and Chemotherapy* **26**, 1237–1243 (2020).

181. Tamma, P. D. *et al.* Infectious Diseases Society of America 2022 Guidance on the Treatment of Extended-Spectrum β-lactamase Producing Enterobacterales (ESBL-E), Carbapenem-Resistant Enterobacterales (CRE), and *Pseudomonas aeruginosa* with Difficult-to-Treat Resistance (DTR-P. . *Clin Infect Dis* **75**, 187–212 (2022).

182. Lee, G. C. & Burgess, D. S. Treatment of *Klebsiella Pneumoniae* Carbapenemase (KPC) infections: a review of published case series and case reports. *Ann Clin Microbiol Antimicrob* **11**, 32 (2012).

183. Paul, M. *et al.* European Society of Clinical Microbiology and Infectious Diseases (ESCMID) guidelines for the treatment of infections caused by multidrug-resistant Gram-negative bacilli (endorsed by European society of intensive care medicine). *Clinical Microbiology and Infection* **28**, 521–547 (2022).

184. Tamma, P. D. *et al.* Infectious Diseases Society of America 2024 Guidance on the Treatment of Antimicrobial-Resistant Gram-Negative Infections. *Clinical Infectious Diseases* (2024) doi:10.1093/cid/ciae403.

185. Wale, Y. M., Roberts, J. A., Wolie, Z. T. & Sime, F. B. Is there evidence on the optimal duration of aminoglycoside therapy in β-lactam/aminoglycoside combination regimens used for the treatment of gram-negative bacterial infections? A systematic review. *Int J Antimicrob Agents* **64**, 107297 (2024).

186. Montero, M. M. *Pseudomonas aeruginosa* multiresistente: aspectos epidemiológicos, clínicos y terapéuticos. 109 (2012).

187. Herbig, M. E., Evers, D.-H., Gorissen, S. & Köllmer, M. Rational Design of Topical Semi-Solid Dosage Forms-How Far Are We? *Pharmaceutics* **15**, 1822 (2023).

188. EUCAST. Guidance document EUCAST breakpoints in brackets. *European Society of Clinical Microbiology and Infectious Deseases* 1–2 (2023).

189. Nicoloff, H., Hjort, K., Levin, B. R. & Andersson, D. I. The high prevalence of antibiotic heteroresistance in pathogenic bacteria is mainly caused by gene amplification. *Nat Microbiol* **4**, 504–514 (2019).

190. Hermes, D. M. et al. Evaluation of heteroresistance to polymyxin B among carbapenem-susceptible and -resistant Pseudomonas aeruginosa. *J Med Microbiol* **62**, 1184–1189 (2013).

191. Montero, M. M. et al. Time-Kill Evaluation of Antibiotic Combinations Containing Ceftazidime-Avibactam against Extensively Drug-Resistant *Pseudomonas aeruginosa* and Their Potential Role against Ceftazidime-Avibactam-Resistant Isolates. *Microbiol Spectr* **9**, (2021).

192. Sykes, J. E. & Papich, M. G. Principles of Antiinfective Therapy. *Canine and Feline Infectious Diseases* 46–53 (2014) doi:10.1016/B978-1-4377-0795-3.00006-5.

193. Ren, H. *et al*. Synergistic bactericidal activities of tobramycin with ciprofloxacin and azithromycin against *Klebsiella pneumoniae*. *Journal of Antibiotics* **74**, 528–537 (2021).

194. Promega. BacTiter-Glo ™ Microbial Cell Viability Assay. 67 (2012).

195. Cáñez-Carrasco, M. G. & García-Alegría, A. M. Validación De Un Método Analítico Para La Determinación De Fósforo Por Espectrofotometría Ultravioleta-Visible. *Biotecnia* **17**, 32 (2015).

196. OIE. Principios y Métodos de Validación de las pruebas de diagnóstico de las enfermedades infecciosas. *Manual Acuático de la OIE* 2012 20 (2012).

197. Tam, V. H. & Nikolaou, M. A Novel Approach to Pharmacodynamic Assessment of Antimicrobial Agents: New Insights to Dosing Regimen Design. *PLoS Comput Biol* 7, e1001043 (2011).

198. Cai, Y. *et al.* Elimination of extracellular adenosine triphosphate for the rapid prediction of quantitative plate counts in 24 H time-kill studies against carbapenem-resistant gram-negative bacteria. *Microorganisms* **8**, 1–15 (2020).

199. WATANABE, A. *et al.* Use of ATP Bioluminescence Assay to Evaluate Oral Streptococci. *Biocontrol Sc*i **27**, 229–233 (2022).

200. Zhang, H. *et al*. Quenching the firefly bioluminescence by various ions. *Photochemical and Photobiological Sciences* **15**, 244–249 (2016).

201. Vogel, S. J., Tank, M. & Goodyear, N. Variation in detection limits between bacterial growth phases and precision of an ATP bioluminescence system. *Lett Appl Microbiol* **58**, 370–375 (2014).

202. Micek, S. T. et al. Empiric Combination Antibiotic Therapy Is Associated with Improved Outcome against Sepsis Due to Gram-Negative Bacteria: a Retrospective Analysis. *Antimicrob Agents Chemother* **54**, 1742–1748 (2010).

203. Thy, M., Timsit, J.-F. & de Montmollin, E. Aminoglycosides for the Treatment of Severe Infection Due to Resistant Gram-Negative Pathogens. *Antibiotics* **12**, (2023).

204. Mensa, J. *et al.* Antibiotic selection in the treatment of acute invasive infections by *pseudomonas aeruginosa*: Guidelines by the Spanish society of chemotherapy. R*evista Española de Quimioterapia* **31**, 78–100 (2018).
205. Avent, M. L. *et al.* Evaluating Mono- and Combination Therapy of Meropenem and Amikacin against *Pseudomonas aeruginosa* Bacteremia in the Hollow-Fiber Infection Model. *Microbiol Spectr* **10**, (2022).

206. Tamma, P. D., Cosgrove, S. E. & Maragakis, L. L. Combination therapy for treatment of infections with gram-negative bacteria. *Clin Microbiol Rev* **25**, 450–470 (2012).

207. Chamot, E., El Amari, E. B., Rohner, P. & Van Delden, C. Effectiveness of combination antimicrobial therapy for Pseudomonas aeruginosa bacteremia. *Antimicrob Agents Chemother* **47**, 2756–2764 (2003).

208. Dudley, M. N., Blaser, J., Gilbert, D., Mayer, K. H. & Zinner, S. H. Combination therapy with ciprofloxacin plus azlocillin against pseudomonas aeruginosa: Effect of simultaneous versus staggered administration in an in vitro model of infection. *Journal of Infectious Diseases* **164**, 499–506 (1991).

209. Bowers, D. R. *et al.* Outcomes of appropriate empiric combination versus monotherapy for *pseudomonas aeruginosa* bacteremia. *Antimicrob Agents Chemother* **57**, 1270–1274 (2013).

210. Thy, M. & Timsit, J. Aminoglycosides for the Treatment of Severe Infection Due to Resistant Gram-Negative Pathogens. 1–14 (2023).

211. Medscape. Amikacin (Drug Monograph). *Medscape Reference* (2025).

212. De Winter, S. *et al.* Higher versus standard amikacin single dose in emergency department patients with severe sepsis and septic shock: a randomised controlled trial. *Int J Antimicrob Agents* **51**, 562–570 (2018).

213. Nicolau, D. P. Pharmacokinetic and pharmacodynamic properties of meropenem. *Clinical Infectious Diseases* **47**, (2008).

214. Doern, C. D. When Does 2 Plus 2 Equal 5? A Review of Antimicrobial Synergy Testing. *J Clin Microbiol* **52**, 4124–4128 (2014).

215. Igbinosa, E. O. *et al.* Antibiotic Synergy Interaction against Multidrug-Resistant *Pseudomonas aeruginosa* Isolated from an Abattoir Effluent Environment. *The Scientific World Journal* **2012**, 1–5 (2012).

216. Vardakas, K. Z., Tansarli, G. S., Bliziotis, I. A. & Falagas, M. E. β-Lactam plus aminoglycoside or fluoroquinolone combination versus β-lactam monotherapy for *Pseudomonas aeruginosa* infections: A meta-analysis. *Int J Antimicrob Agents* **41**, 301–310 (2013).

217. Hagihara, M. *et al. In vivo* study assessed meropenem and amikacin combination therapy against carbapenem-resistant and carbapenemase-producing *Enterobacteriaceae* strains. *Journal of Infection and Chemotherapy* **26**, 1–7 (2020).

218. Del Barrio-Tofiño E, López-Causapé C, Cabot G, Rivera A, Benito N, Segura C, Montero MM, Sorlí L, Tubau F, Gómez-Zorrilla S, Tormo N, Durá-Navarro R, Viedma E, Resino-Foz E, Fernández-Martínez M, González-Rico C, Alejo-Cancho I, Martínez JA, Labayru-Echve, O. A. Genomics and Susceptibility Profiles of Extensively Drug-Resistant Pseudomonas. *Antimicrob Agents Chemother* 1–13 (2017).

219. Cheng, Y.-S., Williamson, P. R. & Zheng, W. Improving therapy of severe infections through drug repurposing of synergistic combinations. *Curr Opin Pharmacol* **48**, 92–98 (2019).

220. Kulengowski, B., Clark, J. A. & Burgess, D. S. Killing activity of meropenem in combination with amikacin against VIM- or KPC-producing *Enterobacteriaceae* that are susceptible, intermediate, or resistant to amikacin. *Diagn Microbiol Infect Dis* **93**, 372–375 (2019).

221. El-Halfawy, O. M. & Valvano, M. A. Antimicrobial heteroresistance: an emerging field in need of clarity. *Clin Microbiol Rev* **28**, 191–207 (2015).

222. Alonso, A., Campanario, E. & Martínez, J. L. Emergence of multidrug-resistant mutants is increased under antibiotic selective pressure in *Pseudomonas aeruginosa*. *Microbiology (Reading)* **145** (**Pt 1**, 2857–2862 (1999).

223. Cadwell, J. The Hollow Fiber Infection Model for Antimicrobial Pharmacodynamics and Pharmacokinetics. *Adv Pharmacoepidemiol Drug Saf* **01**, (2012).

224. Roch, M., Sierra, R. & Andrey, D. O. Antibiotic heteroresistance in ESKAPE pathogens, from bench to bedside. *Clinical Microbiology and Infection* **29**, 320–325 (2023).

225. Lu, Y. *et al.* Quorum sensing regulates heteroresistance in *Pseudomonas aeruginosa*. *Front Microbiol* **13**, (2022).

226. Sherman, E. Methods to Evaluate Colistin Heteroresistance in Acinetobacter baumannii. *Methods Mol Biol.* **1946**, 39–50 (2019).

227. Gianvecchio, C. *et al.* Variation in mutant prevention concentrations. *Front Microbiol* **10**, 1–9 (2019).

228. Le, J., McKee, B., Srisupha-Olarnc, W. & Burgessc, D. S. In Vitro Activity of Carbapenems Alone and in Combination With Amikacin Against KPC-Producing *Klebsiella Pneumoniae*. *J Clin Med Res* **3**, 106–110 (2011).

229. Onufrak, N. J., Forrest, A. & Gonzalez, D. Pharmacokinetic and Pharmacodynamic Principles of Anti-Infective Dosing. *Clin Ther* **38**, 1930–1947 (2016).

230. Steffens, N. A., Zimmermann, E. S., Nichelle, S. M. & Brucker, N. Meropenem use and therapeutic drug monitoring in clinical practice: a literature review. *J Clin Pharm Ther* **46**, 610–621 (2021).

231. Germovsek, E., Barker, C. I. & Sharland, M. What do I need to know about aminoglycoside antibiotics? *Archives of disease in childhood - Education & practice edition* **102**, 89 LP – 93 (2017).

232. Thy, M. & Timsit, J. Aminoglycosides for the Treatment of Severe Infection Due to Resistant Gram-Negative Pathogens. 1–14 (2023).

233. Karaiskos, I., Lagou, S., Pontikis, K., Rapti, V. & Poulakou, G. The “Old” and the “New” Antibiotics for MDR Gram-Negative Pathogens: For Whom, When, and How. *Front Public Health* **7**, (2019).

234. Tängdén, T., Karvanen, M., Friberg, L. E., Odenholt, I. & Cars, O. Assessment of early combination effects of colistin and meropenem against *Pseudomonas aeruginosa* and *Acinetobacter baumannii* in dynamic time-kill experiments. *Infect Dis* **49**, 521–527 (2017).

235. Alonso, A., Campanario, E. & Martínez, J. L. Emergence of multidrug-resistant mutants is increased under antibiotic selective pressure in *Pseudomonas aeruginosa. Microbiology (Reading)* **145 (Pt 10)**, 2857–2862 (1999).

236. El-Halfawy, O. M. & Valvano, M. A. Antimicrobial heteroresistance: An emerging field in need of clarity. *Clin Microbiol Rev* **28**, 191–207 (2015).

237. Zhang, F. *et al.* Carbapenem-resistant K. pneumoniae exhibiting clinically undetected amikacin and meropenem heteroresistance leads to treatment failure in a murine model of infection. *Microb Pathog* **160**, 105162 (2021).

07
Appendix

8. Appendix A: Scientific publication

ATP Bioluminescence Assay To Evaluate Antibiotic Combinations against Extensively Drug-Resistant (XDR) *Pseudomonas aeruginosa*

Microbiol Spectr. 2022 Aug 31;10(4):e0065122. doi: 10.1128/spectrum.00651-22. Epub 2022 Jul 25.

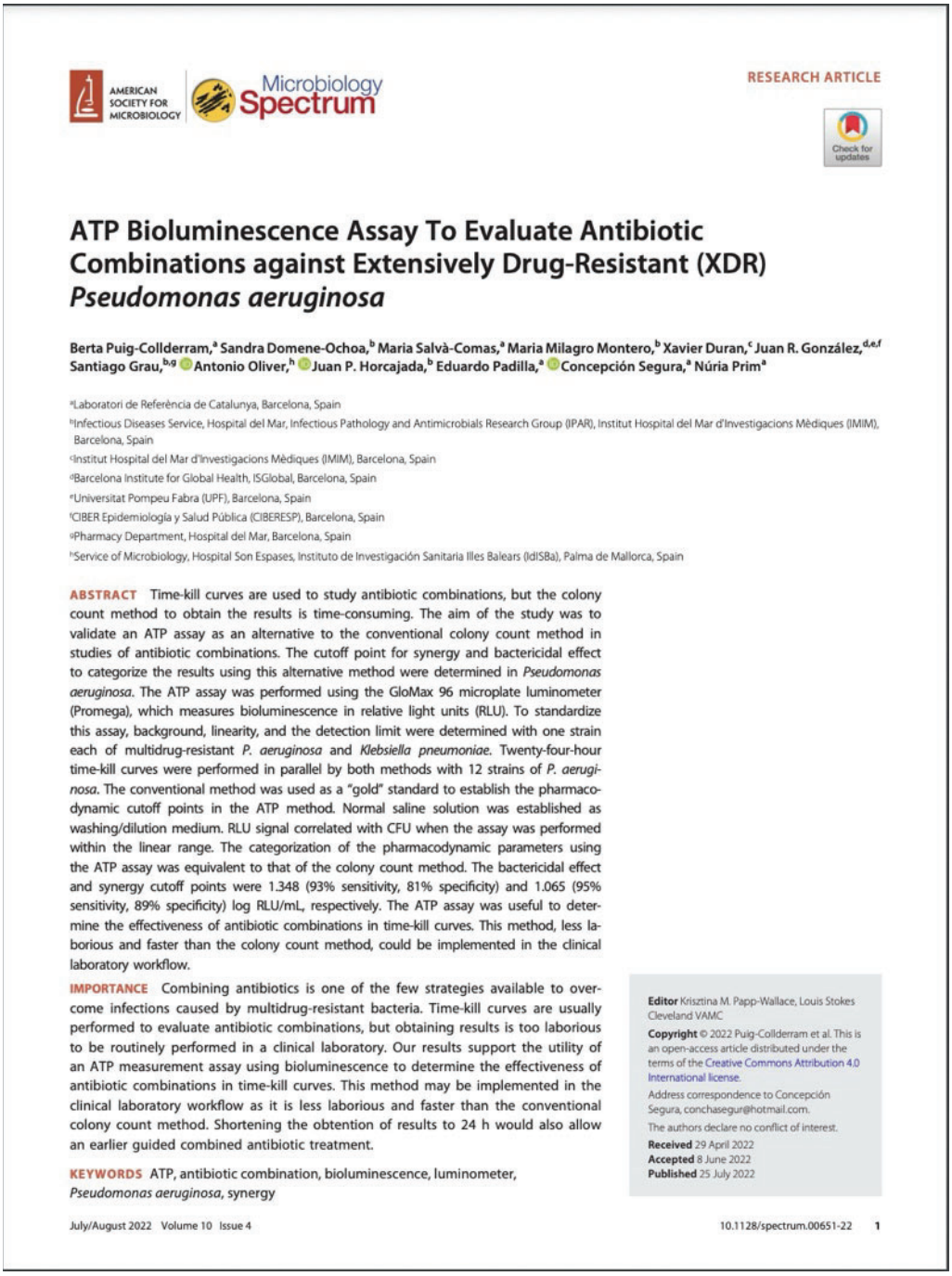

AMERICAN SOCIETY FOR MICROBIOLOGY | Microbiology Spectrum

RESEARCH ARTICLE

ATP Bioluminescence Assay To Evaluate Antibiotic Combinations against Extensively Drug-Resistant (XDR) *Pseudomonas aeruginosa*

Berta Puig-Collderram,[a] Sandra Domene-Ochoa,[b] Maria Salvà-Comas,[a] Maria Milagro Montero,[b] Xavier Duran,[c] Juan R. González,[d,e,f] Santiago Grau,[b,g] Antonio Oliver,[h] Juan P. Horcajada,[b] Eduardo Padilla,[a] Concepción Segura,[a] Núria Prim[a]

[a]Laboratori de Referència de Catalunya, Barcelona, Spain
[b]Infectious Diseases Service, Hospital del Mar, Infectious Pathology and Antimicrobials Research Group (IPAR), Institut Hospital del Mar d'Investigacions Mèdiques (IMIM), Barcelona, Spain
[c]Institut Hospital del Mar d'Investigacions Mèdiques (IMIM), Barcelona, Spain
[d]Barcelona Institute for Global Health, ISGlobal, Barcelona, Spain
[e]Universitat Pompeu Fabra (UPF), Barcelona, Spain
[f]CIBER Epidemiología y Salud Pública (CIBERESP), Barcelona, Spain
[g]Pharmacy Department, Hospital del Mar, Barcelona, Spain
[h]Service of Microbiology, Hospital Son Espases, Instituto de Investigación Sanitaria Illes Balears (IdISBa), Palma de Mallorca, Spain

ABSTRACT Time-kill curves are used to study antibiotic combinations, but the colony count method to obtain the results is time-consuming. The aim of the study was to validate an ATP assay as an alternative to the conventional colony count method in studies of antibiotic combinations. The cutoff point for synergy and bactericidal effect to categorize the results using this alternative method were determined in *Pseudomonas aeruginosa*. The ATP assay was performed using the GloMax 96 microplate luminometer (Promega), which measures bioluminescence in relative light units (RLU). To standardize this assay, background, linearity, and the detection limit were determined with one strain each of multidrug-resistant *P. aeruginosa* and *Klebsiella pneumoniae*. Twenty-four-hour time-kill curves were performed in parallel by both methods with 12 strains of *P. aeruginosa*. The conventional method was used as a "gold" standard to establish the pharmacodynamic cutoff points in the ATP method. Normal saline solution was established as washing/dilution medium. RLU signal correlated with CFU when the assay was performed within the linear range. The categorization of the pharmacodynamic parameters using the ATP assay was equivalent to that of the colony count method. The bactericidal effect and synergy cutoff points were 1.348 (93% sensitivity, 81% specificity) and 1.065 (95% sensitivity, 89% specificity) log RLU/mL, respectively. The ATP assay was useful to determine the effectiveness of antibiotic combinations in time-kill curves. This method, less laborious and faster than the colony count method, could be implemented in the clinical laboratory workflow.

IMPORTANCE Combining antibiotics is one of the few strategies available to overcome infections caused by multidrug-resistant bacteria. Time-kill curves are usually performed to evaluate antibiotic combinations, but obtaining results is too laborious to be routinely performed in a clinical laboratory. Our results support the utility of an ATP measurement assay using bioluminescence to determine the effectiveness of antibiotic combinations in time-kill curves. This method may be implemented in the clinical laboratory workflow as it is less laborious and faster than the conventional colony count method. Shortening the obtention of results to 24 h would also allow an earlier guided combined antibiotic treatment.

KEYWORDS ATP, antibiotic combination, bioluminescence, luminometer, *Pseudomonas aeruginosa*, synergy

Editor Krisztina M. Papp-Wallace, Louis Stokes Cleveland VAMC

Address correspondence to Concepción Segura, conchasegur@hotmail.com.

The authors declare no conflict of interest.

Received 29 April 2022
Accepted 8 June 2022
Published 25 July 2022

Use and abuse of antibiotics have led to an increase in antibiotic-resistant bacterial strains. Acquired resistance to antimicrobials is an issue challenging health systems. Antibiotic resistance can be caused by different mechanisms, ranging from inactivation or alteration of the antimicrobial or its binding site to changes in porins or in efflux pumps, which result in a lower accumulation of antibiotic. Infections caused by multidrug-resistant (MDR) microorganisms may be difficult to treat, which is translated into an increase in their mortality and morbidity rates.

The emergence of antibiotic resistance in bacteria usually involved in nosocomial infections, has generated special alarm because these infections can compromise the lives of critical and/or immunosuppressed patients. *Pseudomonas aeruginosa* and *Klebsiella pneumoniae*, together with *Escherichia coli*, are the bacterial species most frequently involved in nosocomial infections. These infections are often caused by MDR high-risk clones within these species (1–4).

Optimization of the strategies to combat MDR microorganisms is essential due to the limited therapeutic options. Combining antibiotics to obtain a synergistic effect against MDR bacteria may be also a therapeutic option. The efficacy of an antibiotic combination can be evaluated by different techniques. The time-kill curve is a dynamic method in which bacterial death is analyzed in the presence of fixed concentrations of antibiotic in relation to time (5). Results from time-kill curves are obtained 48 h after starting the experiment. Based on the results obtained in the curves, other complex pharmacokinetic/pharmacodynamic studies can be carried out, such as the "hollow fiber" model (6). This two-compartment model allows the evaluation of changes in antibiotic concentration over time, mimicking physiological conditions. Both techniques are very laborious and complicated when implemented in the clinical diagnostic routine in a microbiology laboratory. A less laborious and faster technique than the classical methodology to count viable cells would facilitate the laboratory workflow and shorten the time for results, allowing the implementation of studies of antibiotic combinations in the clinical routine.

Methods for bacterial detection and counting based on bioluminescence have been described. These methods correlate cell viability with metabolic activity by measuring NAD or ATP. The presence of these molecules in cells makes its detection symptomatic of the presence of living organisms (7).

Luminometers allow the quantification of bioluminescence. The increase in bioluminescence is directly proportional to the amount of ATP, which in turn correlates with the living organisms present in the sample (8). These systems are widely used, especially in industry and in health care settings, to evaluate the effectiveness of cleaning and/or sterilization processes (8, 9). The potential use of this technique to evaluate antibiotic activity by studying the bactericidal effect has been also reported (10). To our knowledge, the pharmacodynamic parameter of synergy has not been determined before using this technique in time-kill curves.

The aim of the present study was to validate the use of this ATP measurement assay using bioluminescence as an alternative to the colony count of viable cells for the study of antibiotic combinations. The ultimate goal is the implementation of this technique in the laboratory routine.

RESULTS

Luminometer standardization. The background average values obtained from 30 observations were 10^3 and 10^2 relative light units (RLU)/mL for cation-adjusted Mueller-Hinton broth (CA-MHB) and normal saline solution (NSS), respectively. Below these values bacterial RLU readings could not be differentiated from the corresponding RLU value of the medium. Background oscillation was considered relevant enough to be removed in further assays. The detection limits obtained for both CA-MHB and NSS were 10^4 and 10^3 CFU/mL, respectively. The range of linear relationship between log RLU per milliliter and log CFU per milliliter were 10^4 to 10^8 CFU/mL (R^2 = 0.99 to 1) in CA-MHB, and 10^3 to 10^9 CFU/mL (R^2 = 0.98 to 1) in NSS (Fig. 1). No significant differences were observed at

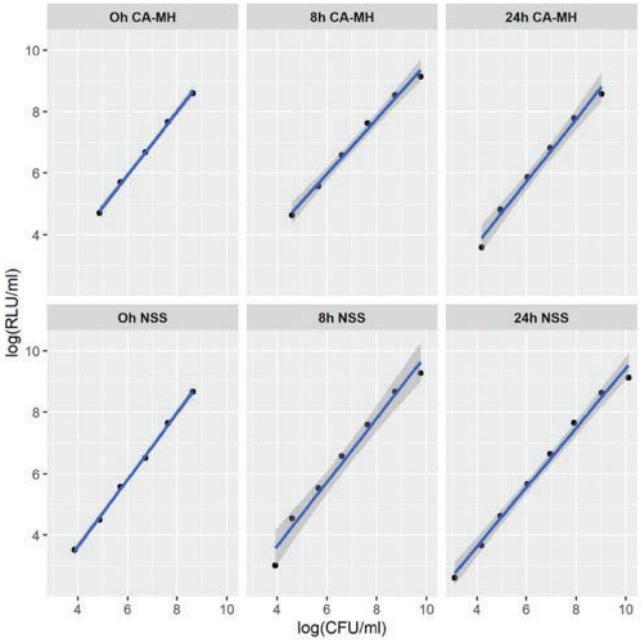

FIG 1 Linearity study of *Pseudomonas aeruginosa* at 0, 8, and 24 h with cation-adjusted Mueller-Hinton broth (CA-MHB) and normal saline solution (NSS) (below).

different times or for the different species. NSS was established in further studies as the medium used to wash and dilute the samples.

The relative standard deviations (RSDs), in both the CA-MHB and NSS data, were equal to or inferior to the corresponding RSDs of the conventional method for the different times, concentrations, and strains analyzed (data not shown).

Comparative analysis. The comparative analysis was performed analyzing the results from the *P. aeruginosa* curves by the conventional colony count method and the ATP assay in parallel. The growth curve study was performed from the values obtained under the experimental condition without antibiotic. The Pearson correlation coefficient (*r*) was 0.93, and the infraclass coefficient correlation (ICC) was 0.88 (95% confidence interval [CI], 0.816 to 0.923).

The graphical comparison of time-kill curves for some isolates is shown in Fig. 2. The results obtained at 24 h by the conventional colony count method (CFU per milliliter) were used as a gold standard to determine the pharmacodynamic parameters in RLU per milliliter. The cutoff point for bactericidal effect was established using the values obtained from antibiotics as single agents and combined. The sample size included 257 paired data. The value for the bactericidal effect cutoff was 1.348 log RLU/mL, with a sensitivity of 93%, and a specificity of 78.5%; the area under the curve (AUC) obtained was 0.929 (Fig. 3A).

The cutoff point for synergy was established considering the values obtained from antibiotic combinations. The sample size included 105 paired data. The cutoff point for synergy was 0.9 log RLU/mL, with a sensitivity of 95% and a specificity of 88%; the area

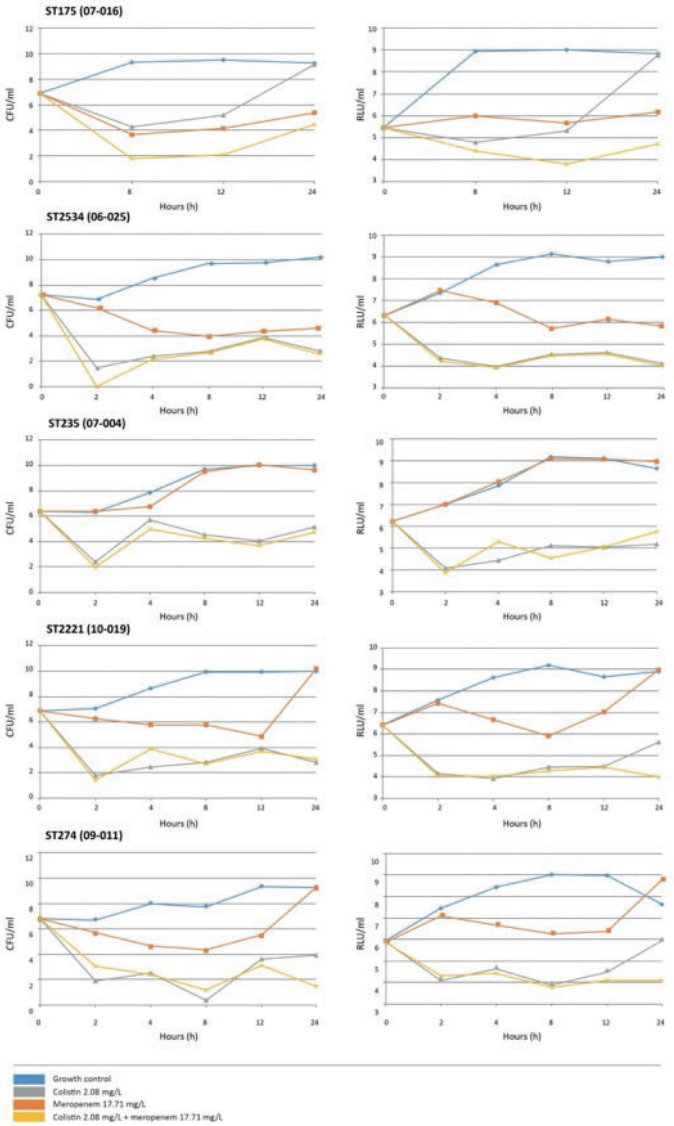

FIG 2 Time-kill curves for *P. aeruginosa* ST175 (07-016), ST235 (07-004), ST274 (09-011), ST2221 (10-016), ST2534 (06-025), and ST2536 (06-001). Results are shown for the conventional colony count method (CFU per milliliter) (left) and ATP

(Continued on next page)

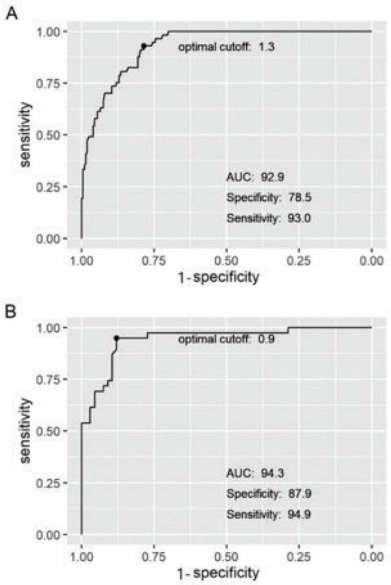

FIG 3 ROC curves for bactericidal effect and synergy. High areas under the ROC curves (0.929 to 0.943) were observed in both pharmacodynamic parameters bactericidal effect (A) and synergy (B).

under the curve (AUC) obtained was 0.9430 (Fig. 3B). When considering a specificity of 100%, the cutoff was 2.199 (53% sensitivity).

DISCUSSION

Combined antibiotic treatments are increasingly used in the clinic due to the burden of infections caused by MDR/extensively drug-resistant (XDR) bacteria. However, antibiotic combination studies are time-consuming and therefore not routinely performed in clinical laboratories. The use of instantaneous luminometer reading to evaluate antibiotic combinations in time-kill curves would avoid the requirement of an overnight culture for a viable cell count. The present study was aimed to validate an ATP measurement technique using bioluminescence as an alternative to the laborious conventional colony count method for the study of antibiotic combinations in time-kill curves.

Background, linearity, and the detection limit were studied for the standardization of the ATP measurement assay. NSS was compared with CA-MHB, which was the medium recommended by the manufacturer and used in previous studies (8, 11, 12). Background oscillation was considered relevant enough to be removed from assays. Linearity showed similar Pearson's correlation coefficients. Given the lower detection limit and the broader range of linearity determined for NSS, this was established as the optimal medium. Considering the initial inoculum (10^6 log CFU/mL), the detection limit obtained with NSS (10^3 log CFU/mL) was considered adequate as the value corre-

FIG 2 Legend (Continued)
measurement assay (RLU per milliliter) (right). Four experimental conditions were studied: growth control, meropenem alone, colistin alone, and meropenem plus colistin. The antibiotic concentrations were 17.71 mg/L for meropenem and 2.08 mg/L for colistin.

sponded to the maximum bacterial load change required to evaluate the pharmacodynamic parameters.

Control of variables affecting the bioluminescence reaction is essential, including the composition of the reading medium. Several ions have been reported to quench the bioluminescence reaction of the firefly luciferase (13). Cations should be strictly controlled while performing the assay, not only because of the potential quenching effect of the medium, but also due to the requirement of magnesium for the activity of this enzyme (11, 14). The concentration of cations included in CA-MHB medium may interfere with the RLU signal, which is in agreement with our standardization results that support the use of NSS instead of CA-MHB medium. Extracellular ATP may also affect the signal, as previously reported by Cai et al. (10). While these authors removed enzymatically extracellular ATP, the double centrifugation we performed to eliminate the antibiotic may have also contributed to its removal.

The correlation between CFU and RLU had been previous reported to diminish at 24 h, depending on the bacterial species (15). They attributed those discrepancies to metabolic differences between growth phases, slowing down the ATP production at the stationary phase. However, the decreases in correlations were observed because readings above the upper limit of what the authors had considered their linearity range were included. In contrast, in the present study no differences were found in the correlation at different growth phases—probably because the readings were within the linearity range.

The categorization of antibiotic combinations obtained using the ATP measurement assay was equivalent to the results obtained with the colony count method. Specificity should be prioritized over sensitivity when considering the therapeutic benefit of a combination. Therefore, 100% specificity cutoff points for synergy should be used to avoid false positives and unnecessary side effects. Synergy should be confirmed by the colony count method when the bacterial load decrease is between the cutoff with maximum sensitivity and specificity and the 100% specificity cutoff point. In this situation, the same aliquot could be further evaluated by the conventional method.

Our study had some limitations. The present study included only *Pseudomonas aeruginosa*. Other Gram-negative bacilli and Gram-positive bacteria should also be evaluated to validate its use in clinical isolates. One of the strengths of our study was the large sample size of readings to establish the cutoff points for *P. aeruginosa*. Another strength was the number of different antibiotic combinations, which supports its potential in a clinical background.

Our results support that the ATP assay could be used for the study of antibiotic combinations against MDR/XDR strains. Furthermore, as this method is less laborious and faster than the colony count, it could be implemented in the clinical laboratory workflow routine for the study of effective treatments against clinical isolates.

MATERIALS AND METHODS

Bacteria. This study examined 12 clinical isolates of extensively drug-resistant (XDR) *P. aeruginosa* from nine Spanish hospitals previously characterized at a phenotypical and molecular level (see the supplemental material) (16). The isolates belonged to the following sequence types: ST111, ST175, ST179, ST235, ST244, ST253, ST274, ST2221, ST2533, ST2534, ST2535, and ST2536. KPC-containing *K. pneumoniae* ATCC BAA 1706 was included for standardization.

Culture media and antibiotics. Columbia blood agar (COS) (bioMérieux) were used to culture the isolates. Cation-adjusted Mueller-Hinton broth (CA-MHB) (Becton, Dickinson) was used to perform the time-kill curves, and Mueller-Hinton agar (MH) plates (bioMérieux) were used for the quantification of CFU per milliliter.

The antibiotics used were meropenem, aztreonam, colistin, and amikacin (all from Sigma-Aldrich), and ceftolozane-tazobactam (Zerbaxa; MSD). The antibiotic stocks were prepared according to the Clinical and Laboratory Standards Institute (CLSI). The final concentrations used in the time-kill assays corresponded to the AUC over 24 h (Table 1) (17–21).

Time-kill curves. A starter culture was performed from the overnight (O/N) culture in CA-MHB and incubated in a water bath shaker at 37°C for 90 min to achieve early exponential growth.

Each flask containing 30 mL of CA-MH was supplemented with either a single antibiotic or combination at the corresponding concentration (Table 1), except the growth control condition. The antibiotic combinations tested are shown in the supplemental material. Flasks were inoculated with 10^6 CFU/mL

TABLE 1 Antibiotics used in the time-kill curves[a]

Antibiotic	Concn (mg/L)	Equivalent clinical dose
Meropenem	17.71	2 g q8h
Aztreonam	43.75	2 g q8h
Ceftolozane-tazobactam	38/6.25	3 g q8h
Colistin	2.08	4.5 IU q12h
Amikacin	8.17	1 g q24h

[a]The corresponding concentration and its equivalent clinical dose are shown for each antibiotic.

and incubated at 37°C in the water bath shaker for 24 h. From each flask, 1-mL aliquots were collected at different times (0, 8, and 24 h) and centrifuged at 5,000 rpm for 5 min. After the supernatants were discarded, bacterial cells were resuspended twice with saline solution to eliminate the antibiotic from the medium. Each aliquot was analyzed in parallel using two methods: (i) conventional viable cell count (CFU per milliliter) and (ii) the ATP measurement assay (RLU per milliliter).

Conventional viable cell count (CFU per milliliter). Ten-fold dilutions of the aliquots were inoculated onto MH agar plates and incubated at 37°C for 18 to 24 h. Only plates with 30 to 300 colonies were considered.

The bactericidal effect and synergy were the pharmacodynamic parameters defined based on conventional viable cell count. The bactericidal effect is defined as the reduction of ≥3 log CFU/mL at 24 h from the start of the experiment with the starter culture (5). Synergy is defined as the reduction of ≥2 log CFU/mL from the final count of colonies in the antibiotic combination compared to the result of the most effective of the two components (22).

ATP quantification technique by bioluminescence (RLU per milliliter). The quantification of viable cells through ATP was performed using the BacTiter-Glo microbial cell viability assay kit (Promega) and the GloMax 96 microplate luminometer (Promega) (11). The reagent was prepared and preserved following manufacturer's instructions. After bacterial lysis, free ATP reacts with luciferase enzyme (Ultra-Glo recombinant luciferase) that induces a luminescent signal. This assay is based on the ability of firefly luciferase to catalyze the oxidation of D-luciferin in the presence of a magnesium salt and ATP, and the light intensity emitted has been shown to be proportional to the ATP content and hence to the viable bacterial cells in any sample.

ATP measurement was performed using 96 opaque-walled multiwell plates. Time-kill curve samples were analyzed in triplicate and samples from the linearity assay five times. The same number of controls with background medium was included in each assay. The procedure was done by adding 100 μL sample and 100 μL BacTiter-Glo reagent. The plate was incubated at 37°C in the dark for 5 min and placed into the luminometer with a 1-s integration time. Mean background RLU values were then subtracted from the RLU sample values.

ATP assay standardization. Background, linearity, precision, and the limit of detection were analyzed using *P. aeruginosa* ST175 and *K. pneumoniae* ATCC BAA-1706 to set the experimental conditions to perform the time-kill curve tests. Each test of each strain was performed in duplicate.

Background was determined to control any significant oscillation of the reading medium. Data were gathered from linearity assays and corresponded to the values obtained with CA-MHB and normal saline solution (NSS) alone. The average and the standard deviation (SD) were calculated.

Linearity was calculated performing 10-fold dilutions of the bacterial culture in CA-MHB. This bacterial culture was performed as described for the time-kill curves. Two aliquots of each dilution were obtained at 0, 8, and 24 h to test two different backgrounds (i.e., CA-MHB and NSS). For the NSS condition, one aliquot was centrifuged at 5,000 rpm for 5 min, the supernatant was discarded, and the bacterial cells were resuspended twice with NSS. For the CA-MHB broth, there were no additional steps prior to the reading. Each aliquot was 10-fold diluted and analyzed in parallel using the luminometer and performing cultures onto MH plates in duplicate.

For every time and background, graphical representations of the results expressed in $\log_{10}$ scale were plotted. CFU were represented in the x axis and RLU in the y axis. Linear regression was used to evaluate the correlation between CFU and RLU using the R^2 statistic.

Precision corresponded to the relative standard deviation (RSD) (coefficient of variation). This parameter was calculated for each time, viable cell count, and background (14).

The limit of detection was calculated from the control wells of the linearity assay as the average luminescence (RLU) + 3 SD (23).

Statistical analyses. The comparative study between the conventional method and the ATP assay included a correlation study throughout the growth curves. The average of time-kill curve results (CFU and RLU) was converted to a $\log_{10}$ scale. The values from the *P. aeruginosa* growth control (without antibiotic) were used to confirm the correlation between CFU and RLU along the 24-h growth curves. A Shapiro-Wilk test for normal data was performed prior to calculation of the Pearson correlation coefficient and the intraclass correlation coefficient (ICC) with Stata version 15.

Receiver operating characteristic (ROC) curves, sensitivity, specificity, area under the ROC curve (AUC), and the optimal cutoff for the ATP assay were computed using an R library called pROC. Figures were created in R using the ggplot library. The bactericidal effect and synergy cutoff points were determined with a Youden test (14) using the conventional colony count method as the gold standard. The chosen cutoff point values were those with maximum sensitivity and specificity. Nonetheless, the

sensitivity and specificity of these parameters can be adjusted through the modification of the cutoff point values according to the aim of the test.

SUPPLEMENTAL MATERIAL

Supplemental material is available online only.

SUPPLEMENTAL FILE 1, PDF file, 0.1 MB.

ACKNOWLEDGMENTS

This work was performed using internal resources.

We thank Promega (Biotech Ibérica) for technical support and the kind supply of equipment and reagents.

B.P.-C., N.P., M.S.-C., X.D., and C.S. contributed to the conception and design of the study and acquisition, analysis, and interpretation of data. C.S., N.P., and J.R.G. contributed drafting the article and revising it critically for important intellectual content. J.P.H., S.D.-O., M.M.M., E.P., and A.O. gave the final approval of the version to be submitted. All authors approved the final version of the manuscript to be submitted.

We declare no conflict of interest.

REFERENCES

1. Oliver A, Mulet X, López-Causapé C, Juan C. 2015. The increasing threat of Pseudomonas aeruginosa high-risk clones. Drug Resist Updat 21–22:41–59. https://doi.org/10.1016/j.drup.2015.08.002.
2. Mathers AJ, Peirano G, Pitout JDD. 2015. The role of epidemic resistance plasmids and international high-risk clones in the spread of multidrug-resistant Enterobacteriaceae. Clin Microbiol Rev 28:565–591. https://doi.org/10.1128/CMR.00116-14.
3. Breidenstein EBM, de la Fuente-Núñez C, Hancock REW. 2011. Pseudomonas aeruginosa: all roads lead to resistance. Trends Microbiol 19:419–426. https://doi.org/10.1016/j.tim.2011.04.005.
4. Banerjee R, Johnson JR. 2014. A new clone sweeps clean: the enigmatic emergence of Escherichia coli sequence type 131. Antimicrob Agents Chemother 58:4997–5004. https://doi.org/10.1128/AAC.02824-14.
5. Leber AL (ed). 2016. Clinical microbiology procedures handbook, 4th ed. American Society for Microbiology, Washington, DC.
6. Drusano GL, Neely MN, Yamada WM, Duncanson B, Brown D, Maynard M, Vicciarella M, Louie A. 2018. The combination of fosfomycin plus meropenem is synergistic for Pseudomonas aeruginosa PAO1 in a hollow-fiber infection model. Antimicrob Agents Chemother 62:e01682-18. https://doi.org/10.1128/AAC.01682-18.
7. Shama G, Malik DJ. 2013. The uses and abuses of rapid bioluminescence-based ATP assays. Int J Hyg Environ Health 216:115–125. https://doi.org/10.1016/j.ijheh.2012.03.009.
8. Cai Y, Leck H, Lim TP, Teo J, Lee W, Hsu LY, Koh TH, Tan TT, Tan T-Y, Kwa AL-H. 2015. Using an adenosine triphosphate bioluminescent assay to determine effective antibiotic combinations against carbapenem-resistant Gram negative bacteria within 24 hours. PLoS One 10:e0140446-15. https://doi.org/10.1371/journal.pone.0140446.
9. Aragonès L, Escudé C, Visa P, Salvi L, Mocé-Llivina L. 2012. New insights for rapid evaluation of bactericidal activity: a semi-automated bioluminescent ATP assay. J Appl Microbiol 113:114–125. https://doi.org/10.1111/j.1365-2672.2012.05320.x.
10. Cai Y, Ng JJ, Leck H, Teo JQ, Goh J-X, Lee W, Koh T-H, Tan T-T, Lim T-P, Kwa AL. 2020. Elimination of extracellular adenosine triphosphate for the rapid prediction of quantitative plate counts in 24 h time-kill studies against carbapenem-resistant Gram-negative bacteria. Microorganisms 8:1489–1415. https://doi.org/10.3390/microorganisms8101489.
11. Promega. 2012. BacTiter-Glo microbial cell viability assay. 67. Promega, Madison, WI.
12. Cai Y, Seah CL, Leck H, Lim T-P, Teo JQ, Lee W, Tan T-T, Koh T-H, Ee PLR, Kwa AL. 2018. Rapid antibiotic combination testing for carbapenem-resistant Gram-negative bacteria within six hours using ATP bioluminescence. Antimicrob Agents Chemother 62:e00183-18. https://doi.org/10.1128/AAC.00183-18.
13. Zhang H, Bai H, Jiang T, Ma Z, Cheng Y, Zhou Y, Du L, Li M. 2016. Quenching the firefly bioluminescence by various ions. Photochem Photobiol Sci 15:244–249. https://doi.org/10.1039/c5pp00432b.
14. OIE. 2012. Principios y métodos de validación de las pruebas de diagnóstico de las enfermedades infecciosas. Man Acuático OIE 2012:20.
15. Vogel SJ, Tank M, Goodyear N. 2014. Variation in detection limits between bacterial growth phases and precision of an ATP bioluminescence system. Lett Appl Microbiol 58:370–375. https://doi.org/10.1111/lam.12199.
16. Del Barrio-Tofiño E, López-Causapé C, Cabot G, Rivera A, Benito N, Segura C, Montero MM, Sorlí L, Tubau F, Gómez-Zorrilla S, Tormo N, Durá-Navarro R, Viedma E, Resino-Foz E, Fernández-Martínez M, González-Rico C, Alejo-Cancho I, Martínez JA, Labayru-Echve OA. 2017. Genomics and susceptibility profiles of extensively drug-resistant Pseudomonas. Antimicrob Agents Chemother 61:e01589-17. https://doi.org/10.1128/AAC.01589-17.
17. Kitzes-Cohen R, Farin D, Piva G, De Myttenaere-Bursztein SA. 2002. Pharmacokinetics and pharmacodynamics of meropenem in critically ill patients. Int J Antimicrob Agents 19:105–110. https://doi.org/10.1016/S0924-8579(01)00474-5.
18. Smith PF, Ballow CH, Booker BM, Forrest A, Schentag JJ. 2001. Pharmacokinetics and pharmacodynamics of aztreonam and tobramycin in hospitalized patients. Clin Ther 23:1231–1244. https://doi.org/10.1016/S0149-2918(01)80103-X.
19. Wooley M, Miller B, Krishna G, Hershberger E, Chandorkar G. 2014. Impact of renal function on the pharmacokinetics and safety of ceftolozane-tazobactam. Antimicrob Agents Chemother 58:2249–2255. https://doi.org/10.1128/AAC.02151-13.
20. Marchand S, Lamarche I, Gobin P, Couet W. 2010. Dose-ranging pharmacokinetics of colistin methanesulphonate (CMS) and colistin in rats following single intravenous CMS doses. J Antimicrob Chemother 65:1753–1758. https://doi.org/10.1093/jac/dkq183.
21. Garraffo R, Drugeon HB, Dellamonica P, Bernard E, Lapalus P. 1990. Determination of optimal dosage regimen for amikacin in healthy volunteers by study of pharmacokinetics and bactericidal activity. Antimicrob Agents Chemother 34:614–621. https://doi.org/10.1128/AAC.34.4.614.
22. Lim T-P, Cai Y, Hong Y, Chan ECY, Suranthran S, Teo JQ-M, Lee WH, Tan T-Y, Hsu L-Y, Koh T-H, Tan T-T, Kwa AL-H. 2015. In vitro pharmacodynamics of various antibiotics in combination against extensively drug-resistant Klebsiella pneumoniae. Antimicrob Agents Chemother 59:2515–2524. https://doi.org/10.1128/AAC.03639-14.
23. Cáñez-Carrasco MG, García-Alegría AM. 2015. Validación de un método analítico para la determinación de fósforo por espectrofotometría ultravioleta-visible. BIOtechnia 17:32. https://doi.org/10.18633/bt.v17i1.15.